Universidade de Aveiro Departamento de Engenharia de Materiais e Cerâmica
2012

Sarah Hélène Christine Henry

Cerâmica islâmica em corda seca de Mértola dos séculos X a XIII

"Cuerda seca" Islamic ceramics from the X-XIIIth centuries of Mértola

Universidade de Aveiro
Ano 2012
Departamento de Engenharia de Materiais e Cerâmica

Sarah Hélène Christine Henry

Cerâmica islâmica em corda seca de Mértola dos séculos X a XIII

"Cuerda seca" islamic ceramics from the X-XIIIth centuries of Mértola

Dissertação apresentada à Universidade de Aveiro para cumprimento dos requisitos necessários à obtenção do grau de Mestre em Ciência e Engenharia de Materiais, realizada sob a orientação científica do Doutor Joaquim Manuel Vieira, Professor Catedrático do Departamento de Engenharia de Materiais e Cerâmica da Universidade de Aveiro, e co-orientação do Doutor e da Doutora Susana Gomez Martinez, Investigadora do Centro de Estudos Arqueológicos das Universidades de Coimbra e Porto e Co-Diretora de Escavações Arqueológicas do Campo Arqueológico de Mértola

o júri

Presidente	Professora Doutora Maria Margarida Tavares Lopes de Almeida Professora Auxiliar da Universidade de Aveiro
Vogais	Professor Doutor Joaquim Manuel Vieira Professor Catedrático da Universidade de Aveiro (Orientador)
	Professor Doutor João Paulo Pereira Freitas Coroado, Professor Coordenador da Escola Superior de Tecnologia de Tomar, Instituto Politécnico de Tomar
	Professora Doutora Ana Margarida Madeira Viegas de Barros Timmons Professora Auxiliar da Universidade de Aveiro
	Professor Doutor Pedro Manuel Lima de Quintanilha Mantas Professor Auxiliar da Universidade de Aveiro (Co-orientador)
	Doutora Susana Gómez Martinez Investigadora do Programa Ciência 2008 da FCT, Universidade de Coimbra - CEAUCP / Campo Arqueológico de Mértola (Co-orientadora)

agradecimentos

Support from FAME Master/Erasmus Mundus is acknowledged by the author. Access to the electron microscopy infrastructures of RNME Pole of Aveiro, FCT Project: REDE/1509/RME/2005 is gratefully acknowledged.

I am very grateful Doctor Susana Gomez and the camp of archaeological Mértola for their hospitality and above all their confidence.

I especially want to express my gratitude to Pr. Joaquim M. Vieira, Pr. Pedro Q. Mantas and Marta C. Ferro for their help and their support all long my internship in the laboratory of CICECO.

The help of Dr. António Fernandes and Doctor Diogo Mata and permission of the Physics Department of the University of Aviero for providing me the Raman spectrometry for this study is gratefully acknowledge too.

Is also acknowledged the entire team group RNME – National Network of Electron Microscopy, Pole of Aveiro, for their hospitality which allowed me to do my internship is very good conditions..

palavras-chave

Química analitica, cerâmicas islâmicas, corda seca, arqueologia, microscopia electrónica de varrimento, vidrados de chumbo, fosfato, Mértola.

resumo

O trabalho presente pretende fazer a caracterização introdutória da estrutura, fases e composição química da pasta e vidrado de um conjunto de seis peças de cerâmica islâmica em "corda seca" dos séculos X-XIII fornecidas pelo Campo Arqueológico de Mértola. É espetável que os resultados do trabalho possam vir a ser úteis para uma futura identificação da origem das peças, das relações de comércio implícitas ou para lançar luz sobre as antigas tecnologias de fabricação de cerâmica.

Foram selecionadas para este estudo várias das técnicas instrumentais disponíveis. A microscopia eletrónica de varrimento com espectrometria EDS como a ferramenta mais geral foi extensivamente utilizada na determinação da morfologia e da composição química aproximada do vidrado e da pasta. As fases cristalinas presentes na pasta foram identificadas por difração de raios-X. Recorreu-se à espetroscopia UV e ao colorímetro de refletância CIELab para organizar as pastas segundo a cor com o suporte de índices quantitativos. Para questões específicas da composição e microestrutura da zonagem observada no vidrado de algumas amostras recorreu-se ainda à espetrometria micro-Raman e microscopia de luz polarizada refletida para complemento do estudo.

Algumas das amostras apresentaram quantidades importantes de fósforo na camada do vidrado. Nesta matéria, é comummente aceite nos estudos arqueológicos que o fósforo detetado em cerâmica ou vidros antigos que estiveram enterrados vem de águas residuais. Tal interpretação encaixa verosimilmente nos resultados, em parte apenas das amostras arqueológicas estudadas. Observou-se que as fases com fósforo são caracterizadas por uma proporção específica dos elementos Pb, P e Ca apresentando dois tipos de morfologia que são discutidos. Sabe-se que os vidros contendo fósforo podem apresentar intervalo de miscibilidade, com um de vidro de fósforo / chumbo / cálcio que tenderá a separar-se da composição rica em silicato. A implicação, ainda que especulativa, seria de que as cinzas ósseas poderiam estar a ser utilizadas como matéria-prima para a preparação de vidrados cerâmicos de baixo ponto de fusão. Partir desta perspetiva poderá justificar o aprofundamento do estudo para separação entre os efeitos de intemperismo e a hipotética utilização técnica de fosfatos.

A tese começa com um prólogo curto sobre o contexto histórico das amostras investigadas seguido pela descrição resumida dos principais métodos experimentais utilizados. Os dois capítulos com resultados experimentais incluem um estudo introdutório com uma coleção de quatro peças de tempos mais recentes e o da caracterização das amostras históricas da cerâmica em "corda seca"

keywords

Analytical chemistry, Islamic ceramics, “cuerda seca”, archeology, scanning electron microscopy, lead glazes, phosphate, Mértola

abstract

The present work intended to give a introductory characterization of structure, phases and chemical composition of the paste and glaze of a set of six pieces of Islamic ceramics of “cuerda seca” type from the X-XIIIth centuries provided by the Mértola archeological site. The results will expectedly be a contribution to the identification of origin of the pieces, the trading that can be implied or to shed light and on ancient ceramic fabrication technologies.

Several instrumental techniques made available were selected for the study, the Scanning Electron Microscopy with EDS spectrometry as a general tool to determine morphology and the chemical elemental composition of the glaze and paste, X-ray diffraction for the crystalline phases in the paste, UV-spectroscopy and colorimetric to organize the pastes by their color with quantitative indexes. For special cases micro-Raman spectrometry and reflected polarized light microscopy were added to complement the study.

Some of the samples showed important amounts of phosphor in glazed layers. In this matter, it is commonly accepted that the phosphor in archeological ceramics or glasses that were buried comes from runoff water, such interpretation seemingly fits our results in part of the archeological samples.

It was observed that phosphor phases are characterized by a specific ratio of the elements Pb, P and Ca with two types of morphology that are further discussed. It is known that phosphor containing glasses may present miscibility gaps, phosphorous/lead/calcium glass tending to separate from the silicate rich composition. It would speculatively imply that bone ashes as raw material for preparation of low melting point glazes could have been in use. From this perspective, the distinction between weathering effects and a technical phosphor may mean continuation of the study.

The thesis starts with short prologue on the historical context of samples followed by the short description of the main experimental methods used. The two chapters with experimental results include an introductory study with a collection of four pieces of more recent times and the comprehensive characterization of the “cuerda seca” historical samples.

TABLE OF CONTENTS

LIST OF FIGURES

LIST OF TABLES

Chapter 1 - Prologue

The project of this thesis was divided into three moments; first, learning a new technique that was the scanning electron microscopy. Then, to lead me to the use of this new technology and the study of ancient pieces, I conducted a preliminary study of some samples found in the region of Aveiro. Finally, thanks to the collaboration with the Archaeological Museum of Mértola and with the archaeologist Susana M. Gomez who provided us the samples, we were able to make an extensive study of a set of six samples of the type "cuerda seca" from the X-XIIIth centuries. Historical samples have specific values regarding the heritage. Their study responds to specific needs namely to the improvement of the knowledge on economical, cultural and evolution of the technologies along time (Claire Déléry 2008, Susana Gomez 2009). For this kind of analysis, a specific strategy has to be adopted; archaeological samples, due to their fragility, and most of the time, their poor conservation, are difficult to prepare for the analysis. Indeed, they are not always adapted to the analytical techniques because of their specific shape and should not be modified or destroyed because they are precious and unique samples.

The samples come from two places in Mértola: below an ancient Christian cemetery and from a sceptic pit. A first study has been performed by Claire Déléry on a set of samples coming from another site of the archaeological zone in Mértola (Claire Déléry 2006). This study was conducted in order to have a better understanding of the technique of "cuerda seca", cultural and economical dynamics through the analysis of the glaze and the paste of a large collection of samples.

In the Middle-Age, the Al-Andalus territory was an important space for cultural exchanges and traffic in goods because of its position in west of the Mediterranean in a time that a common Islamic rule linked East and West. With harbours in Mediterranean coast that give access to the shores of Maghreb and to the Near East harbours, Al-Andalus was in a front position to receive new techniques. Almeria was one of the most important of these harbours. Through this port passed materials, artisans and slaves in transit to the beautiful capital of the Caliphate, Cordoba (Gomez 2009).

In this time, large ceramic production centres started to develop in Al-Andalus. Polychrome glaze decoration spread from the south-east to the other side of Al-Andalus, by Atlantic harbours such as Lisbon. Mediterranean played the role of centre for diffusion of techniques, Mértola and Lisbon also contributing with local productions of ceramics, figures 1 and 2 (Molera 2001, Gomez 2009).

Figure 1. Map of the Al-Andalus region corresponding to most of the Iberian Peninsula with exception of regions in north and north-east of the territory (Molera 2001).

The trade of ceramics in Al-Andalus appears to be better represented by glazed materials: honey colored and manganese glaze and ceramics decorated with “cuerda seca” technique. From the Xth to the XIIth century, the “cuerda seca” production sites could only be found in Al-Andalus (Claire Déléry 2006). Thanks to Al-Andalus harbours, the cuerda seca technique arrived not just to the Maghreb but also to the south of France at the end of the Xth century. With the political and economical changes in the region from the XIth to the XIIth century, the exportation of the “cuerda seca” potteries grew to Italy, Egypt and other large harbours with an increase of exchanges between Occident and the Mediterranean Orient.

Mértola became one of the communication centers in Garb Al-Andalus. The town played an important role in the redistribution of objects in an extended trade network. Mértola was the central point of the economy in the south-west of Al-Andalus, a wide region that overlaps with the present territories of south of Portugal and west of the autonomous communities of Extremadura and Andalusia in Spain. Indeed, Mértola was considered as an inland seaport tied to the Mediterranean economy since Iron Age and was already the site with palladium and forum during the early Roman period (mid-2th century BC) (Gomes, 2007). This port was located at the most northerly navigable point of the Guadiana river, at the intersection between regional commercial networks and Mediterranean maritime trade routes, figure 2 (Gomez 2009).

Figure 2. Main places of Portugal and Spain territories involved in the“cuerda seca” exchange (Susana 2006)

Mértola provided us 6 samples to bring new information and make a comparison between our results and the results obtained by Claire Déléry and to be able to understand the cultural and economical trades in this type of ceramics. The aim of this study is to determine their structure compositions in order to establish where and how samples were made and their techniques of fabrication. Several techniques of characterization were used: Scanning Electron Microscopy, to determine the morphology and the elemental composition of the glaze, and X-ray diffraction, to give information about the phases of the ceramic body. UV-spectroscopy, colorimetric and micro-Raman analyses were also used.

The following of the thesis is divided into three parts. The first part describes the experimental techniques listed above. The second part is a short study about the preliminary steps in characterizing some samples. Finally, the third part is the characterization of the set of historical samples from the Mértola archaeological site.

The aims of the preliminary study were to establish some routine and protocol concerning the analyses of archaeological samples (understanding the composition of the ceramics, especially the glaze) and to become familiar with the SEM technique (solving the difficulties of sample preparation) and with the analyses themselves. The analysis of a set of four samples of different sate of conservation and ages allowed me to improve the knowledge in formulation of ceramics. This study also allowed me to develop approaches in sample preparation that should be the less destructive as possible within the spirit of conservation.

The main part of the thesis concerns the study of the glazes of the set of “cuerda seca” samples. The term “cuerda seca” was coined in 1558 to describe the décor on ceramic materials with which the

different glazes are isolated from each other by a line of different composition, mostly manganesium oxide composed with fat. The technique of glazing ceramic bodies was firstly used by the, Achaemenid known as the first Persian Empire in the Ist millenary BC (Encyclopedia Universalis).

The second half of the Xth century was a time for art and culture development in Al-Andalus. Orient influenced polychrome decor of ceramics appeared in the Iberian Peninsula. The potters started the production of the first polychrome glazes; honey coloured and manganese decoration, followed by those decorated with the “cuerda seca” technique. In Orient, the centres of production were Kashan, Damas, Fostât and the Caire. Following the route of faiences and Muslim expansion, the “cuerda seca” arrived in Spain in the Xth century and in Malaga later in the XIIth century. In Cristian reconquested territories of Spain the “cuerda seca” décor was mainly fabricated in Seville and Toledo (Encyclopedia Universalis).

During the study, analyses showed important amounts of phosphor. Usually, phosphor found in ancient pieces is considered as the result of weathering by the archaeologists. The phosphorous pollution usually comes from runoff water coming through cemetery, or treatment of the ground with phosphates. In the case of this set of “cuerda seca” ceramics, the findings seem more complex because three kinds of morphology were observed. In two samples, phosphor was only observed at the surface of the sample which can be considered as external pollution. Because of the particular morphology and an obvious correlation between samples concerning the repartition of phosphorous matter (similar ratio Pb/P/Ca) one opted to give room in this study on other potential sources of phosphor in those samples beyond the effects of the burials.

Chapter 2 - Experimental Methods and Techniques

1. Sample preparation

Depending on the sample and on the analysis to be performed (SEM or optical microscopy), there are several sample preparations techniques of selection. The sample can be directly analyzed without modification in the case of topography analyses. In that case, the sample is fixed on a metallic holder with carbon cement or tape. If the sample is non-conductive, a carbon coating (or AOPD) is used to allow the conduction of the electrons through the sample. Samples are often polished in order to offer a flat surface for the study of chemical composition with more accurate measurements.

For the study of the cross-sections, the cut bits of the samples were mounted in epoxy (80% *araldite-AY103* and 20% *hardener*) left to cure overnight. Once it is hardened, the mounting is grinded and the polished in two main steps on silicon-carbide paper follow by fine polishing with diamond paste on cloth. According to the sample (soft or hard material), one can use several grit sizes paper and pastes. For the preparation of the samples of this study three silicon-carbide paper; P400, P800 and P1000 and four diamond paste; #15, #6, #3, #1 (μm) were used. The higher the grit numbers the smaller the abrasive grain sizes are. At the end of the polishing, the sample can be removed from the epoxy mounting or directly glued on a metallic holder and coated with carbon or AOPD.

For the facing analysis by SEM, the taken bits of the glazes were directly glued on a metallic SEM sample holder with carbon cement. The carbon cement allows better adherence of the samples than the carbon tape sticks but it needs 5 hours drying. After drying, the samples were coated with a carbon film. As the ceramics samples are non-conductive materials, one applied two layers of C coating.
Polished samples were glued on metallic SEM sample holders and coated with carbon (as for facing analyses), figure 3.

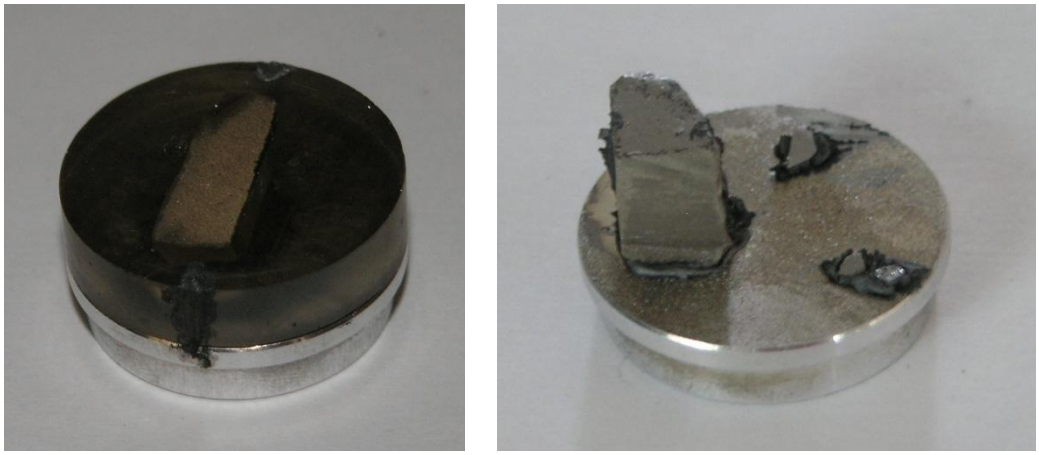

CROSS-SECTION FACING

Figure 3. Images of two mounted samples, prepared for microscopy; mounted in epoxy for cross-section (left) and directly glued on SEM sample holder for face analysis (right).

The polishing is very important in SEM microscopy to have good atomic number contrast in high resolution images the sample must have the lowest relieve as possible. It is equally important in EDS analysis in order to allow quantitative measurement of the chemical composition of the samples (Henri Paqueton and Jacky Ruste, Techniques de l'ingénieur). The quality of polishing of two samples can be observed in the images optical microscope in figure 4.

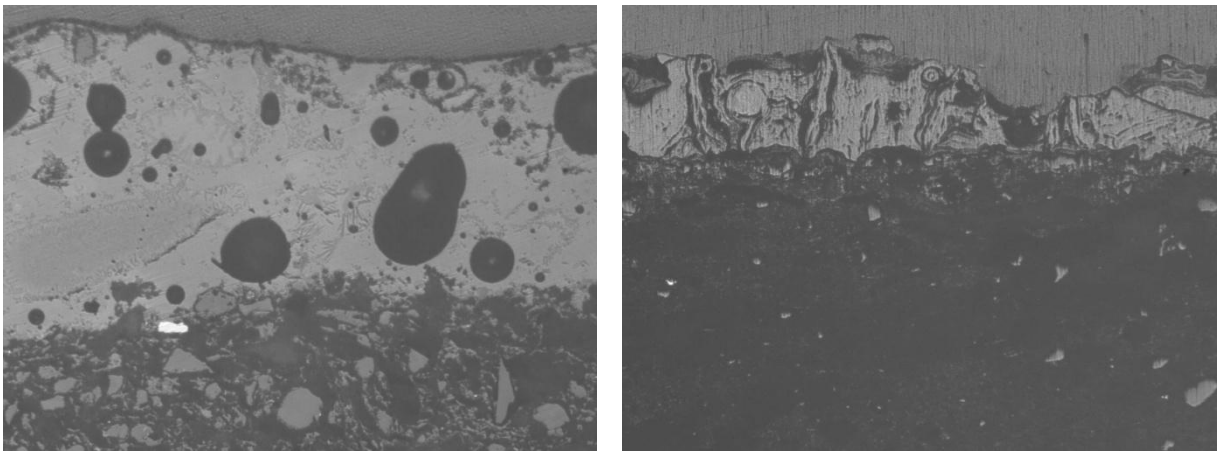

GOOD POLISHING POOR POLISHING

Figure 4. Optical images of the polished cross-sections of sample HBR-0206 (left) and HBR-0207 (right) taken with JENAPHOT microscope.

For the XRD measurement, small amount of ceramic body were cut from samples reduce into fine powder which was pressed in the sample holder of the X-Ray powder diffractometer.

2. Principle and technical characteristics of SEM

The scanning electron microscopy (SEM) is a powerful technique for surface topography observations with elemental analyses by X-ray energy (EDS) or wavelength spectrometry (WDS). It uses the signals created at the surface of solid specimen by the interaction of the fine focus electron beam-sample to give information about the texture, the chemical composition and the crystalline structure of the sample. SEM technology is used to generate a 2-dimensional image of a selected area of the surface of the sample with a lateral resolution of 2 to 10 nm, a magnification ranging from 20 to 400 000X. Analysis can also be performed in a specific point, especially useful in EDS (Energy Dispersive Spectroscopy) measurements.

A finely focusing electron beam with a specific kinetic energy scans the surface of the sample and signals produced by the sample are detected. Under the electron beam, the sample emits several signals coming from secondary electrons (giving the SEM image), backscattered electrons and photons (visible light or X-ray allowing the EDS), Auger electrons and transmitted electrons (in thin section as in STEM microscopy), figure 5.

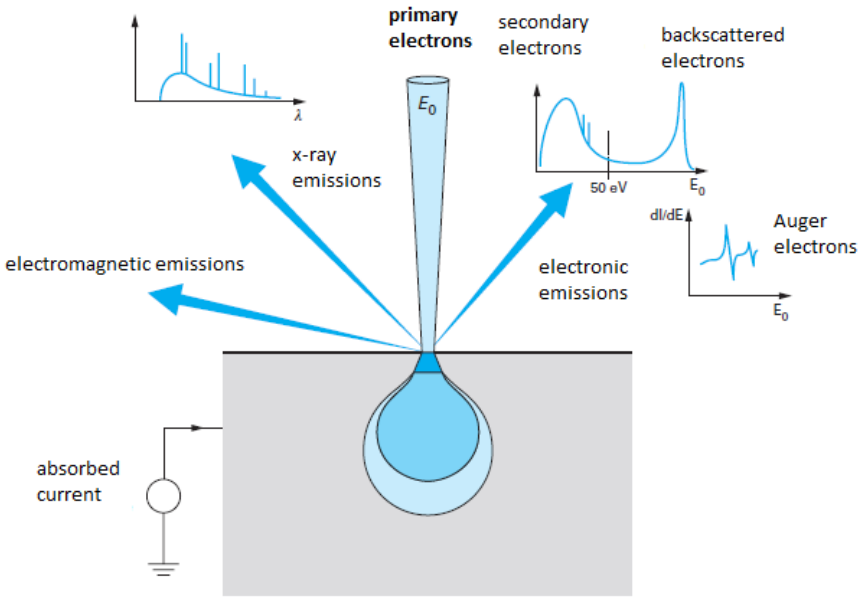

Figure 5. Scheme of the interaction electron/sample during SEM (Paqueton 2004)

Secondary electrons produce the image point by point of the scan surface and show the morphology and topography of the sample. Backscattered electrons are valuable for illustrating contrast in composition in heterogeneous samples. X-rays are produced by inelastic collisions of the incident electrons with electrons in the orbital of the atoms. After this excitation, the electrons of the atoms return to lower energy state producing specific x-rays with characteristic wavelength corresponding to specific chemical species. The produced x-ray gives qualitative and may yield quantitative measures of the concentration of the elements present in the sample.

A scanning electron microscope is composed of: an electron source “GUN” most of the time a tungsten filament, electron lenses used to focus the beam, a sample stage (sample holder), several detectors for the different signals and finally display and data devices.

Also really important for the good work of the SEM microscope are: i) Vacuum system: prevent interaction of the beam with particles of the air, ii) Cooling system, iii) Vibration-free floor and iv) Room free of ambient magnetic and electric fields.

The SEM/EDS analysis were preformed with the SEM/EDS Hitachi S4100 with FEG electron gun and accelerating voltages in 500V a 30kV range, equipped with the Rontec EDS dectector. EDS software provides subroutines for correction of the X-Ray detection conditions in SEM and standarless analysis of chemical composition being feasible.

3. X-Ray diffraction (XRD)

X-ray diffraction is an analytical technique giving information about the crystal structure, chemical composition and physical properties of materials and thin films. X-ray domain, goes from 0.1 Å (γ-Ray limit) to 100 Å (far-UV limit) corresponding to the energy range 0.1 to 100 keV (E=hv=h.c/λ).
The X-ray diffractometry as analytical method can only be used on crystallized materials such as minerals, metals, ceramics, semi-crystalline polymers and organic crystallized samples but not on amorphous material such as the glasses. Yet, crystalline inclusions and precipitates of glazes can be analysed by XRD.
There are many possibilities for the X-rays to interact with the matter; in diffraction, the beam can be diffracted elastically or inelastically. In XRD, one are talking about elastic diffraction; meaning that the incident and the diffracted beams have the same wavelength and the same energy. The kinetic energy of the incident particles is conserved, only their direction of propagation is modified.

In powder-XRD, a focused X-ray beam is diffracted by a sample composed of a big number of microcrystals with random orientation. The microcrystals have a size between 0.01 and 0.001 mm. As there are a lot of microcrystals, one can count that enough of them have a family of reticular plane that matches with the Bragg relation. Indeed, one can represent the crystal network as a series of parallel and equidistant lattice planes. Bragg's law provides the condition for a plane wave to be diffracted by a family of lattice planes:

$$n.\lambda = 2d_{hkl}.\sin\theta \qquad \text{(Eq. 1)}$$

Where d is the lattice spacing, θ the angle between the wave vector of the incident plane wave, k_0, and the lattice planes, λ its wavelength and n is an integer corresponding to the order of the reflection. It is equivalent to the diffraction condition in reciprocal space and to the Laue equations.

For peak identification using the Bragg equation (Eq.1) for each peak, one calculates the corresponding distance crystalline distance d_{hkl}. With the series of d_{hkl} one can determine the series of planes hkl which is related to the lattice parameters. JCPDS files constitute a database of almost known crystalline compounds at the present time. Identification of the phases is based on the comparison of the values distances and peak relative intensity with the files, assisted specialized search tools provided by dedicated software.
From other methods of treating information provided by XRD, such as Rietveld method or Fourrier transforms, one can obtain more information about the sample, namely: i) quantitative analysis: determine the composition of a mixture, ii) determination of preferential orientation of the crystal (texture study), iii) determination of the phase transitions, iv) crystalline structure determination.
The XRD analysis was performed with the Rigaku XDMAX powder diffractometer at room temperature using monochromatic Cu Kα radiation (λ = 1.54056 Å).

4. Optical microscopy

By using polarized light in optical microscopy birefringent materials have the optical contrast increased by the rotation of the vector the electromagnetic field of light. Polarised light analysis of rocks or man-made materials is more often done with transmitted light microscopy. As such, it allows quantitative analysis as usually done in geology, mineralogy or even in chemical studies. Reflection of light on the surfaces of the solids also induces rotation of the vector of the electromagnetic field of light. In partially transparent materials or in presence of surface thin films the reflected light may create interference effects of the polarized light beam that are exposed by using the analyser, as found in Kern optical microscopy (Weaver 2003).

In this study the polished sections of glazes of selected samples were observed in reflected polarized light microscopy with a Nikon microscope equipped with 2 Mb digital photographic camera.

5. Raman spectroscopy

Raman spectroscopy is based on the inelastic scatter of light by the vibration excitation modes of molecules and atomic bonds of the materials. Phonons may be created (Stokes process) or annihilated (Anti Stokes process) in this excitation processes. The Raman shift of the frequency of the scattered beam in relation to the incident beam measures the energy associated to the Stokes/ anti Stokes processes and yields information on the specific energy of chemical bonds of the material being analysed. Raman spectroscopy is frequently restricted to narrow wavenumber range 50-1000 cm^{-1}, which is close to the range selected also for this study. Rules of mutual exclusion correlated the ouputs of Raman spectroscopy to the results of IR FT spectrometry.

The use of laser beams finely focused by the optics of the microscope can give very narrow, highly monochromatic, coherent beam excitations in very small volumes of the surface of the sample as in micro-Raman spectroscopy (Gardiner 1989, Ferraro 2003). For the present study the micro Raman Spectrometer Jobin Yvon 64000 of the Department of Physics was used. It has the following main features: spatial resolution (1 micron), spectral resolution (1 cm^{-1}), range: 40 cm^{-1} to 8000 cm^{-1}, laser excitation of Argon and Ti-saphire.

6. Colorimetric analyses

6.1 UV- spectroscopy

The spectrometer UV-3100 (UV-VIS-NIR) recording spectrophotometer with halogen and deuterium lamps covering the spectrum from 190 to 1000 nm was used to analyse the six samples of

archaeological ceramics and determine the color of their ceramic bodies the cross-sections of in the non-glazed back surfaces, depending on the piece wall thickness.

6.2CIEL*a*b* coordinates

A second colorimetric analysis was performed using CIELab coordinates in order to determine if samples showing the same absorption peak have the same color. For this purpose, a Minolta CM-508D spectrometer with a D65 illuminator and 10 º viewing angle was used. The system of selected coordinates L* a* b*, introduced in 1976, is a measurement model of the CIE (International Commission on Illumination, CIE, 1978).

This three-dimensional representation of color is formed by the two axes a* and b*. The parameter a* can have negative values (-a*) which indicate the green color whereas positive part (a*) stands for red, figure 6. For the b* coordinate, the color ranges from blue (-b*) to the yellow (b*). The third axis is the vertical one, represents the lightness or luminance L* of the color. This quantity varies from L* = 0 (black) to L* = 100 (white) and determines color intensity. These parameters assign a location to the each color in a well defined system and allow comparison of color between different tested samples too.

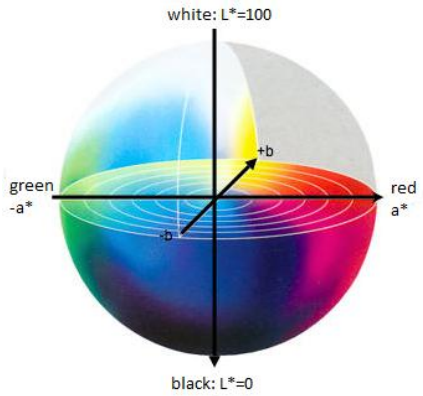

Figure 6. CIELab system of color coordinates (Schanda, 2007)

The CIELab color coordinates were converted to the equivalent RGB values by using the EasyRGB color calculator (http://www.easyrgb.com/index.php?X=CALC#Result), the RGB codes yielding the shading colors of the corresponding heading boxes of table 7. The pastes of samples HBR-0206 and CR/CSP/0023 have red tainted colors. The sample HBR-0001 has a pinkish component in a color of low luminance. The sample CR/CSP/0022 has yellowish taints in a color of the lowest luminance. Finally, samples HBR-0207 and HBR-0072 show colors with greenish components faded by the intense luminance, the HBR-0207 being of clear cream color.

The color of a ceramic body depends on firing temperature, amount of iron in its composition and oxy/reduction conditions in the furnace atmosphere. For two samples that have the same composition, it is expected that the higher L* is the lower the firing temperature might have been (Schanda, 2007)

Chapter 3 - Preliminary study

An introductory laboratory study of tiles and pottery shreds from the 17th to the 20th century

An introductory analysis of tiles found in the ground of the town of Aveiro was done to show the evolution of glazes along different historical moments. It was also an objective of this first laboratory study to solve difficulties expected from poor conditions of the pastes and fragility of the glaze layers mainly during polishing of cross-section

The set of our samples included three modern ceramic pieces (one dark blue tile, a blue and yellow decorated tile, both of most recent production technologies of the 20th century and a blue and white earthenware faience also from the 20th century), and one azulejo tile probably from the 17th century. The three tiles are known as azulejos because they have coloured glazes that shine on their surface (Basso 2009). The decorations of the glaze of the four samples are shown in figure 7. The reference codes, paste thickness and XRD composition are given in table 1. The two samples with MSJ-TILE reference were picked from the ground of the old yard of Santa Joana Coventry (XVth century restored in late 20th century). The other two samples were picked from the grounds in town of Aveiro in Esgueira (ESG) and Mário Sacramento street (RMS) and were selected for the styles of decoration. The numbers indicate the date of collection in 2012.

a) MSJ-TILE-3 25-REST

outside - inside
b) ESG-POT-3 24

c) RMS-TILE-3 31-3C

d) MSJ-TILE-3 25-3C

Figure 7. Optical images of the four samples: a) MSJ-TILE-2-25-REST, b) ESG-POT-3-24, c) RMS-TILE-3 31-3C and d) MSJ-TILE-3 25-3C

This short study is divided into two parts: the characterization of the pastes and the establishment of the main differences among glazes. The results of the XRD analyses of the pastes of the four pieces

are summarized in table 1. The approximate elemental composition of the body and glaze of the four pieces determinated by EDS are given in table 2.

Table 1. Summary of the information of the four samples of the set

Sample	**Paste**	**Thickness (mm)**	**Glazed decoration**	**Paste composition (DRX)**
MSJ-TILE-3 25-REST	White - gray	9.5	Blue and dark blue	Quartz, mullite
ESG-POT- 3 24	cream	---	White and blue (outside); White (inside)	Quartz, diopside, anorthite
RMS-TILE- 3 31-3C	white	5.5	Blue, yellow and White (diffused)	Quartz, diopside, gehlenite, anorthite, mullite
MSJ-TILE-3 25-3C	cream	14	White, yellow and blue (trace)	Quartz, calcite, albite, gehlenite, hematite, diopside, mullite

Table 2. EDS of the glazes and the pastes of the four samples (mol. %).

SEM	Na_2O	MgO	Al_2O_3	SiO_2	K_2O	CaO	TiO_2	Fe_2O_3	CuO	SnO_2	PbO	BaO	ZrO_2	ZnO
MSJ-TILE-3 25-REST														
Paste 1	2.2	2.5	13.0	77.5	3.7			1.1						
Glaze 1			13.7	59.0	2.7	10.0					2.4	3.4	2.8	6.1
ESG-POT- 3 24														
Paste 2		5.1	12.7	61.6	4.5	14.9		1.2						
Glaze 2	5.7		4.3	69.9	4.7	1.0		0.3		5.0	9.1			
RMS-TILE- 3 31-3C														
Paste 3		5.4	10.9	62.5	1.6	19.0		0.6						
Glaze 3			6.9	49.2		10.4	2.5	0.4			17.4		8.1	5.1
MSJ-TILE-3 25-3C														
Paste 4	3.6	3.9	8.8	45.5	1.0	35.0		2.2						
Glaze 4	4.6		4.8	76.2	3.9	0.9				3.3	6.3			

1. The pastes

Without further analysis, one can already have an idea of the age of the tiles regarding the thickness and decoration elements. Tile pressing technology has evolved towards ever thinner section of the tile to save weight; the thicker the tile is, the elder it may be. This can be explained by the evolution of the techniques of production along ages. Such explanation is not expected to hold for the pottery pieces. Ceramic objects used as tableware are usually thin to be light and easily portable.

Thin wall pottery pieces are commonly found in ancient greek amphora collections, high quality Roman terra sigillata, as well as in the present study with the elegant cuerda seca pieces of Islamic production. One can rank the three tile pieces by the increasing the value of their thickness, figure 8 and table 1.

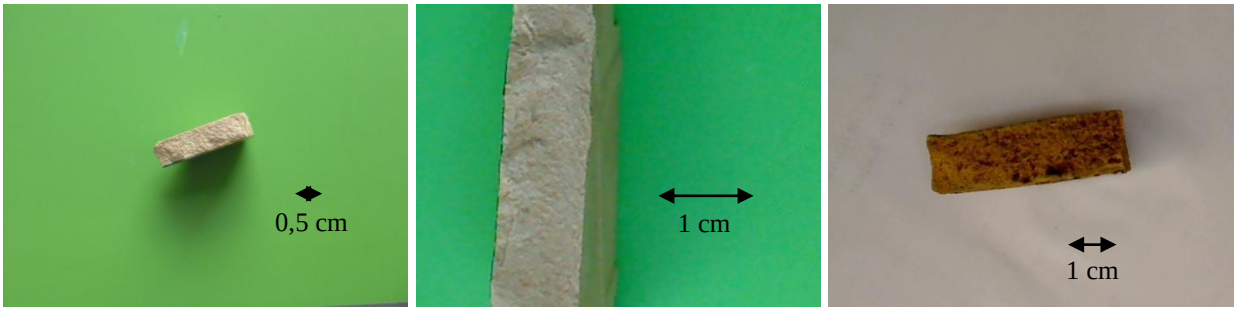

a) RMS-TILE-3 31- 3C: 5. 5 mm b) MSJ-TILE-3 25-REST: 9. 5 mm c) MSJ-TILE-3 25- 3C: 14 mm

Figure 8. Dimension of the samples: a) MSJ-TILE-2-25-REST c) RMS-TILE-3 31-3C and d) MSJ-TILE-3 25-3C

1.1Scanning Electron Microscopy

In the following, for each image of microscopy, the glaze layer is seen on the top and the paste is on the bottom part of the image.

In a morphological point of view, one can make several observations including:
-glaze/interface/paste
-porosity distribution

For each of these categories the four samples are similar. Indeed the three samples MSJ-TILE-3 25-REST, ESG-POT-3 24 and MSJ-TILE-3 25-3C present a well defined interface, without diffusion of the glaze into the paste. This is often interpreted as resulting from a double firing, or can be the effect of single firing when non fritted glazes are used. The paste has been fired before the glaze was applied.
For the sample RMS-TILE-3 31-3C, the interface between the glaze and the ceramic body is not so neatly defined. It can be because of poor regulation of temperature during firing or, in a different way, because reaction of the glaze and clay in the case of a single firing.
One can only give a qualitative description of the porosity as no measures were taken. Regarding size, quantity and distribution of the pores in the four SEM figures 9, one can group the samples (1) with (2) and the samples (3) with (4). The two azulejos 3 and 4 seem to have less but bigger pores

and more heterogeneously distributed than the two other samples. These differences can indicate different production techniques or compositions.

MSJ-TILE-3 25-REST

(1)

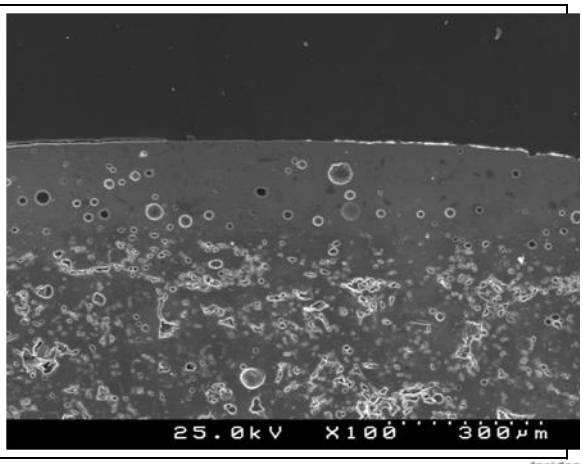

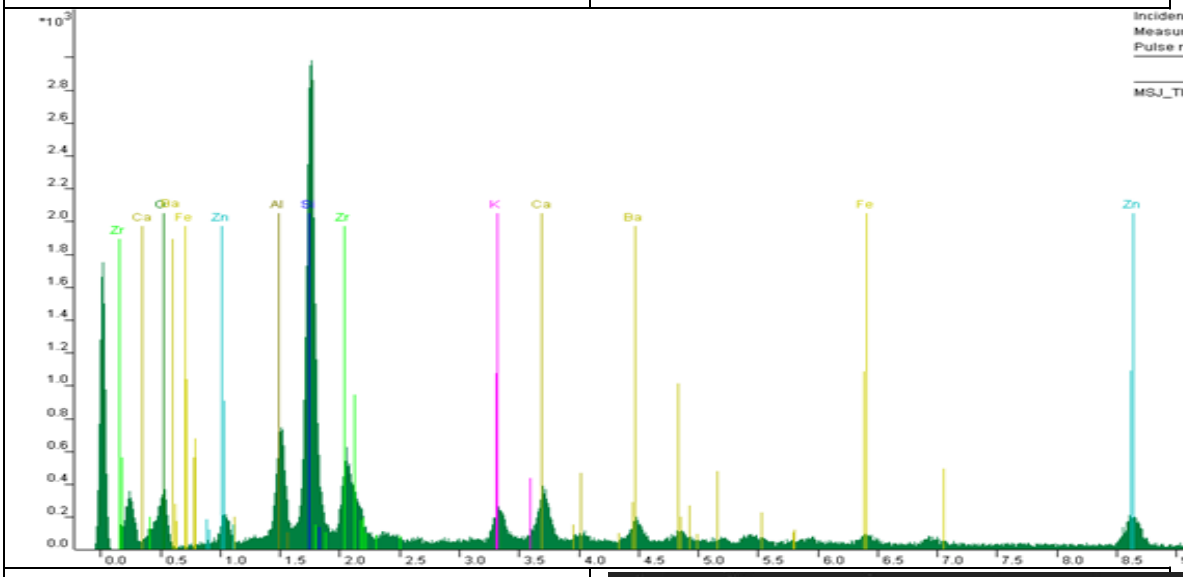

ESG-POT-3 24

(2)

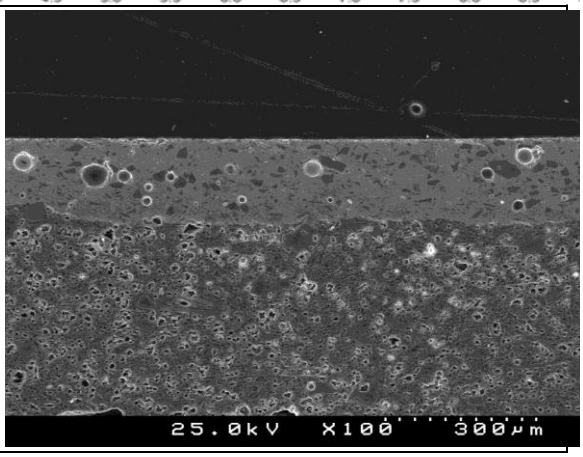

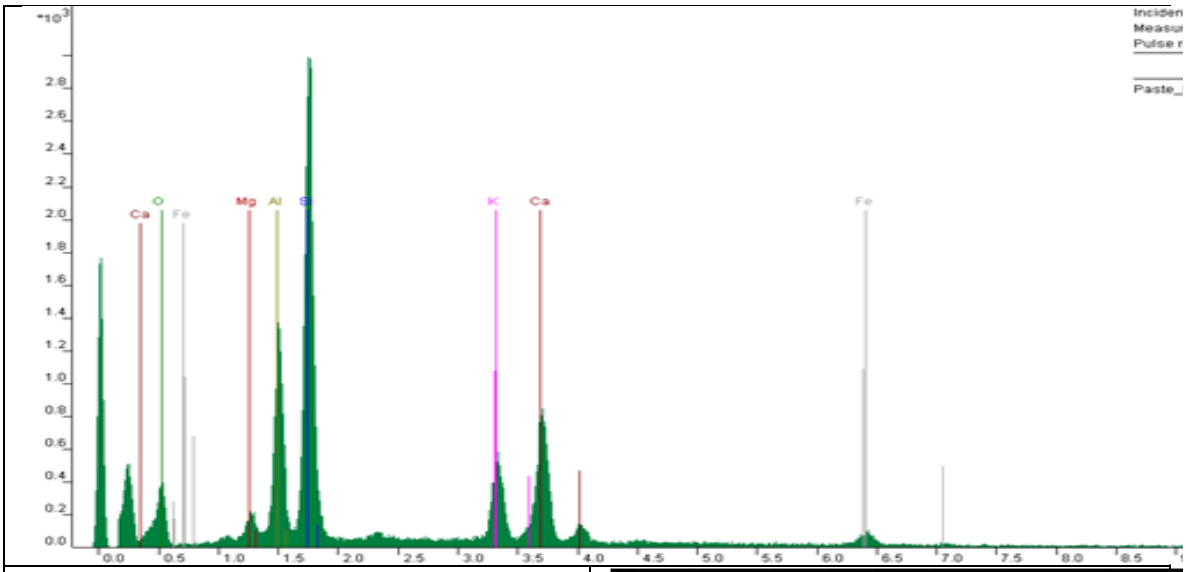

RMS-TILE-3 31- 3C

(3)

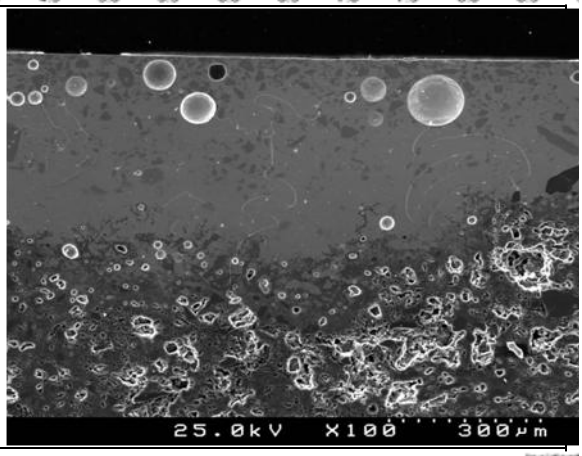

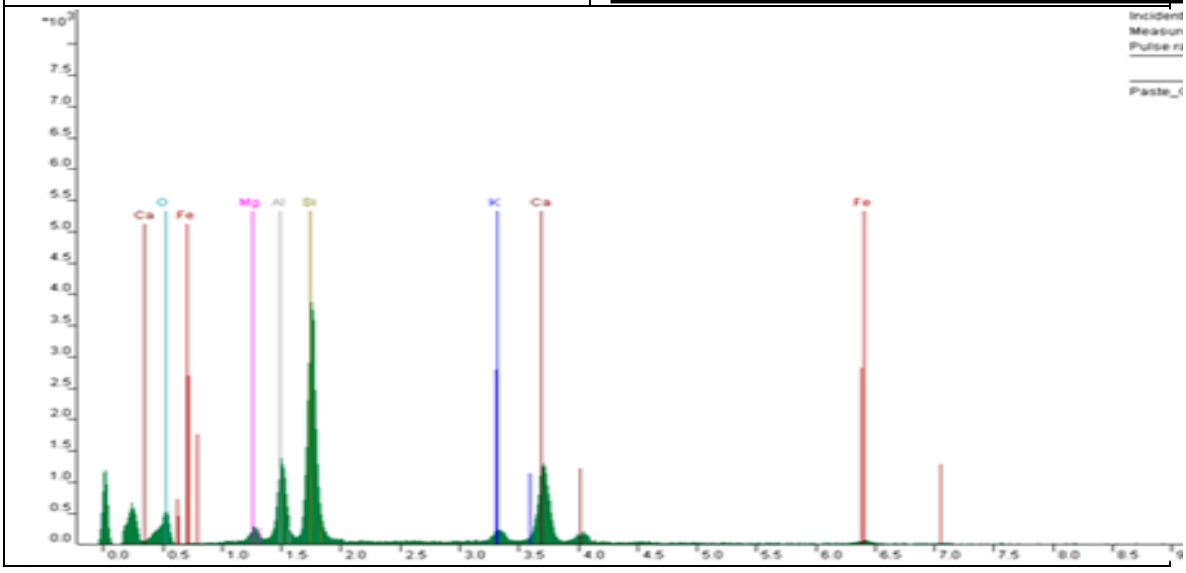

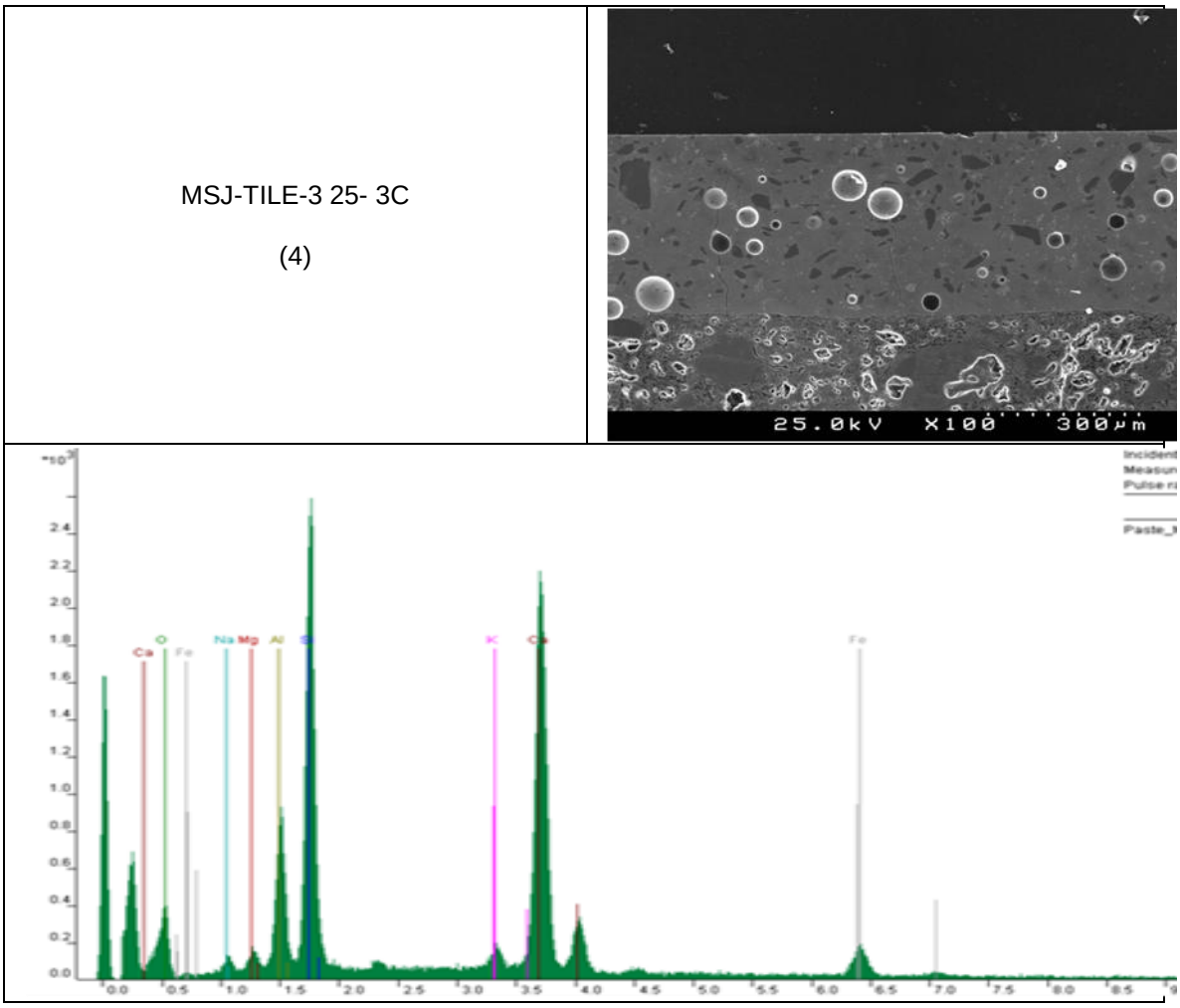

Figure 9. SEM cross-section images and EDS spectra of the paste and glaze of the four ceramic pieces.

The analysis of the paste shows that three samples present the same set of elements. The base of a natural clay, figure 9 and table 2: silicon (Si), calcium (Ca) and aluminium (Al) and common elements present in minerals such as iron (Fe), sodium (Na), magnesium (Mg) and potassium (K), present in hematite, feldspars and other minerals. The differences among these three pastes are derivative proportion of these elements. Sample (4) has a higher level of calcium and more iron than the other two samples.

Sample (1) presents a different composition; with “modern” elements such as barium (Ba) and zirconium (Zr), used to improve the production. These corroborate the thickness and the element of style and shows that this sample is a modern tile from the late 20st century industry.

1.2X-Ray Diffraction

The pastes are mostly composed of silicate derivatives of clay. Above all the intensities, in the crystalline phases in the body one find the silica (SiO2) as the mineral quartz. One also finds more complex silicate minerals such as mullite, diopside, anorthite, gehlenite and albite, table 3. Some of these silicates are the reaction products of others. Indeed, the minerals gehlenite, mullite and anorthite

come from the kaolin, calcite and other mineral of the natural clay (mineral kaolinite, $Al_2Si_2O_5$ (OH) $_4$) as follows:

Table 3. Clay mineral transformation as a function of temperature firing (Cultrone 2001)

MINERALS	TRANSFORMATION	
Metakaolin: $Al_2Si_2O_7$	Temperature of formation: 550-600°C	
Mullite: $Al_6Si_2O_{13}$	Temperature of formation: 1050°C	
Gehlenite: $Ca_2Al_2SiO_7$	Chemical reaction: + Calcium oxide	Temperature= 800°C
Anorthite: $CaAl_2Si_20_8$		Temperature= 900°C

Also important to note is that kaolinite deposits are associated with quartz and non-decomposed feldspars.

Some silicates are linked too: anorthite and albite for example. Both are part of the plagioclase solid solution series one in the calcium-rich end member (anorthite) and the other in the sodium-rich end member (albite: Na (Si_3Al) O_8), figure 10.

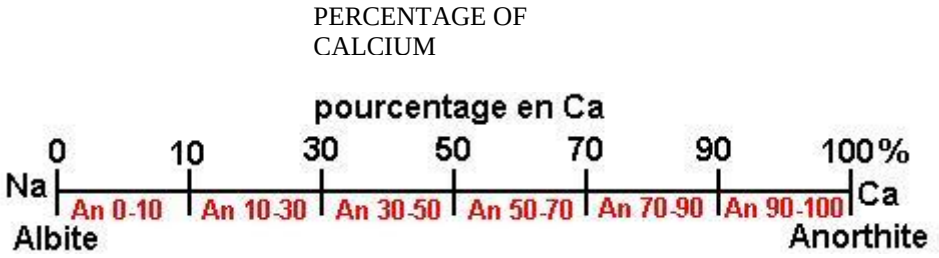

Figure 10. Scale of albite transformation into anorthite state in function of the fraction of calcium (www.minerals.net/mineral/plagioclases.aspx)

Most of these elements are not pure but combined with other elements such as magnesium, sodium, iron, potassium, with traces of titanium and manganese.

Regarding the different spectra, figure 9, one can say that the most recent the ceramics are, the simplest their phases composition is, table 2. That retrieves information about the selection of raw materials (purity of the clay) for the body and control of reactions during firing (in line with the actual mastering of these technologies).

In the case of sample (1), one can say that the clay used was probably kaolin with high purity kaolinite, fired around 1050°C as mullite is the only silicate present. While sample number (3), contains three derivatives of the kaolinite that shows either wider span of temperature or heterogeneity of composition. The presence of calcite in the composition indicates a low firing temperature and the broad phase composition corroborates the use of less pure clay.

XRD	composition
MSJ-TILE-3 25-REST (1)	
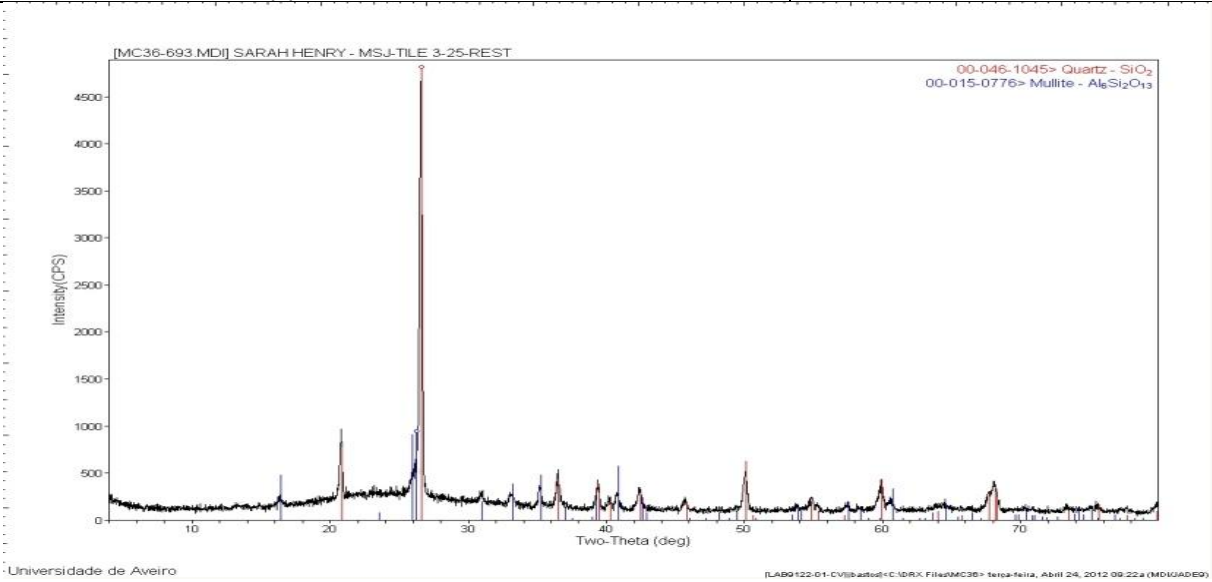 - Quartz: SiO_2, Mullite: $Al_6Si_2O_{13}$	
ESG-POT-3 24 (2)	
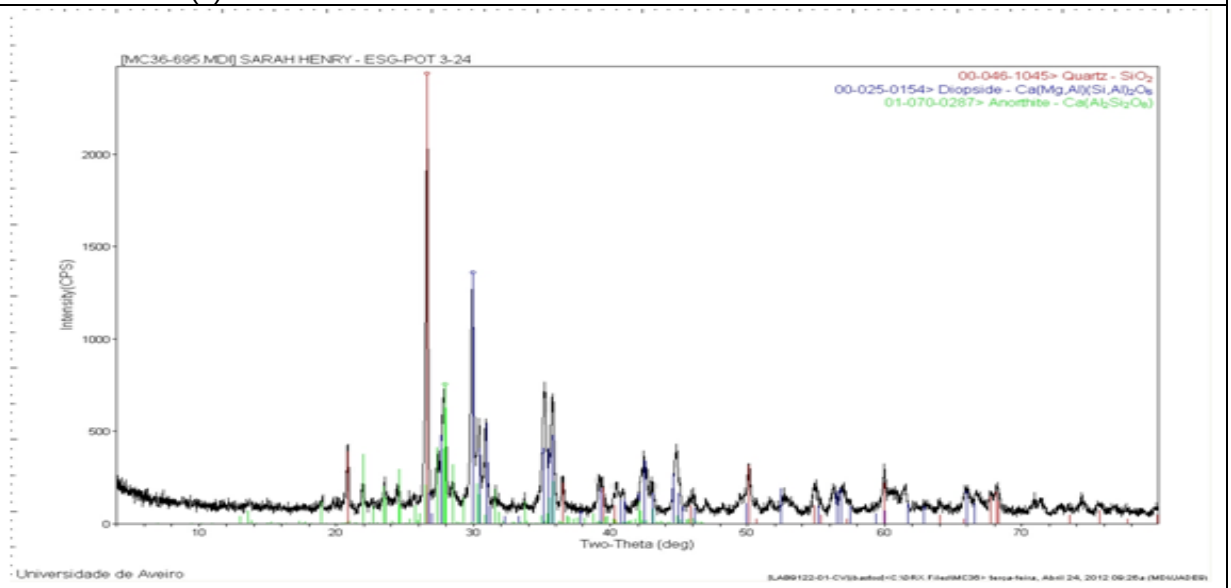 - Quartz: SiO_2, Diopside: Ca $(Mg,Al)(Si,Al)_2O_5$, Anorthite : $Ca(Al_2Si_2O_8)$	
RMS-TILE-3 31- 3C (3)	

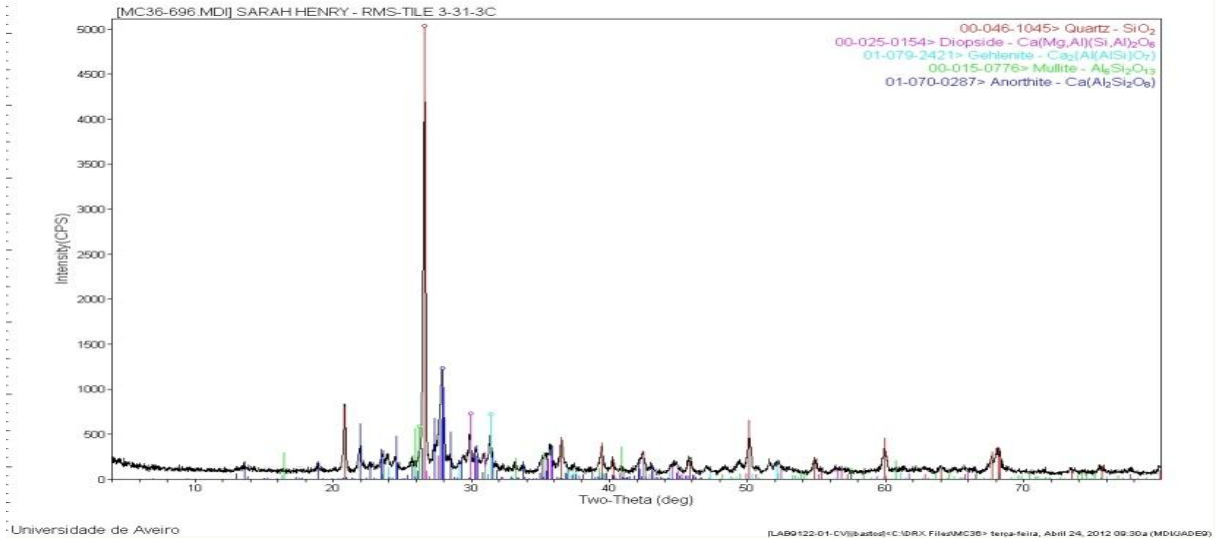

- Quartz: SiO_2, Diopside: Ca (Mg,Al)$(Si,Al)_2O_5$, Gehlenite : Ca_2 $(Al(AlSi)O_7)$, Anorthite : $Ca(Al_2Si_2O_8)$, Mullite: $Al_6Si_2O_{13}$

MSJ-TILE-3 25- 3C (4)

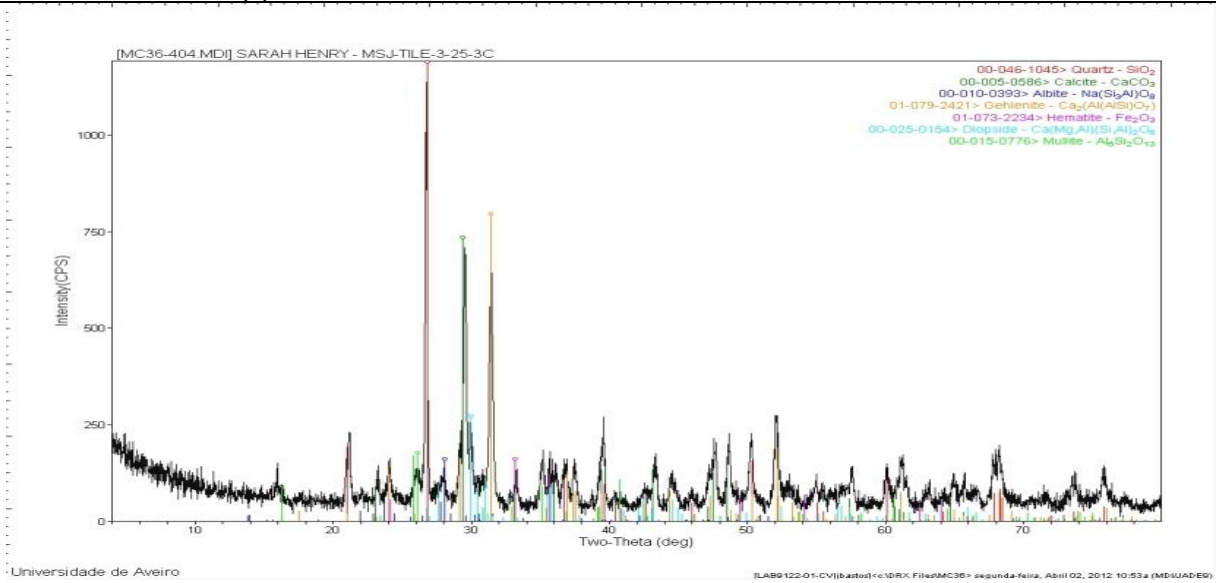

- Quartz: SiO_2, Calcite : $CaCO_3$, Albite : $Na(Si_3Al)$ O_8, Gehlenite : Ca_2 $(Al(AlSi)O_7)$, Hematite: Fe_2O_3, Diopside: Ca $(Mg,Al)(Si,Al)_2O_5$, Mullite: $Al_6Si_2O_{13}$

Figure11. X-ray diffraction results of the samples pastes

2. The glazes

2.1Scanning Electron Microscopy

In the SEM microscopy of the glazes, two kinds of surfaces were analyzed: (a) the cross-section where the samples were cut in two parts in order to give access to the glaze and to the paste, and (b) the face of the glaze surface to access to the different part of the glaze (drawings, coloured areas…).

2.1.1*Cross-sections*

Glazes are calco-sodic siliceous and silica lead glazes. All samples present silicon (Si) and calcium (Ca) but only the samples (2) and (4) have sodium (Na) in sufficient quantity to appear in the spectra. The silicon is the main constituent of the glazes and it becomes the element with the highest intensity with EDS.

One find lead (Pb) and zinc (Zn) in sample 1 and 3 that are silica-lead glazes. These two fluxing elements are used in order to give to the glaze one particular melting point. The study of the ratio Si/Pb gives information about the viscosity of the glaze; the higher the silicon rate, the higher the viscosity, the lowest the fusibility is.

Another category of common used elements are the opacifiers; making the glaze not transparent. In the samples one found the two kinds of opacifiers: in the samples (1) and (3) the zirconium (Zr) and in the sample (2) the tin (Sn). The absence of any opacifier in the sample (4) can be explained by the heterogeneous repartition of tin as opacifier.

Other elements that were also found in the glazes can be explained by diffusion from the paste (Al, Ba) or from the colouring ingredients (Fe).

With their “common” composition and their higher content of lead samples (2) and (4) follow the oldest formulation of glazes were the silica lead glazes in adapted to the thermal expansion of calcia-rich paste (Figueiredo, 2009).

Cross-section	EDS general
MSJ-TILE-3 25-REST (1)	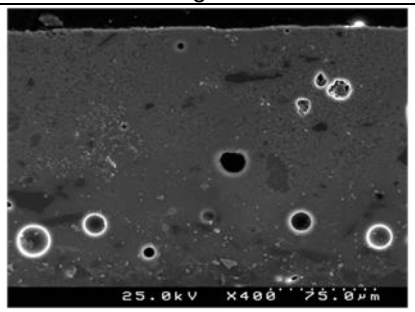

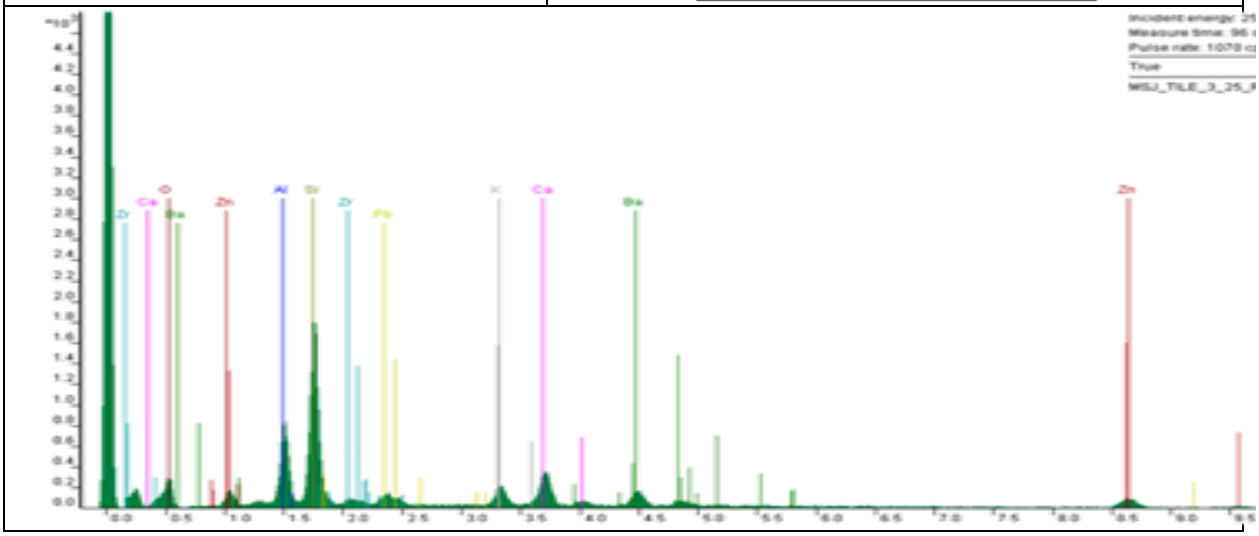

ESG-POT-3 24 (2)	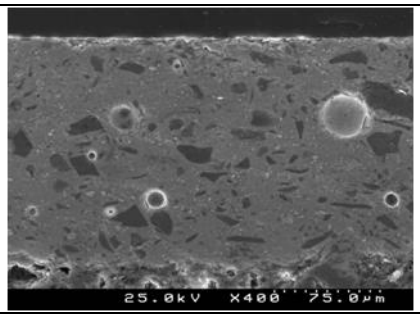
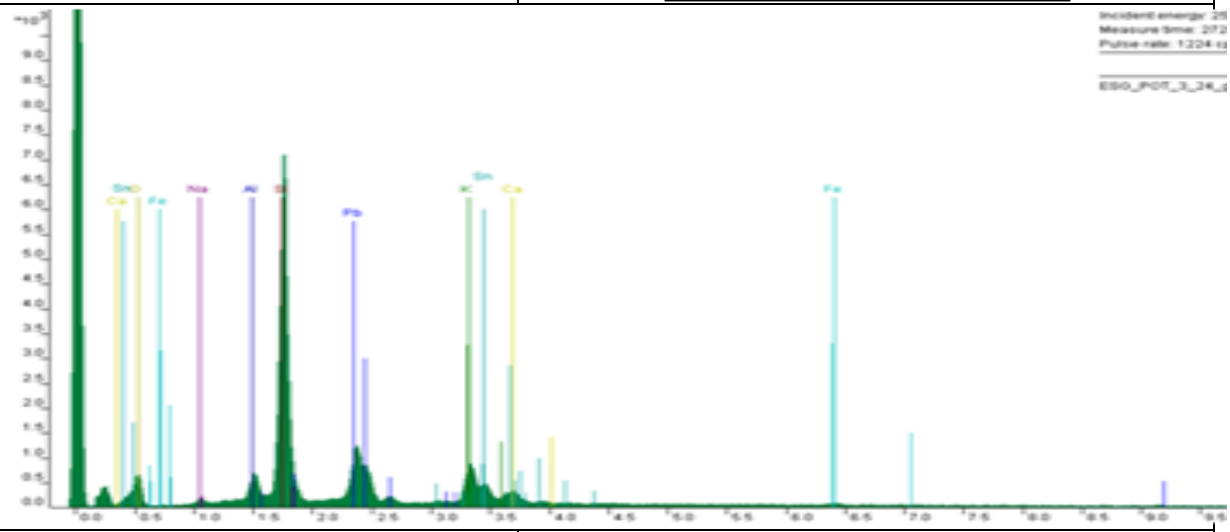	
RMS-TILE-3 31- 3C (3)	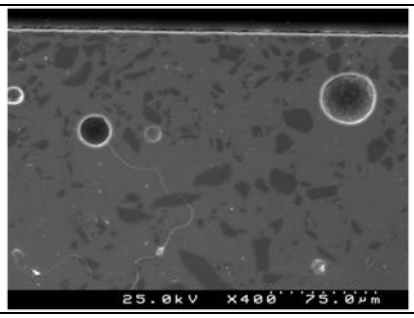
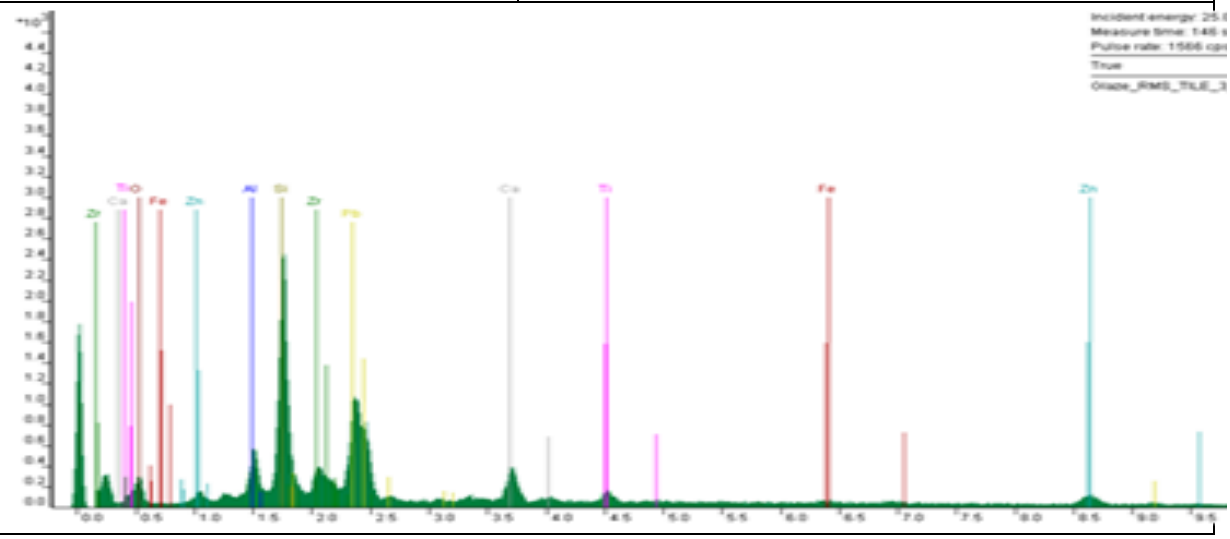	

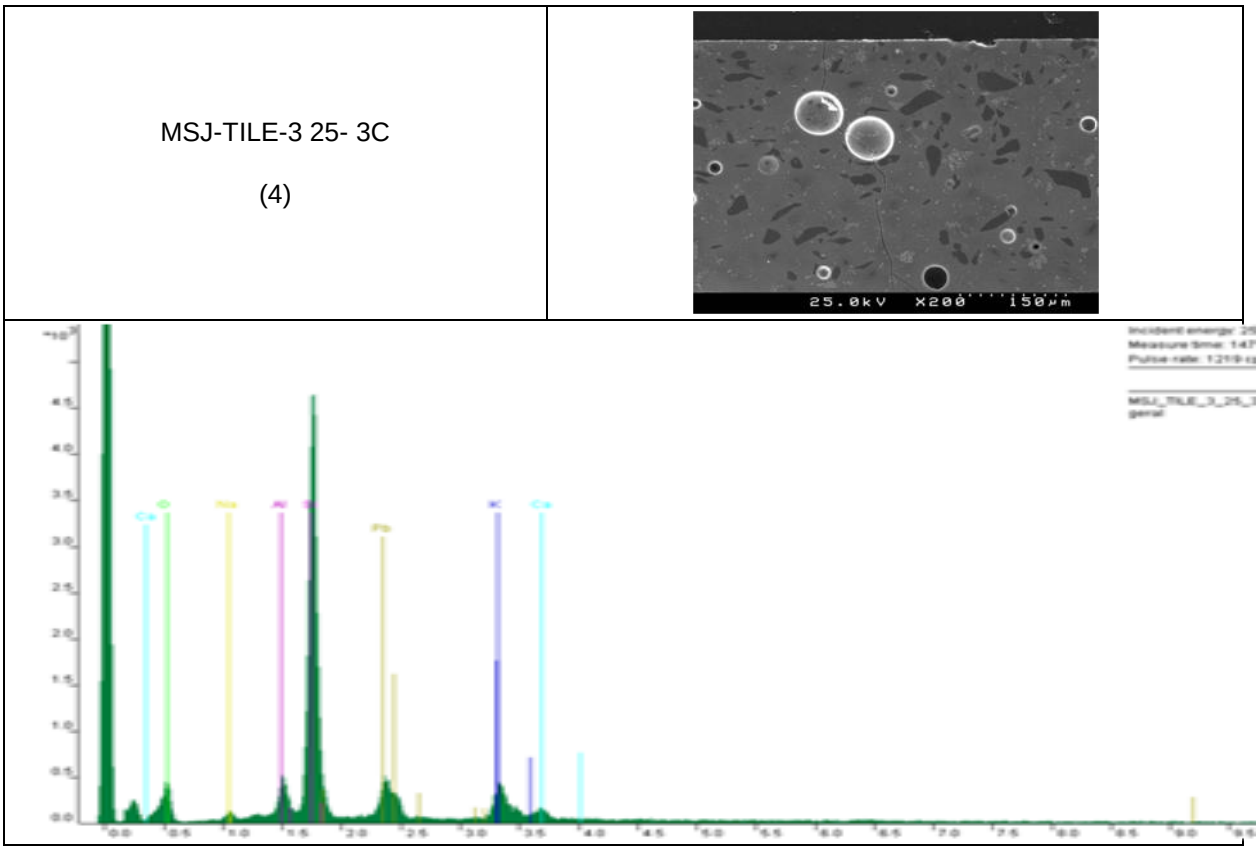

Figure 12. Images obtained with SEM and EDS of the glazes samples

With respect to the morphology of the glazes, one can say that the glaze of samples (2), (3) and (4) have the same aspect with a homogeneous distribution of dark inclusions (SiO_2) and also of white grains (explained in the following). The white grains and the black inclusion present in the sample (4) are unequally dispersed in the glaze. Whereas the black inclusions are in all the samples made of quartz (SiO_2); the white grains have different compositions. EDS analysis of the white precipitates of sample 3 supports the composition as based on zinc.

One can see an evolution between those three samples in figure 13: the white grains of the opacifier of sample (1) and (2) have a circular shape, the white grains of sample 2 being more markedly packed. The sample (4) has opacifier grains of a total different shape; they are circular and clusters in circles. This morphological difference can be explained by difference in composition and firing conditions.
The opacifier regions of sample (2) and (4) have similar composition with tin.

The crystalline inclusions of white contrast of sample (1) figure 13 are composed of many different elements some already found in the corresponding cross-section EDS spectrum, figure 12. The presence of zinc and zirconium as the main opacifiers is matched by equal amount of cobalt and chromium and iron that are the base of the colouring pigments (blue and dark blue).

samples	White grains-SEM
MSJ-TILE-3 25-REST (1)	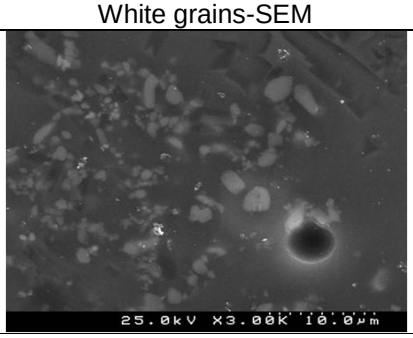
	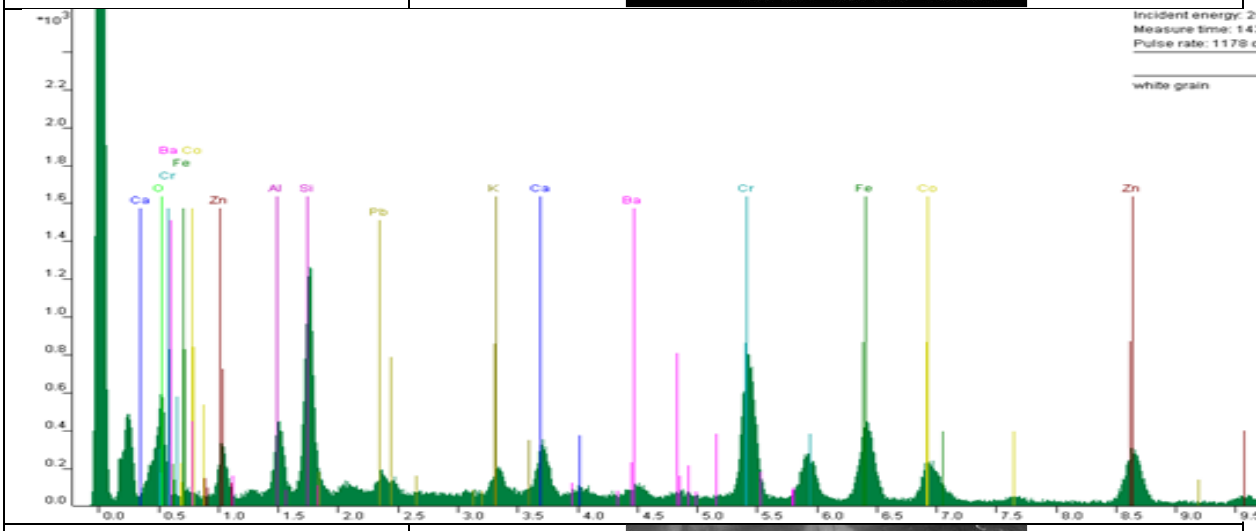
ESG-POT-3 24 (2)	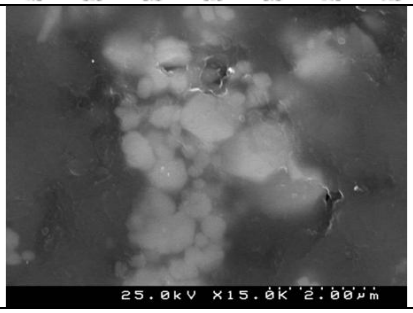
	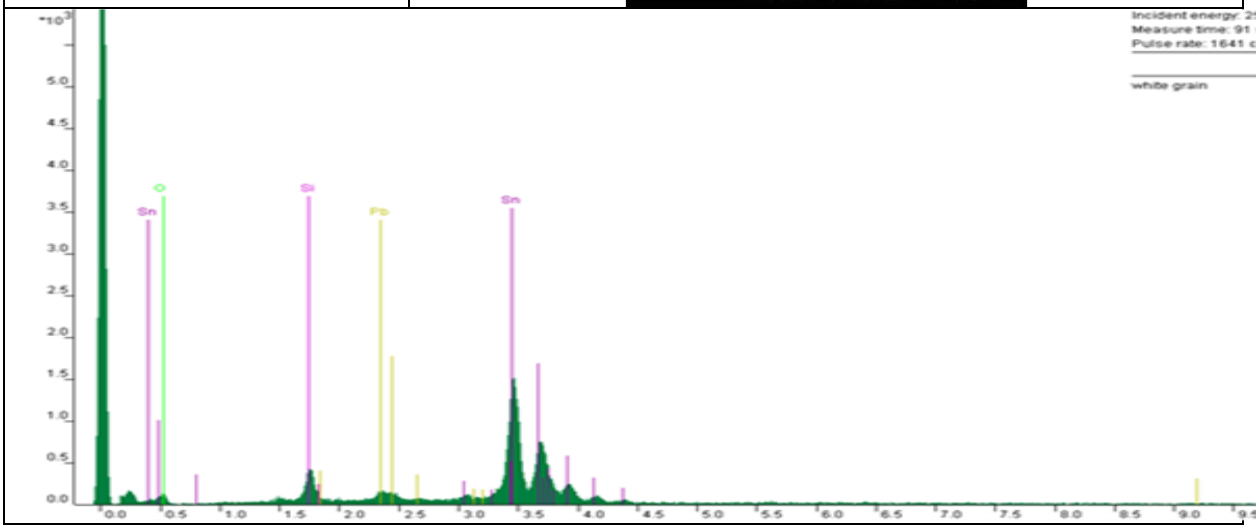

MSJ-TILE-3 25- 3C (4)		

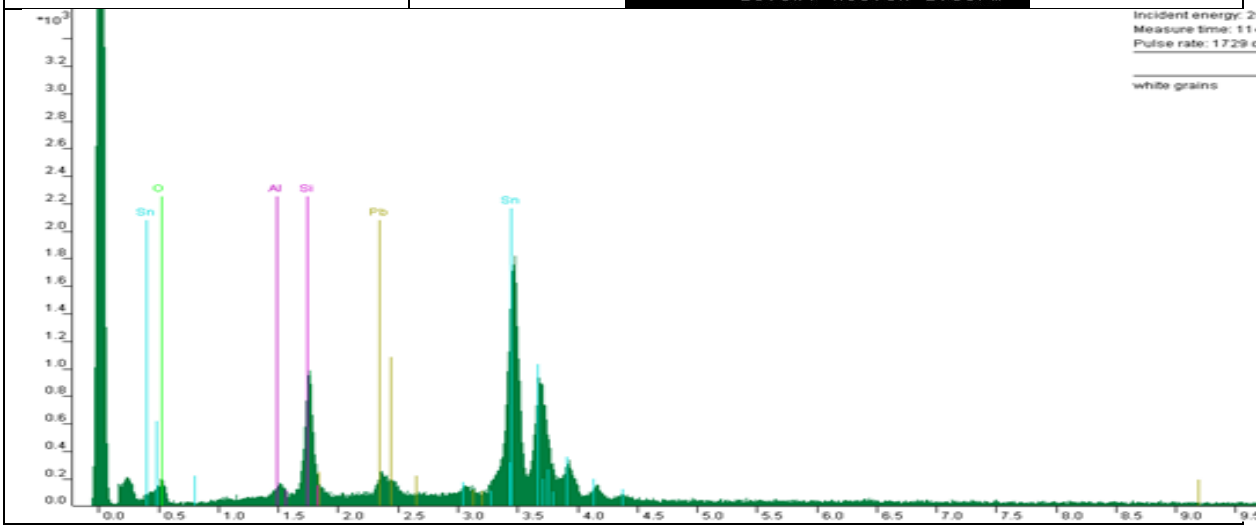

Figure 13. White crystals images obtained with SEM and EDS of the glazes samples

2.1.2 *Face*

The scanning images of the face in figure 14 are used to establish the composition of the different coloured areas or drawings of the glazes (the corresponding EDS spectra are found in Annex 1).

The EDS of the samples (2) and (3) show the same composition as in the analysis made in cross-section, the case being different for the sample (1) and (4), figures 12 and 13. The SEM analyses of the glaze surface of sample 2 and 3 might have missed the coloured areas.

The sample (1) has three distinct zones (see figure 14). The zone with the line seen figure 7-a (probably painted) has the same composition as the glaze. The second zone with the deep blue has coarse quartz inclusions figure 14. One can say that the titanium, the lead, the iron and the barium are coming present in the deep blue zone with a rough surface and less shining aspect.

sample	surfaces		
MSJ-TILE-3 25- REST (1)	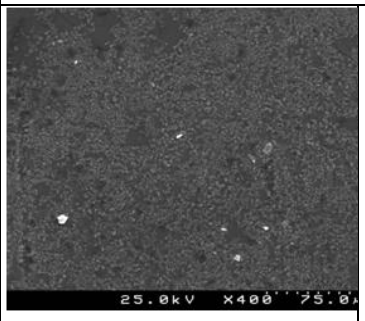	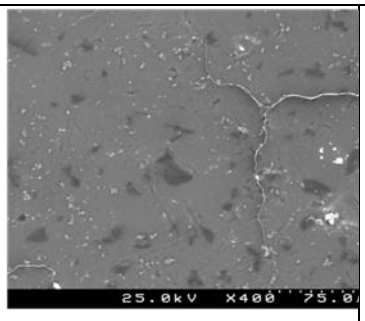	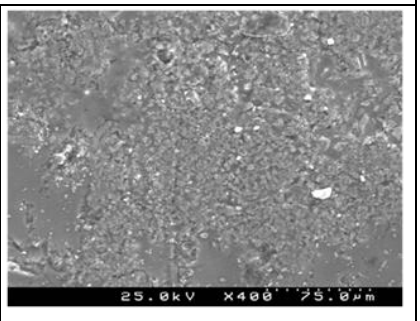

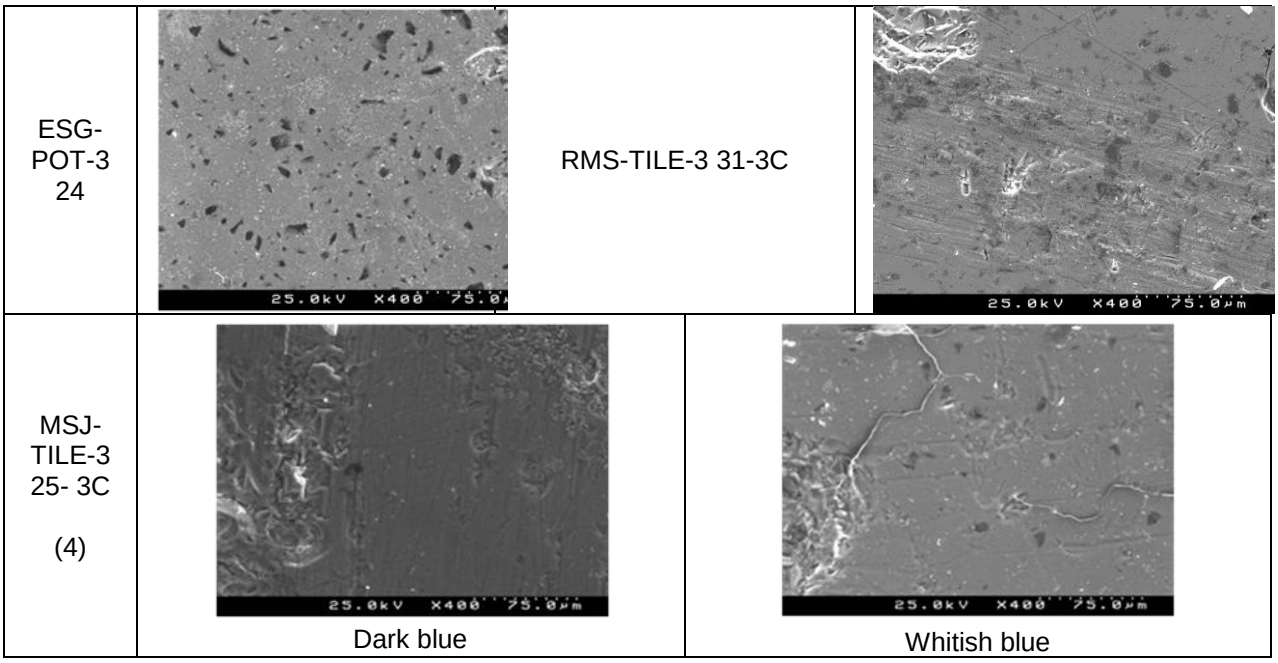

Figure 14. Face images obtained with SEM and EDS of the glazes samples

Of the sample (4), only the dark blue and the whitish blue part of the glaze were analysed. The places where EDS were taken in the bluish white area shows the regular elements found in the cross section of the glaze added with cobalt, nickel, iron and antimony. Besides the blue colouring, the yellow colour linked to Sb may have also diffused to that point. Cobalt oxide is the most common pigment used to make the blue colour.

3. Conclusion

The SEM/EDS and XRD analyses show different composition and morphology of the four samples. Because of complex composition, thickness and decoration style and the presence of modern elements (barium…) one can say that the sample (1): MSJ-TILE-3 25-REST and (3): RMS-TILE-3 31-3C are the most recent tiles of this series. On the contrary, the not so precise composition the sample (4), its thickness and the blue-yellow colouring on white glaze (Basso, 2009) indicates that it is from older sample. It is more difficult to set the age of sample (2: ESG-POT-3 24; it has tin as opacifier.

Chapter 4 – Mértola samples

"cuerda seca"-X-XIIIth centuries

1. Historical context

1.1 “Cuerda seca”

1.1.1 *Technical characteristics*

The “cuerda seca” technique as part of the glazed decoration styles has some specific characteristics that make the difference. There are different ways to make a glazed decor: the decoration made of paint or glaze can be covered by a transparent glaze or applied on the (opaque) glaze, but after firing, glaze and decoration always become just one vitreous layer. One finds this technique on green and manganese decoration. That is the main difference with “cuerda seca”.

In “cuerda seca” decoration, all the surface of the ceramics presents a décor made of painted lines and glazes directly applied on the clay body. There are two types of “cuerda seca”: partial “cuerda seca” where the biscuit is visible and the total “cuerda seca” where the decoration covers the entire surface of the piece. A black line surrounds the drawings and is used to separate apart the different colours of the glaze and prevent their mixing. The line is directly applied on the clay and after firing it is not glazed which differs from the green and manganese decoration technique. The line was made of a mixture of manganese oxide with a blend of animal and vegetal fat that burnt during firing, leaving a black mark. After firing, the coloured glazes, mostly of lead-silica type, become vitrified, but not the “cuerda seca” line, that giving to the décor a relief aspect (Claire Déléry, 2006).

1.2 Decoration

1.2.1 *Glaze*

Glazes are important sources of information to study the evolutions of “cuerda seca” potteries throughout time. Indeed, glazes present different behaviour depending on their composition that varies from one colour to another.

Claire Delery (2006) provides additional details about the different types of glaze in use and their firing.

Glazes are composed of silica, which is vitrified at very high temperature. Fluxing agents such as PbO are mixed with silica to decrease glass melting point. The role of added glass modifiers (Na, K, Ca) is to stabilize the non-vitrifying components. Other metal oxides such as ZnO or PbO are also in use to give the glaze a specific melting temperature. Finally, the addition of opacifiers such as tin oxide makes the glaze non-transparent.

The Si/Pb ratio is systematically calculated as it gives information on the viscosity of the glazes. Indeed, when this ratio is higher than 1, the silicon content is higher than that of lead and the viscosity of the glaze increases. On the contrary, the higher the lead content is the lower the viscosity of the glaze is and more likely the risk of spillage of the glaze over “cuerda seca” lines. During firing, some

elements, including lead, evaporate modifying the original composition of the glaze. In addition, lead has the tendency to migrate to the clay body and Si, Al, Ca to the glaze. This exchange modifies the viscosity and the melting temperature of the glazes with firing time (Déléry 2006).

“Cuerda seca” glazes are typically composed of three colours: white, yellow and blue-green plus the black for the “cuerda seca” lines themselves. For each colour, the compositions of the glazes vary with addition chromogen ionic compounds. The greens are obtained by adding copper and iron / or just copper (Claire Déléry 2006). The dark green can be obtained by increasing the amount of iron or by increasing the thickness of the glaze. The turquoise is obtained with copper, iron and tin, the late being an opacifier. The natural green and dark green are obtained by varying the proportions of copper and iron respectively (~ 2% and 3% and 3% and 1%). The yellow or honeys are tin free glazes coloured with antimony or iron from clays and manganesium. The whites are obtained through a high tin content in the absence of chromogen ions.

1.2.2*Firing*

The potteries can be fired in two different processes, the single step firing and double firing. The double firing process is done in two steps: the ceramic body is first fired without the glaze and second time fired with the glazed decoration. While in single firing, the ceramic with glazing applied on the dried body is fired in just one high temperature cycle. Single firing is usually dictated by economic savings.
The firing process is an important part of production of ceramics as it leads to differences not just in morphology but also in chemical composition of the glazed layers. Indeed, with double firing potters obtain an interface around 20 and 30 µm, whereas with single firing with fritted glazes the interface obtained is wider, between 70 and 100 µm. In the second case, the interface becomes enlarged by the precipitation of several phases due to the reaction between the ceramic body and the glaze (Claire Déléry 2006).

Differences in firing process also lead to differences in colors; clays may contain iron which gives different colors according to the temperature, time of exposure to heat, oxidizing/reduction in the furnace atmosphere and the presence of other elements (Ca, Ti, ...) that change redox conditions of the material. Therefore, one can observe that ceramics coming from double firing are clearer than in single firing due to a lower oxidation state of iron (Claire Déléry, 2006).

2. Samples

The panel is composed of six samples from between the XIth and XIIIth centuries of the archaeological site Mértola. The pieces were found under a Christian cemetery and a sceptic pit.
Four of the samples are partial “cuerda seca” and the remaining ones are total “cuerda seca”.

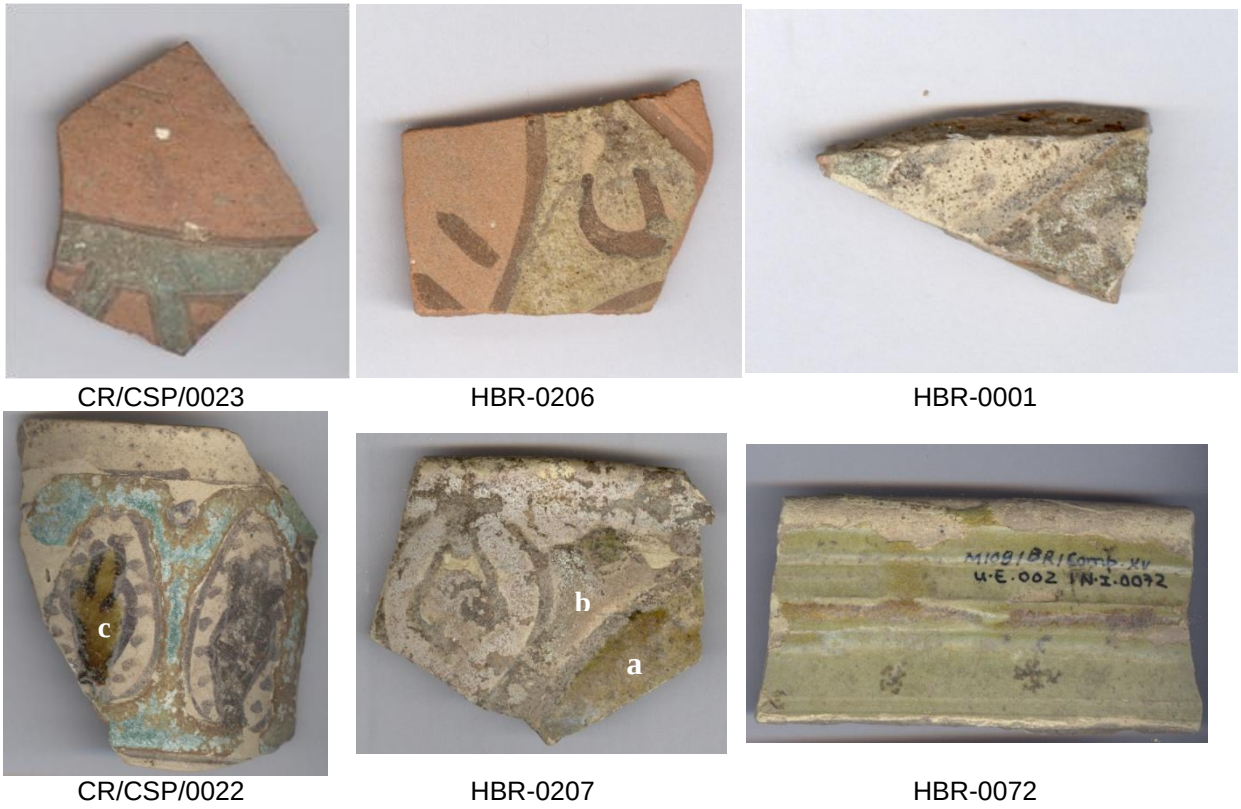

Figure 15. Optical pictures of the six cuerda seca samples

The samples CR/CSP/0023 and HBR-0206 are partial “cuerda seca”. The glaze of sample CR/CSP/0023 is a blue/green glaze delimited by perfect black lines of “cuerda seca”. In spite of the similarities of the perfectly drawn black line of “cuerda seca”, the sample HBR-0206 seems to have a different glaze. The glaze of this sample has a white/green color that seems to be over-fired (rough surface) while the firing temperature of sample CR/CSP/0023 seems to be better adjusted to the glaze.

The sample HBR-0001 is partial “cuerda seca”. The glaze of this sample is in a higher state of degradation than in the two previous samples. The “cuerda seca” is still visible but it is difficult to determine the differences in the color of different glazed areas. Close inspections indicates that the glaze is made of two colors, green and white, separated by “cuerda seca” lines.
HBR-0207 is a total “cuerda seca” and HBR-0072 presents a brown line-like contrast on the circumference relief. The piece HBR-0072 (probably a “jarred”) is covered by a homogeneous green glaze and separated in two areas by a brownish line. The decor of sample HBR-0207 is composed of areas of white and a green glazes separated by “cuerda seca” lines. The difference between the vitreous green (a) and the other zones in green (b) can be explained by the advanced alteration state or because the piece actually has glazes of two different compositions.

Sample CR/CSP/0022 (figure 15) is the whitest piece of the set in visual inspection and also the one of more elaborated drawings. The clear color of the clay surface can come from the kaolinite or derivate materials (3. 2).

The piece CR/CSP/0022 is a partial “cuerda seca”. The drawings of the pottery piece are well preserved. One can observe the lotus flower in the middle of circles (c) and palms separating these elements, the glaze being properly surrounded by “cuerda seca” lines. The glaze seems to be composed of three colors: the blue/green of the palms, the vitreous green in one lotus flower and the black area of the other flower. One is not sure about the black color of this second area; it may come from a firing or glazing accidents, or might have been intentional with some aesthetic purpose.

3. Results

In the following, the results of the study of six samples will be divided into three parts. The EDS analyses showed important quantities of phosphor in the glazes under different forms. Phosphor may lead to a phase separation in the glazes depending on the content in silicates versus phosphorous/lead/calcium phases. The phosphorous phases are characterized by specific ratio of the Pb, P, Ca ions. Two types of morphology were identified.
Therefore, the samples were regrouped by their similarities of morphology phosphor containing areas of their glazes: the samples CR/CSP/0023 and HBR-0001 are grouped together because they showed a visible stratigraphic effect, the samples CR/CSP/0022 and HBR-0206 because of spheres that look like precipitates of phosphorous matter and finally, the samples HBR-0207 and HBR-0072 with their phosphorous sediment layers on the surface of their glazed layers.
It is generally accepted that the phosphorous matter in archaeological ceramics comes coming from runoff water (Clare Déléry, 2009). However, from the results obtained here one may wonder if bone ashes as raw material for low melting point ceramic glazes were already in use. From such perspective, the distinction between technical phosphor and phosphate sediments could be made.

The figures were taken by SEM microscopy with different magnifications. The magnification of each SEM image is indicated below the figure [example: x400]. For each samples several images of the different zones of the samples were taken (tables 18, 19, 22, 23, 24 and 25).
Some of the SEM images were taken in facing (showing only the surface of the glaze) and the others in cross-section (showing the inside of the glaze of the paste). Sometimes, one image corresponds to several EDS spectra because it shows diverse interesting details.

Results of XRD analyses for each of the six samples are given in table 4. These results will be commented in the following subsections of this chapter.

Table 4. XRD of the pastes of the six samples

Sample paste	quartz	diopside	anorthite	augite	gehlenite	mullite
CR/CSP/0023	x	-	x	-	x	x
HBR-0001	x	-	x	x	x	-
CR/CSP/0022	x	-	x	x	x	-
HBR-0206	x	-	x	-	x	x
HBR-0072	x	x	x	x	-	-
HBR-0207	x	-	x	x	-	-

3.1 Colorimetric analysis of the paste

3.1.1*UV- spectroscopy*

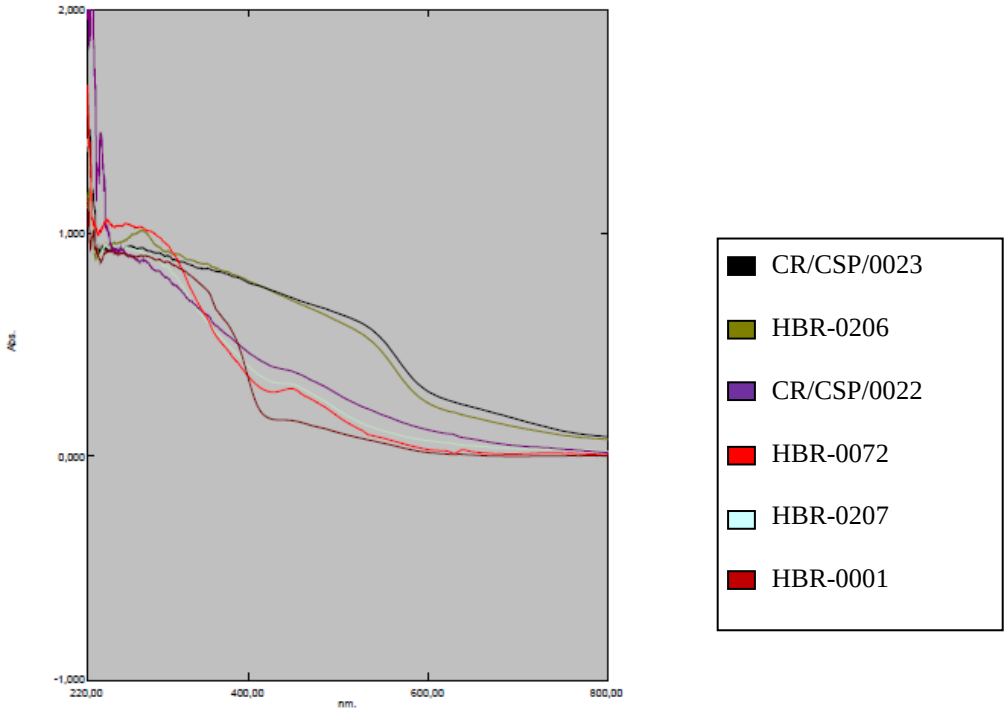

Figure 16. Ultra-violet spectra of the samples CR/CSP/0023, HBR-0206, CR/CSP/0022, HBR-0072, HBR-0207 and HBR-0001

The spectroscopy was used to determine region of absorption of the samples. It allows one to know if the samples have the same color or not, but does not give the exact color.

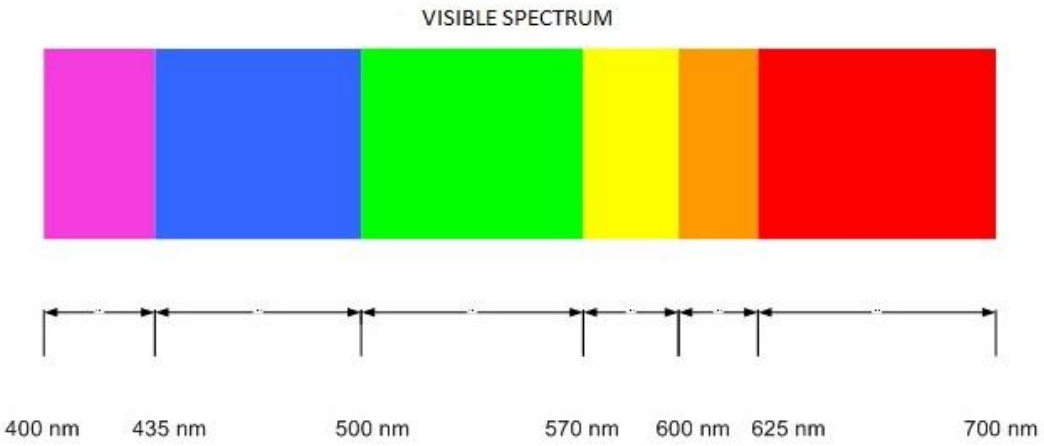

Figure 17: electromagnetic spectrum corresponding to the visible range

According to the visible part of the spectra in figure 8, one can see three categories of samples with:
- absorption around 600 nm corresponding to orange/red,
- absorption around 500 nm corresponding to green/yellow,
- absorption around 400 nm corresponding to pink.

3.1.2*CIEL*a*b* coordinates*

For present study, color of the pastes of six samples was analysed in order to understand links that could exist between them and be able to group samples.

Table 5. Results of the CIELab analyses of color of the ceramic bodies of the archaeological samples

	HBR-0072	HBR-0207	CR/CSP/0022	HBR-0001	HBR-0206	CR/CSP/0023
L*	79.92	97.33	50.11	55.49	51.67	55.76
a*	-4.96	-4.77	-2.39	5.43	10.25	9.10
b*	27.26	27.01	18.14	22.89	27.28	25.83

Samples HBR-0206 and CR/CSP/0023 have close chemical compositions (see XRD analyses in table 4). As they also have similar a* and b* coordinates (giving the color) but slightly different luminance; we can assume that the sample HBR-0206 of lower L* was fired at higher temperature than the sample CR/CSP/0023 of higher L*. This hypothesis will be investigated with the help of XRD results below.

According to the CIELab coordinates scheme and with the direct observation of the samples, one can say that the pieces CR/CSP/0023 and HBR-0206 (figure 15) are made of red clay. Red clays are usually composed of high proportions of hematite and calcite. To determine their composition, the ceramic bodies were studied by XRD and SEM, this results being presented below in the part (3.2/3).

The CIELab coordinates scheme shows that the sample HBR-0001 (figure 15) has a pinkish component of color. This result is interesting because in the visual inspection the surface of the

ceramic body looks whitish. The color determined by color spectrometry can be again explained because of its content in iron, as seen in the following (3. 2).

The results of color analysis of the paste of the samples HBR-0207 and HBR-0072 (figure 15) show greenish components integrating their colors. Such colors are coming from the mixture of the koalinite clay with added elements (see 3. 3).

3.2CR/CSP/0023 and HBR-0001

3.2.1*Microscopy*

These two samples show a specific glaze morphology that forms fine bands or a “stratigraphy” as shown in the following.

For the sample CR/CSP/0023 the selected images in figure 18 show:

- in figure A, the paste and the distribution of pores of the paste. The EDS of the paste detected the presence of elements of main silicates, namely kaolin, and iron.

- in figure B, in a general view of the glaze taken in cross-section is shown. This image can be split into three parts: the interface (in grey above the ceramic body), some black inclusions and the grey matrix. The composition at the interface corresponds to a regular silica-lead glaze base with tin oxide as opacifier (silicates, lead, calcium and tin) [table 7]. Besides tin oxide, precipitates of lead and calcium compounds are usually use as opacifiers and correspond to the white crystals. The sample shows also small proportion of copper (1, 5% and 2, 7%) homogeneously distributed in the glaze corresponding to the pigments that yield blue colour to the glaze. The big black inclusions at the top (1) of the glaze and the two other elongated (2 and 3) in the middle are quartz grains. The two others parts (grey matrix and black zones) are detailed in figures C, D and F.

- in figure C, details the top of the glaze are shown. One can see at the top of the image “lines” detailed and analyzed in the figure E, the dark grey zone being detailed in the figure D and the grey matrix detailed in the figure 18-F.

- in figure D, the dark grey zone has the same composition [table 6] as the glaze in general (silicates, iron, copper from the pigments, lead and tin as main opacifier). The absence of phosphor in those zones is noted; that may correspond to a part of the glaze blend that did not react with phosphor because of a heterogeneous mixing of the powders or because the glass may tend to separated into different glassy phases during firing.

It is interesting to note that the composition at the top of the glaze layer (figure E) and the composition of the glaze (figure F) are the same. The same ratio Pb/Ca/P [table 7] is determined in these two parts

of the glazed layer. Nevertheless, the matrix does not show the same morphology of stratigraphy observed at the top. The only difference that can be reported is a different Si to Pb ratio [table 7] which is 60% higher than in the case of the area with stratigraphy.

CR/CSP/0023

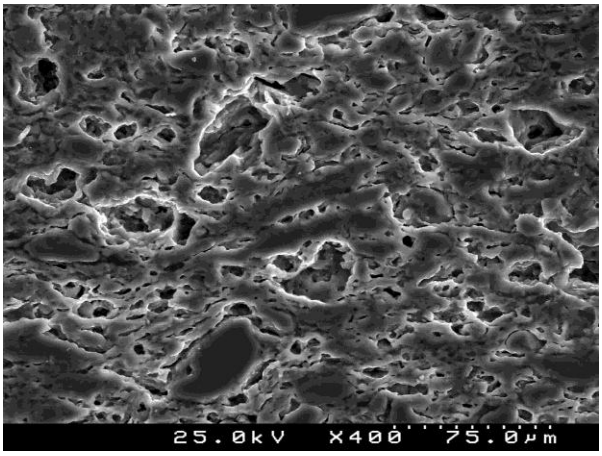

A: cross section SEM= paste

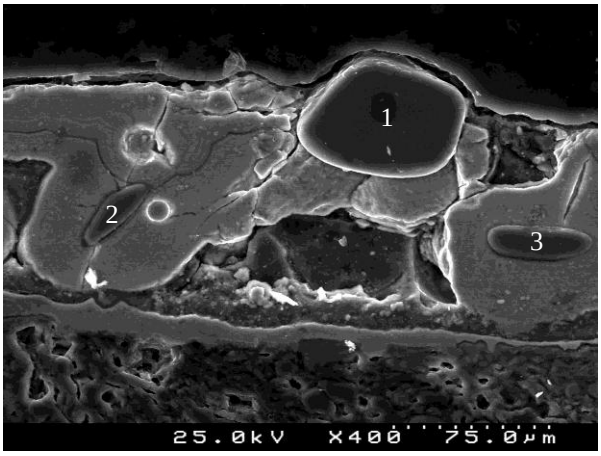

B: cross section SEM=general glaze

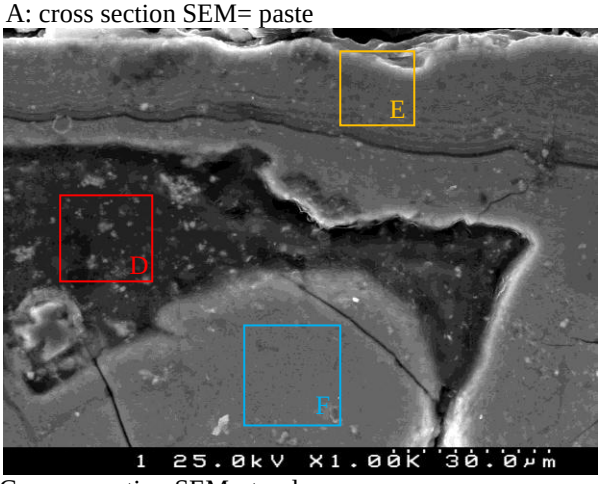

C: cross section SEM= top layer

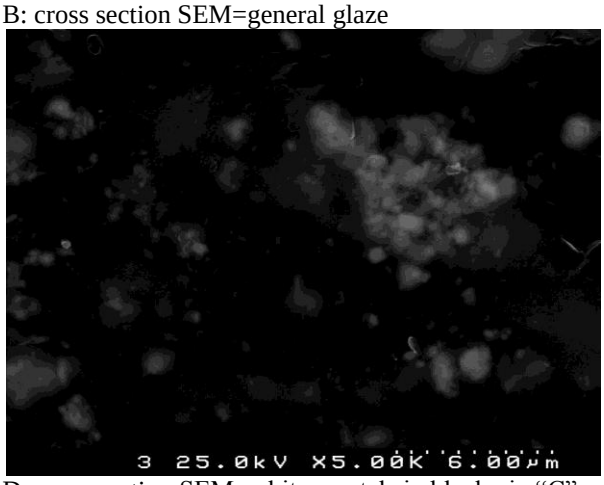

D: cross section SEM=white crystals in black pix "C"

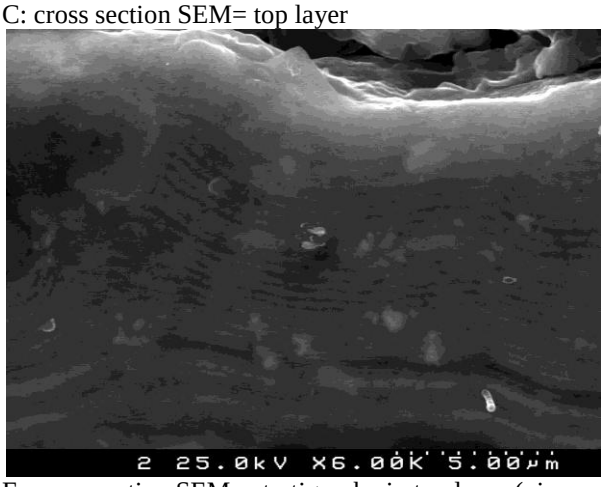

E: cross section SEM= stratigraphy in top layer (pix "C")

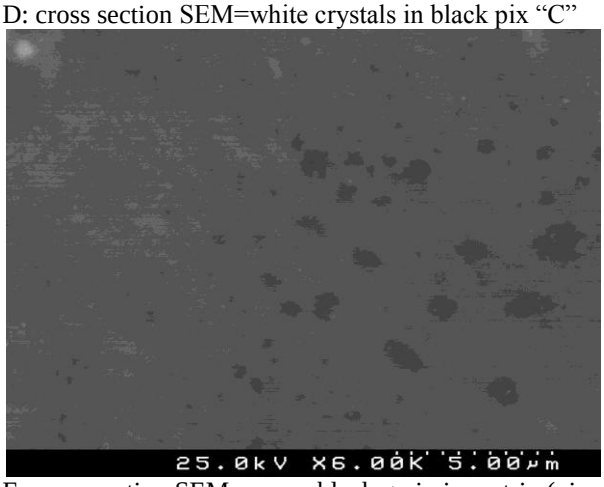

F: cross section SEM= zoom black grain in matrix (pix "C")

Figure18. SEM images of the sample CR/CSP/0023

Table 6. EDS results of the sample CR/CSP/0023 (mol. %)

SEM Paste/glaze	Na_2O	MgO	Al_2O_3	SiO_2	K_2O	CaO	TiO_2	P_2O_5	MnO	Fe_2O_3	CuO	SnO_2	PbO	Si/Pb ratio
Paste (A)	2.1	3.2	8.8	70.9	1.9	10.0	--	--	--	3.2	--	--	--	
General glaze (B)	--	--	4.2	31.6	1.8	18.4	--	10.5	--	0.6	1.8	9.1	22.0	1.44
Black grains (B)	--	--	--	100.0	--	--	--	--	--	--	--	--	--	-
Interface (B)	--	--	4.3	46.0	--	3.9	--	--	--	--	2.9	28.4	14.6	3.16
White grains in interface (B)	--	--	--	25.2	--	--	--	--	--	--	--	68.5	6.3	3.99
White crystals in dark grey zone (D)	--	--	7.4	65.7	--	--	--	--	--	1.0	2.3	15.1	8.5	7.73
Black crystals in dark grey zone (D)	--	--	6.5	66.2	2.6	3.5	--	--	--	0.9	2.4	10.8	7.2	9.26
Top of the glaze : strat (E)	--	--	4.6	18.1	--	26.8	--	12.1	--	--	--	15.1	23.5	0.77
Grey matrix (F)	--	--	--	15.9	--	35.5	--	13.4	--	--	2.0	--	33.2	0.48
Black spot in grey matrix (F)	--	--	3.5	17.7	--	29.6	--	13.4	--	--	2.7	--	33.2	0.53

Table 7. EDS results of the glaze of the sample CR/CSP/0023

element / zones	Pb	P	Ca
General glaze (B)	18.81	17.94	15.69
Top of the glaze : strat (E)	20.14	20.68	22.96
Grey matrix (F)	29.25	23.62	31.29
Black spot in grey matrix (F)	28.41	22.91	25.33

HBR-0001

Sample HBR-0001 has morphology analogous to stratigraphy observed in sample CR/CSP/0023 but in more extensive areas. The images in figure 19 give details of the glaze. Figures A, B and C [figure 21] were taken in facing. At high magnification (x700 and x1800) one already can clearly see the stratigraphy in the structure of the glaze. The EDS analysis of those parts show an important content of phosphor (~27%) in the similar ratio to Pb and Ca as in sample CR/CSP/0023 [table 7]. This specific morphology seems to be centred around spherical inclusions mainly composed of calcium, lead and phosphor. The analysis in cross-section confirms this behaviour. The cross-section allows the observation of what seems to be the sources of the layered stratigraphy. Figures D and E show general views of the glaze at low magnification (x150 and x400). In this sample the specific morphology is homogeneously distributed troughout the entire glaze. In increasing magnification (x1K-x2K), one can distinguish four zones:

- stratigraphy around grey spheres (figure H)
- stratigraphy around dark zones of irregular shape (figure G)
- stratigraphy around grey grains (figure F)
- stratigraphy around black inclusions (figure I)

The grey inclusion has almost the same composition as the stratigraphy area around it. It could be explained by a reaction of the mixture of lead and calcium phosphate when doing the glaze frits. The black inclusions (quartz) and the black zone have no trace of phosphor in the EDS analysis, table 8. At the boundary of the area of dark contrast, there are many white grains of irregular crushed-like shapes that are mainly composed of calcium, lead and phosphor in a specific ratio already observed, [table 9]. Finally, the grey sphere is composed of the regular elements that one can find in glazes and calcium, lead and phosphor always in the proportions close to the ratio [table 9] already observed in face analyses and in the other sample (CR/CSP/0023).

In cross-section, one can see that the lines defining the stratigraphy seem to start around different kinds of spheres and meet without interruption in the spaces between spheres.

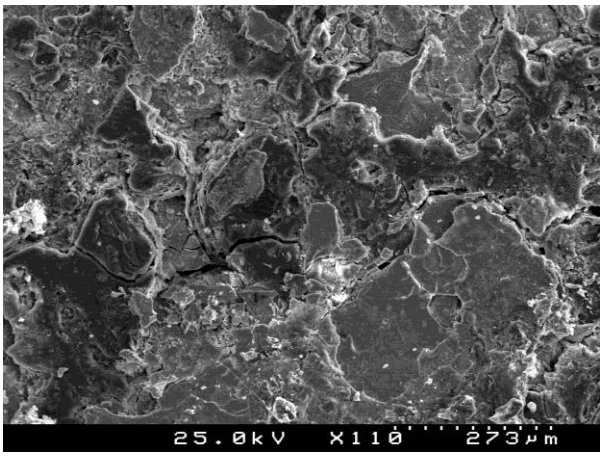

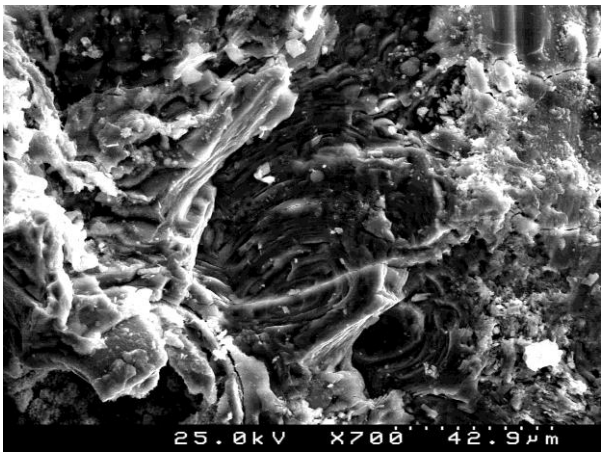

A : face SEM= general view

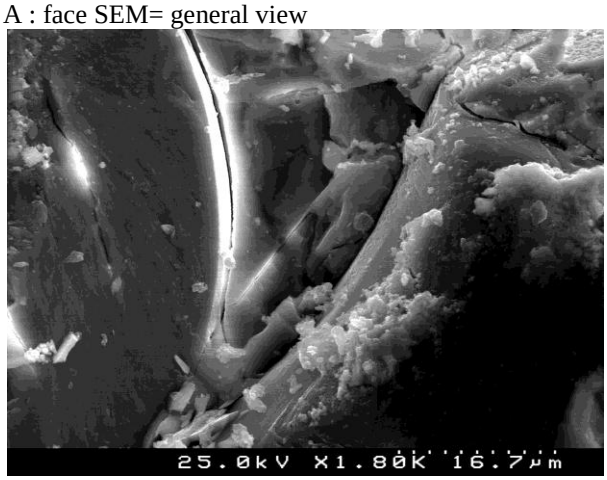

C: face SEM= stratigraphy arount a sphere (Pb, P, Ca)

B: face SEM= Stratigraphy. In grey flat grain

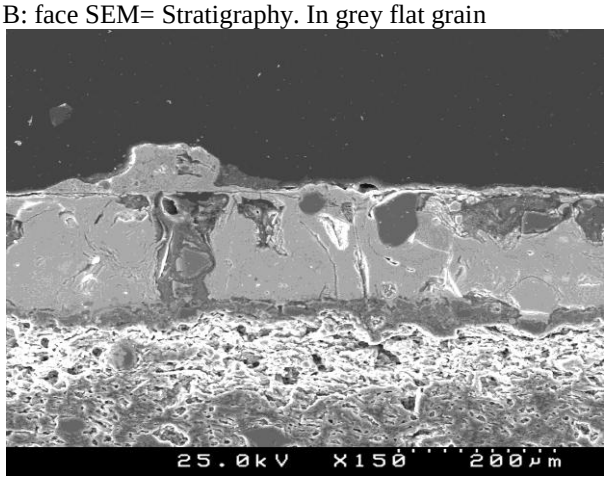

D: cross section SEM= general view- phosphorous sediment

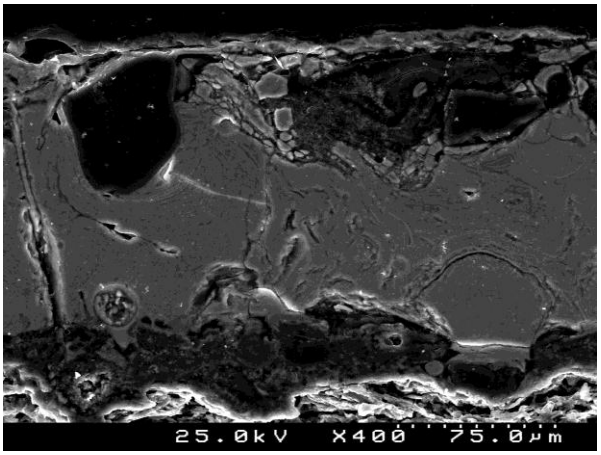

E: cross section SEM= details right

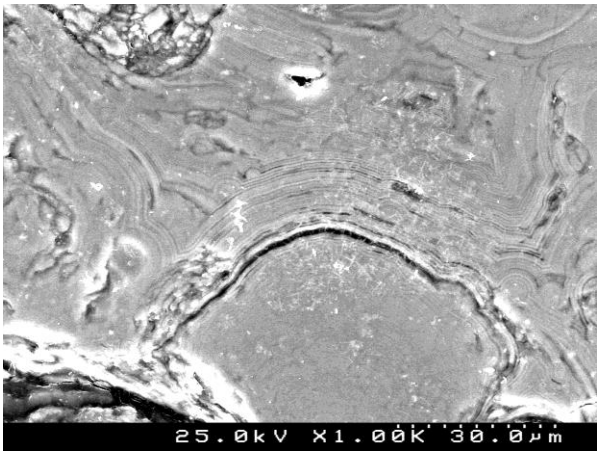

F: cross section SEM= details grey grain

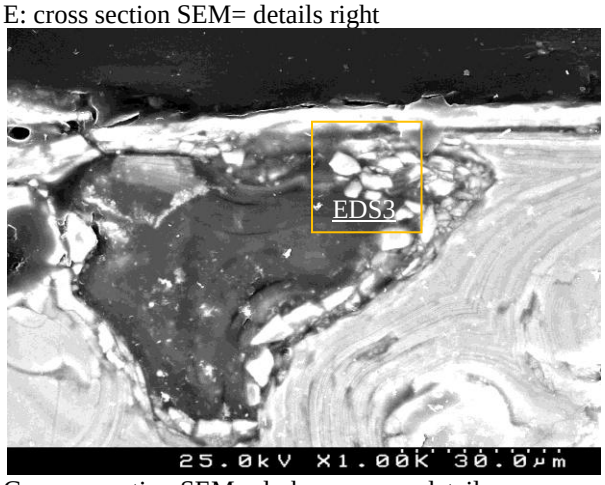

G: cross section SEM= dark grey zone details

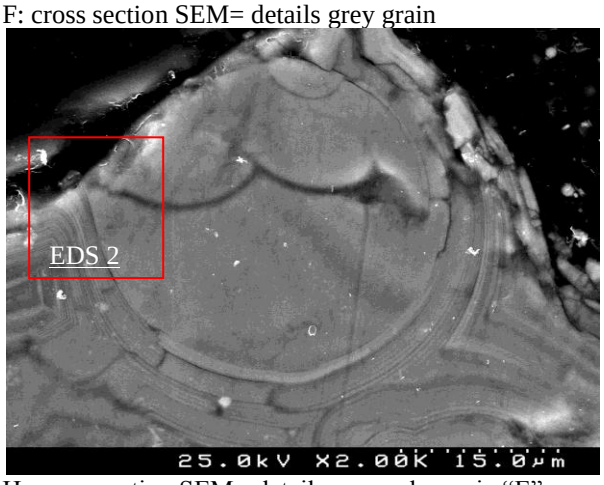

H: cross section SEM= details grey sphere pix “E”

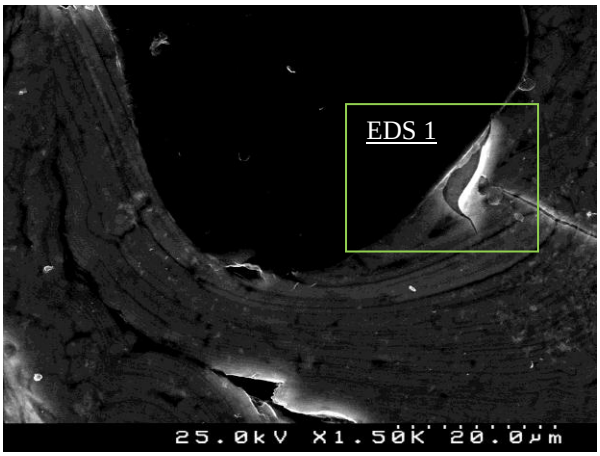

I: cross section SEM= detail black grain

Figure 19. SEM images of the sample HBR-0001

Table 8. EDS results of the sample HBR-0001 (mol. %)

SEM paste, glaze	Na_2O	MgO	Al_2O_3	SiO_2	K_2O	CaO	TiO_2	P_2O_5	MnO	Fe_2O_3	CuO	SnO_2	PbO	Si/Pb ratio
paste	1.9	5.4	9.2	57.3	0.9	21.2	--	--	--	4.1	--	--	--	-
General face (A)	--	--	6.9	38.5	2.4	17.8	--	9.9	--	1.8	--	8.5	14.2	2.72
Strat B (face)	--	--	3.1	10.3	--	36.8	--	15.9	--	0.6	2.3	6.4	24.7	0.42
Strat around sphere C (face)	--	--	2.6	9.0	--	46.0	--	16.2	--	--	3.2	--	23.0	0.39
D (sediment cross section)	--	4.9	7.0	23.5	2.1	29.5	--	12.1	--	1.9	--	--	19.0	1.23
G: black zone	2.5	3.1	7.2	66.5	2.0	5.3	--	--	--	1.1	0.5	7.0	4.7	14.03
G: white crystals in black zone	--	--	8.7	53.1	--	--	--	--	--	0.9	--	33.3	4.0	13.28
G: top white layer	--	5.7	11.5	40.2	3.1	17.5	--	6.9	--	5.2	--	--	9.9	4.05
G: top top white layer	--	4.4	13.3	62.2	3.6	3.9	--	3.8	--	4.2	--	--	4.7	13.28
G: white grains (*EDS 3)	--	--	--	9.5	--	33.1	--	17.3	--	1.6	3.0	7.4	28.0	0.34
G: strat in black zone	--	10.4	5.8	35.9	--	11.3	--	8.3	--	1.2	1.8	9.8	15.4	2.32
H: grey grain	--	--	--	--	--	45.8	--	18.2	--	--	4.7	--	31.3	-
Grey grain (line scan)	--	8.0	2.5	4.2	--	32.9	--	17.2	--	--	3.7	3.8	27.8	0.15
H: strat around grey grain (*EDS 2)	--	--	3.2	8.2	--	39.0	--	16.2	--	--	4.0	--	29.5	0.28
I : black grain	--	--	--	100.0	--	--	--	--	--	--	--	--	--	-
I: strat around black grain (*EDS 1)	--	--	--	15.5	--	27.8	--	15.4	--	--	3.2	7.5	31.4	0.49

Table 9. EDS results of the sample HBR-0001

element / zones	Pb	P	Ca
General face (A)	11.70	16.37	14.67
Strat B (face)	20.62	26.54	30.74
Gradient around sphere C (face)	19.39	27.28	38.76
D(sediment cross section)	15.44	19.58	23.99
G: black zone	4.20	-	4.69
G: top white layer	7.83	10.87	13.79
G: top top white layer	3.75	6.08	3.10
G: white grains	23.54	29.13	27.82
G: strat in black zone	13.34	14.45	9.83
H: grey grain	26.43	30.86	38.73
H: Grey grain (line scan)	23.17	28.58	27.41
H: strat around grey grain	24.69	27.08	32.65
I: strat around black grain	26.62	26.11	23.60

3.2.2*X-ray diffraction*

The results of X-ray analysis in table 4 show that the pastes of the two samples have the silicates derived of decomposition and reaction of a kaolin clay. Differences between the samples can be explained by the use of different firing temperatures.

In the sample CR/CSP/0023, the presence of gehlenite and mullite in this sample indicates that the sample was fired at temperatures between 900ºC (formation of anorthite) and 1050°C, formation of mullite. The calcium that can be present in minor fractions in the primary clay minerals and is abundant in sedimentary deposits as calcite, in mica and other silicates is absorbed during firing.

In the sample HBR-0001 again the gehlenite and anorthite are found that gives the same temperature for the firing. Augite is a mineral from the silicate family that contains traces of calcium, magnesium, iron... This mineral can give information about the origin of the clay used by the potters.

3.2.3 *Polarized light reflected microscopy*

Selected images of reflected polarized light microscopy of samples CR/CSP/0023 and HBR-0001 are given in figure 20. The samples were selected for the observation under polarized light because they have zoning, banded areas at several places, as shown by the SEM images above. The optical images for one and other of these samples were taken under similar values of rotation of the analyser.

a) CR/CSP/0023

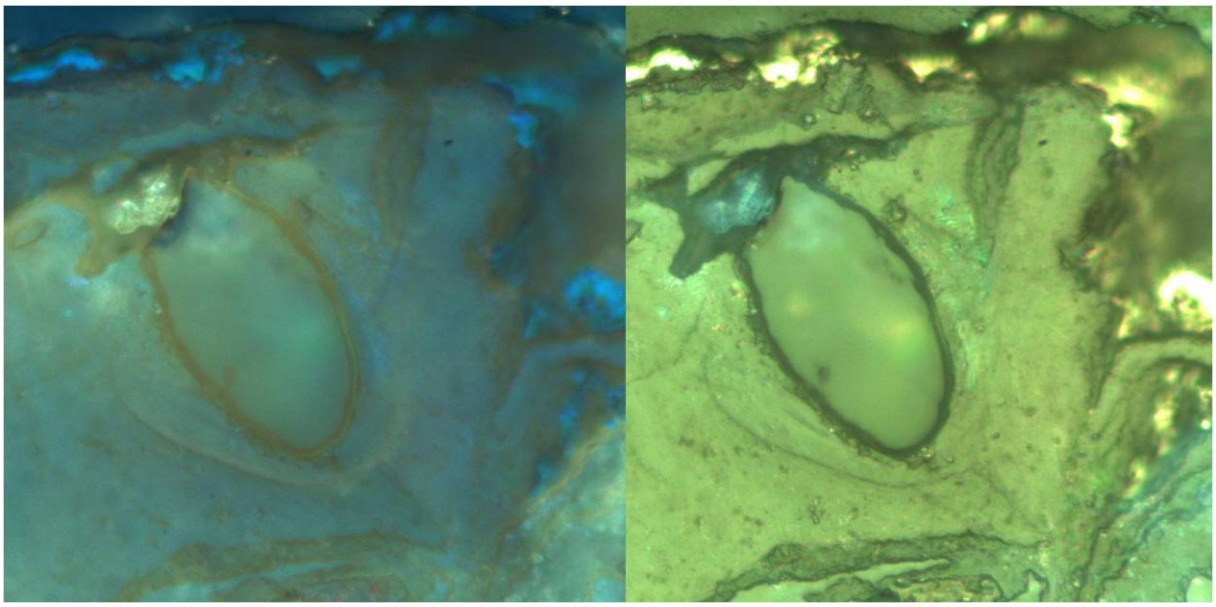

b) HBR-0001

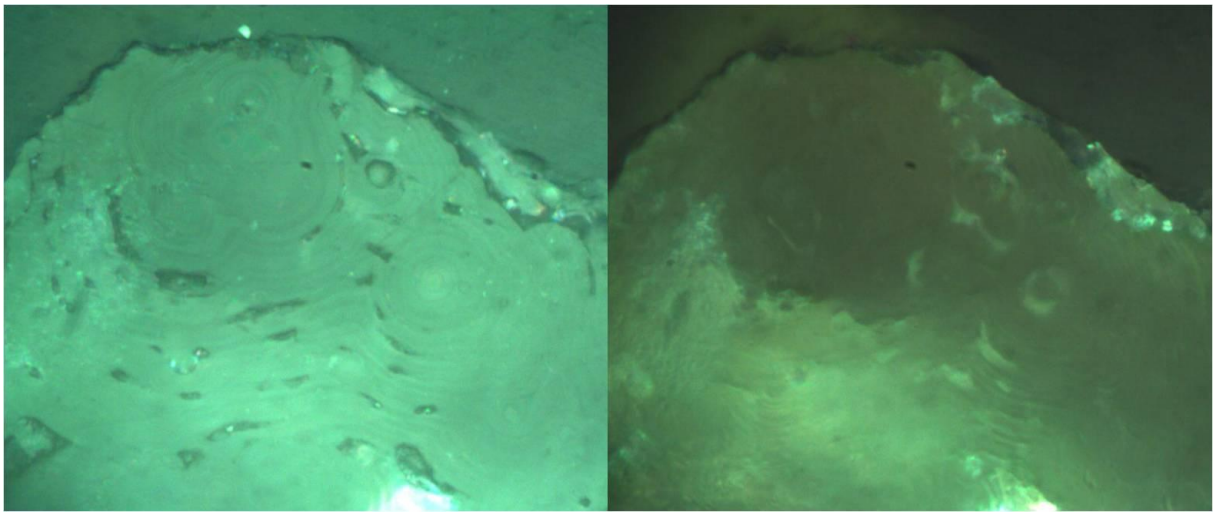

Figure 20. Images of reflected polarized light microscopy illuminated by white. a) Sample CR/CSP/0023. B) Sample HBR-0001.

The change of optical contrast in figure 20 a) with rotation of the analyser reveals some areas with differences of contrast in the matrix that tend to follow the lines of the zoning structure, this effect being feeble. In a different way, the rotation of the analyser produced a rich contrast in the corresponding images of sample HBR-0001, figure 20 b). The zoning as revealed by the optical microscopy develops in optical active inner surfaces concentric with many centres. Often the development of these surfaces seems pinned on voided residual pores. The morphology of the fine porosity is peripheral to the same centres and is seemingly correlated to the observed optical contours. Extensive observation of this glaze along the cross-section proved that the effect shown in figure b) was generally present in the volume of the glazed layer. Optical images of a third sample

(HBR-0206) which did not display zoning in SEM showed only contrast related to the minerals, glass body and other inclusions.

3.2.4 *Micro-Raman spectrometry of sample HBR-0001*

Selected spectra of the micro-Raman analysis done on the polished cross-section of sample HBR-0001 are presented in figure 21. A micro-Raman spectrum of a sintered pellet of calcium hydroxyapatite (Ca-HAP) provided by courtesy of Doctor Diogo Mata (CICECO-University of Aveiro) is also included as reference, this spectrum having been obtained with the same spectrometer, at the same laser light wave length, λo = 532 nm, under comparable conditions of illumination. The reference HAP pure sample was synthesized by solid reaction and a final step of sintering at 800-1000 ºC. The intensity of each of the measured spectrum was recalculated by normalizing the values by the maximum of intensity and a quantity being added to move the spectrum up/down in the plot as needed.

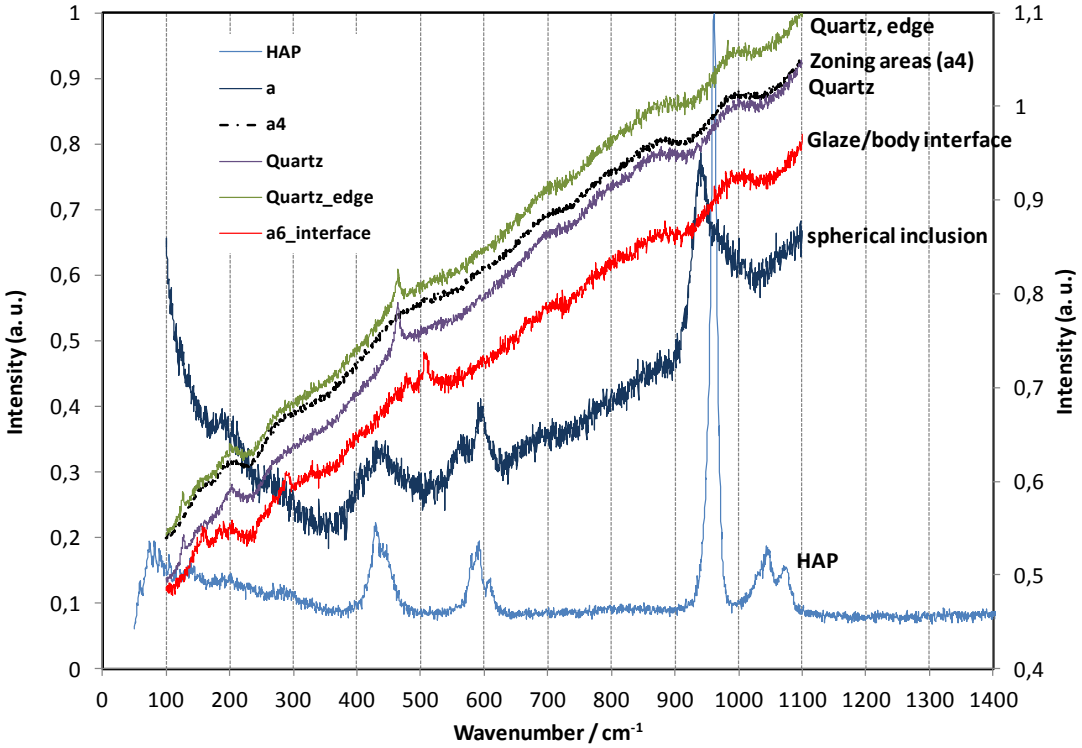

Figure 21. Micro-Raman spectra of phosphate-rich and quartz inclusions, banded matrix area and glaze/ paste interface of sample HBR-0001, and reference micro-Raman spectra of pure, high temperature fired calcium-hydroxyapatite (HAP) (*courtesy of Dr. Diogo Mata*), λo = 532 nm.

Close observation of the Raman spectra of Ca-HAP reveals a large number of peaks at (60, 73, 83, 91, 105, 135, 200b, (431,145), 580, 592, 610), 962, (1029, 1045, 1076) cm^{-1}, all of them being

assigned to the HAP phase accordingly to the bibliography (Ciobanuc and al. 2011). The rising of the intensity of the RAMAN spectra of HAP at low wave numbers (< 300 cm^{-1}) is characteristic of the O-H bond of the HAP phase (Hadrich and al. 2001 b). The micro-Raman spectra of the content in the spherical inclusion (Pb, P, Ca) rich (Figure 21) has a strong line of hydroxypyromorphite-hyadroxyapatite solid solution at 940 cm^{-1} (Hadrich and al. 2001 a). Hyrdroxypyromorphite is also named as Pb-hydroxyapatite.The splitting of the band at 560, 590 cm^{-1} may indicate a high temperature process (glaze firing) as the origin of the solid solution, although precipitation of the solid solution in contact or with a residual hydrated SiO_2 gel could also cause spectral broadening. In the stratigraphy or banded areas contacting the inclusion, the main peak of (Pb,Ca)-HAP is broadened into a band, but it absent in (a4) spectrum taken at a different point of the sample that also has zoning. This same spectra (a4) shows glass like broad and poorly defined bands (Si-O) and there is no noticeable rising of the intensity below 350 cm^{-1}. These zones are also Pb, P, Ca rich (line profile and EDS results above, figure 19).

The main peak of quartz at 465 cm^{-1} is seen in two micro-Raman spectra taken inside and at the edge of quartz inclusion given above in figure 21. Broad bands of a Si-O like glass are also seen in these spectra (Raskovska and al. 2009, Tanesvka and al. 2009). Without further study, the lines observed in the spectrum of the glaze/precipitates taken at the interface, only in a very coarse tentative can these lines be assigned silicates and the broad bands to the glass-like material found there (Raskovska 2009,Tanesvka 2009).

3.3 CR/CSP/0022 and HBR-0206

3.3.1 *Microscopy*

The glazes of these two samples also have phosphor in high quantity, but it does not present the same distribution and is not related to stratigraphy as it as in previous samples HBR-0001 and CR/CSP/0023. In samples HBR-0206 and CR/CSP/0022 the presence phosphor is restricted to spherical inclusions homogeneously distributed inside the entire glaze, figures 22 and 23.

CR/CSP/0022

The glaze of sample CR/CSP/0022 is composed of two colours: blue and green that were analyzed separately in face SEM [figure 22]. Figures A and B correspond to the blue glaze. B details the shapes of the white crystals in figure A. Figures C and D correspond to the green glaze. D details the white crystals that are seen in figure C.

The EDS performed in the glazed surfaces of these two pieces shows that phosphor is only detected in the green glaze. Whereas the white crystals in the blue glaze are compose of tin, iron, aluminium and silicon, the white crystals in the green glaze are made of a mixture of glaze materials with

phospho/lead/calcium [table 11 and 12]. The dark contrasted zones are either quartz or inclusions of silicates.

The images taken on the cross-section allow a better description of the structure of this sample. Figures F, G, H and I [figure 22] give details of the large image of the glaze in figure E.

The glaze can be divided into three parts: the interface, the surface layer and the volume glaze in between these two zones. The volume of the glaze contains big spherical shapes either filled or void (figure F). Because of over exposure in SEM due to the relief of those spheres, the spherical cavities (in white) could not be analyzed by EDS, nor can the holes be analyzed. EDS was limited to the top edge of the layer seen on walls of these cavities. One can observe boundaries delineated around filled spheres.

The EDS analyses show that the content of the spheres or precipitates is a mixture of phosphor, lead and calcium in the same proportions as reported for samples CR/CSP/0023 and HBR-0001 above [tables 6/8]. In some places, smaller spherical inclusions are contained inside larger spheres. The composition of the inner spheres is the same as that the matter of the walls surrounding them. Unlike the previous samples, phosphor is not detected in the glaze volumes contacting these spheres.

Figure G, which is a zoom of the surface layers, shows a structure of two layers on the top of the glaze. EDS analysis indicate that these two layers are parts of just same one layer that delaminated into the two. This layer (2) is composed [table 11] of phosphor/calcium/lead and silicon and minor fractions of iron, tin and copper. Iron and copper are colouring elements of the green glaze. The white crystals presents in the layer (2) (H) are mostly silicates with glaze elements and small quantity of phosphorous/lead/calcium again in the same relative proportions as found above [table 7/9]. Another layer (1) is seen at the top of this layer, figure G. This layer is mainly composed of phosphorous/calcium/lead and a small amount of silicon too, probably coming from the layer underneath. Layer (1) is probably a deposit of phosphates related to weathering. The phosphor found in the layer (2) could have diffused from layer (1).

Besides the content of the spherical cavities the sediment layer, the glaze does not contain any phosphorous matter. One can suppose that the pottery was firstly covered by the green glaze (EDS, image E), covered by a thin layer of blue/green glaze which was altered by phosphates pollutants.

Finally, the body/glaze interface is composed of silicates and main elements of the glaze composition. No phosphor was detected at the interface, neither in the paste, table 10.

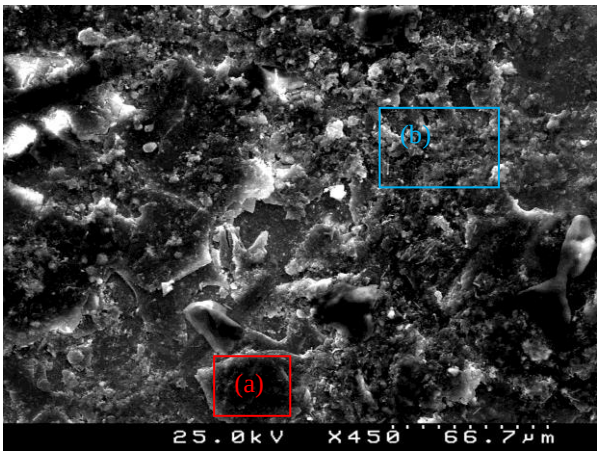

A: face SEM=general view blue glaze

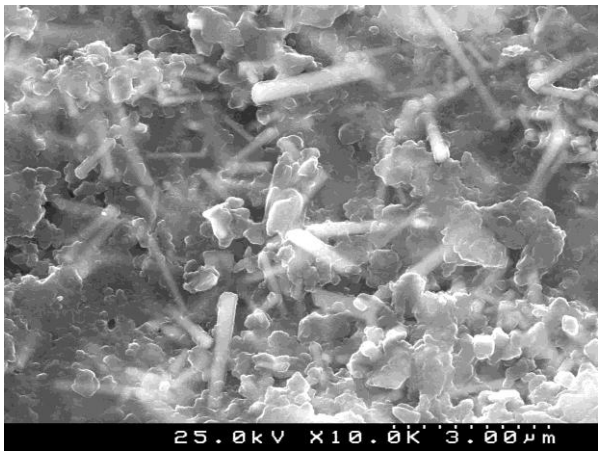

B: face SEM= details white crystals in blue glaze

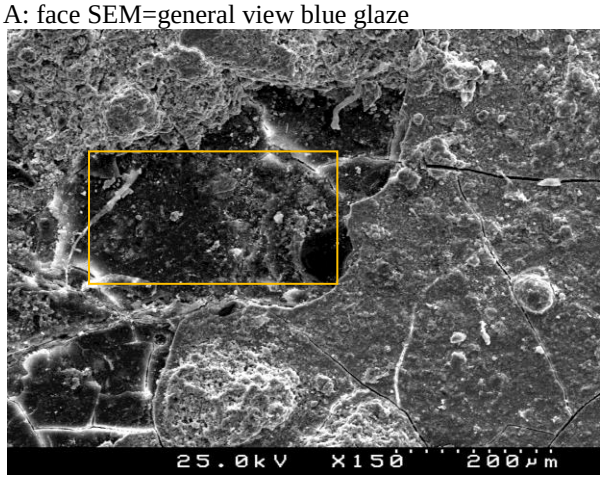

C: face SEM=general view green glaze

D: face SEM= details white crystals green glaze

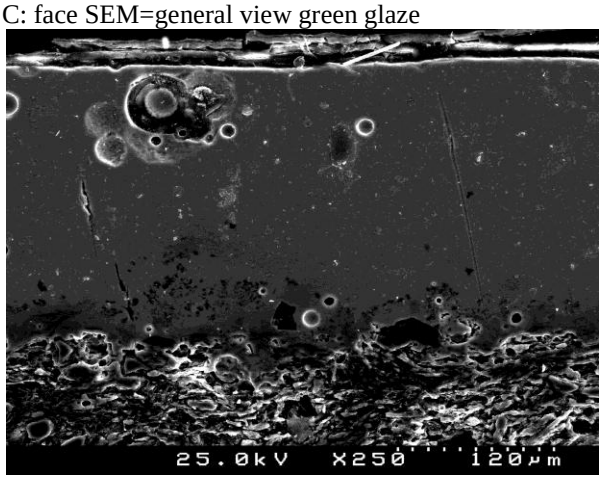

E: cross-section SEM= general view

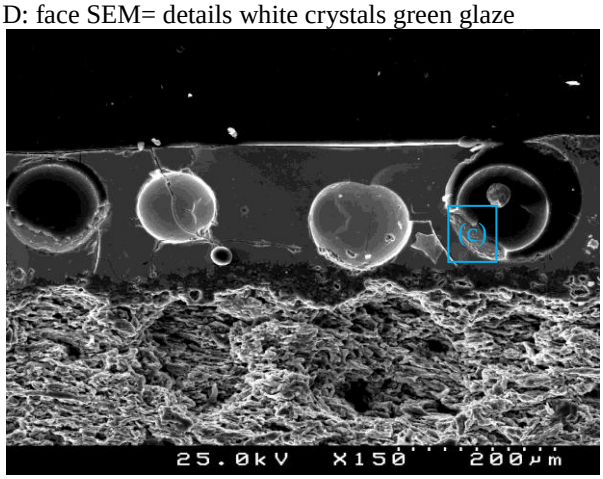

F: cross-section SEM=precipitates

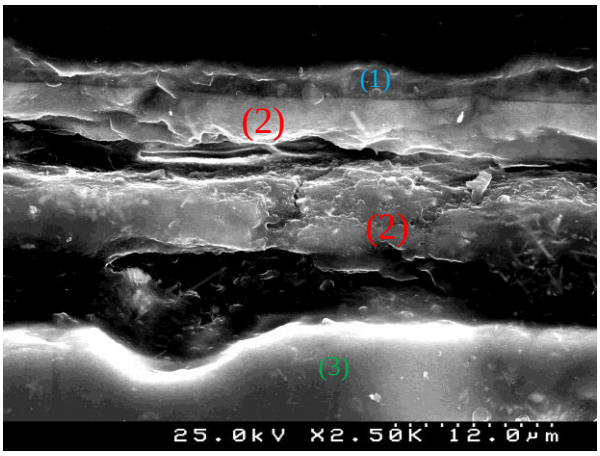

G: cross-section SEM= details top layers

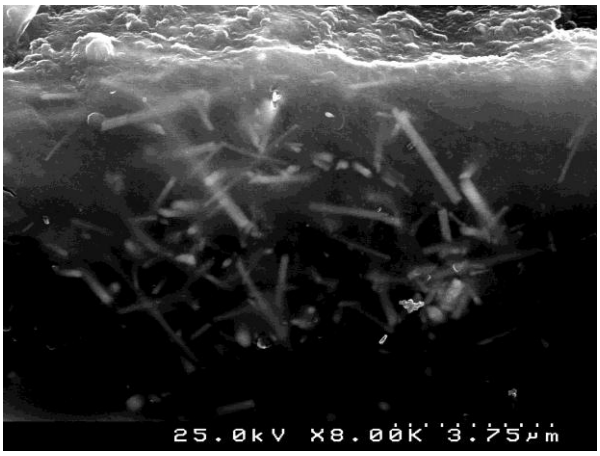

H: cross-section SEM= details crystals in second layer (2)

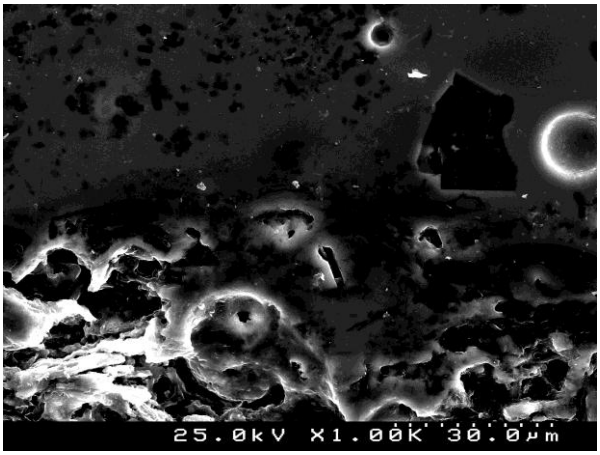

I: cross-section SEM=interface

Figure22. SEM images of the sample CR/CSP/0022

Table 10. EDS results of sample CR/CSP/0022 (mol. %)

SEM Paste/glaze	Na_2O	MgO	Al_2O_3	SiO_2	K_2O	CaO	TiO_2	P_2O_5	Fe_2O_3	CuO	SnO_2	PbO	Si/Pb ratio
paste	3.2	4.2	11.1	53.3	1.7	20.9	0.5	--	3.4	--	--	1.6	32.38
(A) General face blue glaze	12.1	--	3.3	49.1	2.7	7.7	--	--	0.7	4.0	7.8	12.7	3.85
(A) Black zone (a)	--	--	--	100.0	--	--	--	--	--	--	--	--	-
(A) Grey zone (b)	13.7	--	--	55.8	2.6	3.1	--	--	--	3.8	5.5	15.5	3.59
(B) White crystals blue glaze	--	--	6.7	41.6	--	--	--	--	0.9	--	50.8	--	-

SEM Paste/glaze	Na_2O	MgO	Al_2O_3	SiO_2	K_2O	CaO	TiO_2	P_2O_5	Fe_2O_3	CuO	SnO_2	PbO	Si/Pb ratio
(C) general view face, green glaze	--	7.8	3.6	8.8	--	39.7	--	12.8	0.6	1.9	--	24.7	0.35
(C) black part green glaze	--	7.8	4.2	52.9	3.0	10.3	--	--	1.9	1.6	14.1	4.4	11.90
(D) white crystals green glaze	--	--	3.7	12.6	2.4	37.2	--	12.8	0.9	--	--	30.4	0.41
(E) general green glaze	2.3	--	21.5	62.6	10.6	--	--	--	0.6	--	--	2.5	25.07
(E) interface	6.0	3.8	9.4	58.1	4.1	9.9	--	--	2.6	--	--	6.0	9.65
(E) sphere at the interface	9.3	5.3	4.2	47.0	3.0	10.5	--	--	2.1	--	--	18.7	2.52
(F) empty and full sphere= precipitates (general)	8.6	6.7	6.1	16.2	1.8	34.1	--	10.3	1.3	--	--	14.9	1.09
(F) sphere black and white: walls (c)	--	--	5.9	40.1	4.4	17.5	--	7.9	1.1	--	--	23.1	1.74
(F) sphere in sphere	--	--	4.4	31.7	--	22.6	--	11.1	0.8	1.7	--	27.8	1.14
(F) around sphere	--	--	3.9	66.2	--	4.9	--	--	1.6	1.8	12.2	9.5	6.99
(G)top layer (2)	--	--	--	24.7	--	23.1	--	12.5	0.8	1.7	9.3	27.8	0.89
(G) top top layer, sediments (1)	--	--	--	8.9	--	44.1	--	14.3	--	--	--	32.6	0.27
(G) glaze (3)	12.0	11.2	--	46.1	2.2	4.5	--	--	1.6	2.1	5.6	14.8	-
(H) white crystals in top layer (2)	7.5	10.6	4.7	48.4	--	5.8	--	2.9	1.0	1.6	11.5	6.1	7.99
(I) interface	4.1	--	10.3	79.5	4.5	1.3	--	--	0.3	--	--	--	-

Table 11. EDS results of sample CR/CSP/0022

element / zones	Pb	P	Ca
(C) general view face green glaze	21.12	21.95	33.96

(D) white crystals green glaze	25.39	21.41	31.10
(F) empty and full sphere= precipitates	11.63	16.07	26.59
(F) sphere black and white (c)	19.32	13.31	14.69
(F) sphere inside sphere	23.89	19.05	19.43
(G) top layer (2)	24.50	22.13	20.42
(G) top top layer = sediments (1)	28.55	25.08	38.56
(H) white crystals in top layer (2)	5.22	5.03	4.98

HBR-0206

The sample HBR-0206 shows the same morphology found in sample CR/CSP/0022 but it was better preserved and allowed more detailed analyzes.

The two images taken in facing by SEM and the EDS analysis show the paste (figure A) with a small amount of titanium (figure 23 and table 12) which can be interesting to indentify the origin of the clay. The image in figure B corresponds to “cuerda seca” line as manganese was detected there [table 12].

In the cross-section images of this sample one can observe filled spheres (figure D and E). The EDS analysis of the content of those nearly spherical inclusions brings new information to understand this morphology: the matter filling these spaces seems to be precipitates of phosphor/calcium and lead only [tables 12 and 13]. In the surrounding of these spheres, there is no phosphor and the quantity of calcium decreases sharply from 43% inside to 11% in the surroundings.

In figure F (red square) one can see white crystal-like particles inside a spherical cavity. In addition to the regular composition in Pb/P/Ca of the precipitate, a small fraction of silicon was detected too, table 12. One can already think about a partial fusion between something that brought the phosphates and the glaze material. This hypothesis is corroborated by the EDS of the structure of the spherical void in figure G. It is actually a hole, where some matter became adherent against the walls. The crystals that formed on the cavity walls are composed of elements of glaze and phosphates of calcium and lead.

As in sample CR/CSP/0022, there is a thin layer of phosphates (figure 23C) [table 12] that may correspond to adhesion of external pollution.

In that sample, again, as in the previous one, there is no trace of phosphor in the volume of the glaze layer at the outside of the spheres/precipitates, they are surrounded by a boundary of silicate material [table 13]. Neither the paste contains phosphor. The bulk composition of the glaze corresponds to a lead-silica glaze with high potassium content which seemingly is Na-free.

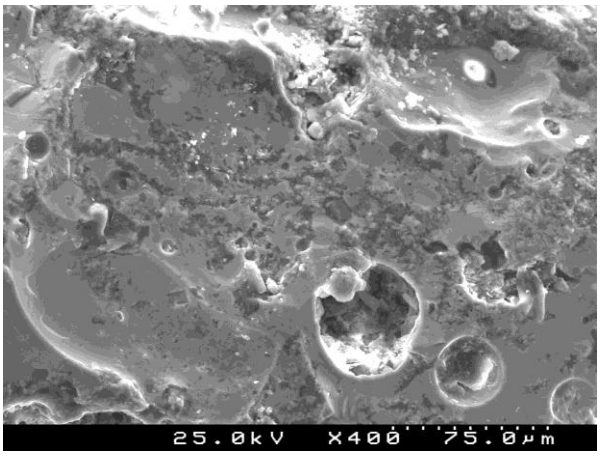

A: unglazed paste (face)

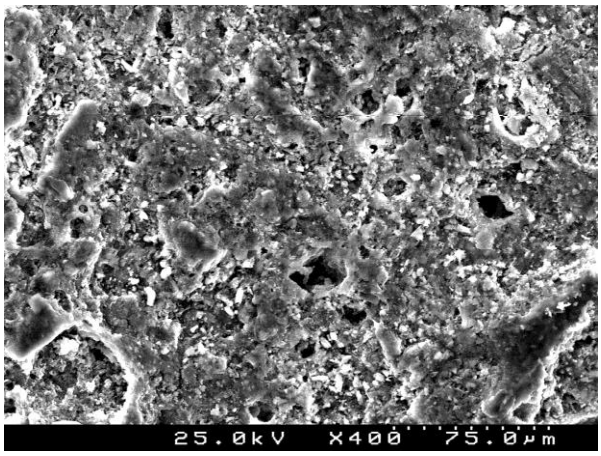

B: “cuerda seca” face

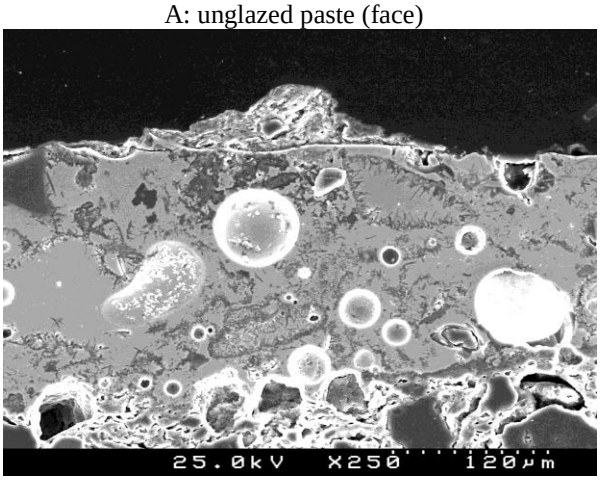

C: general glaze (cross section)

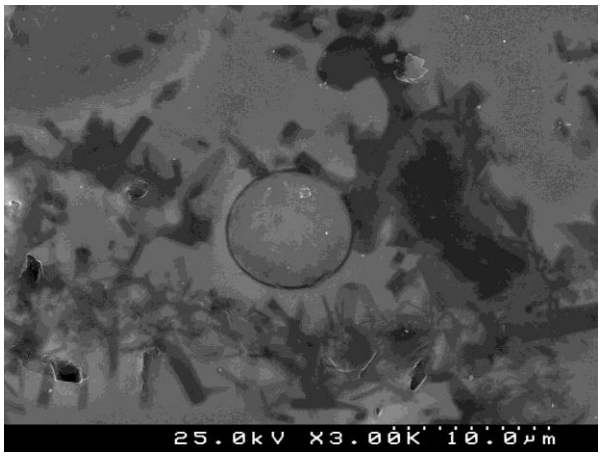

D: P-precipitates

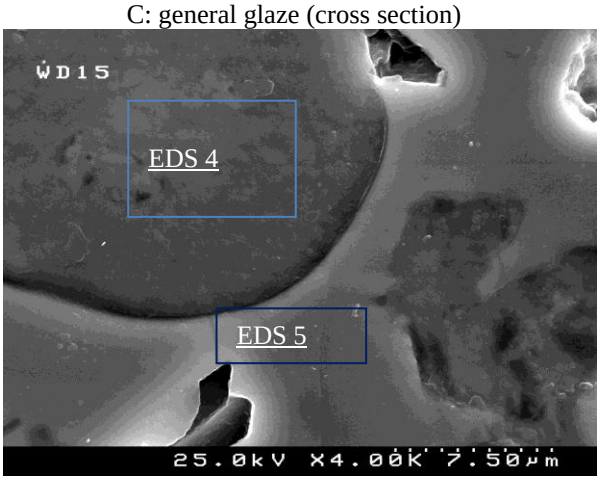

E: zoom P-precipitates

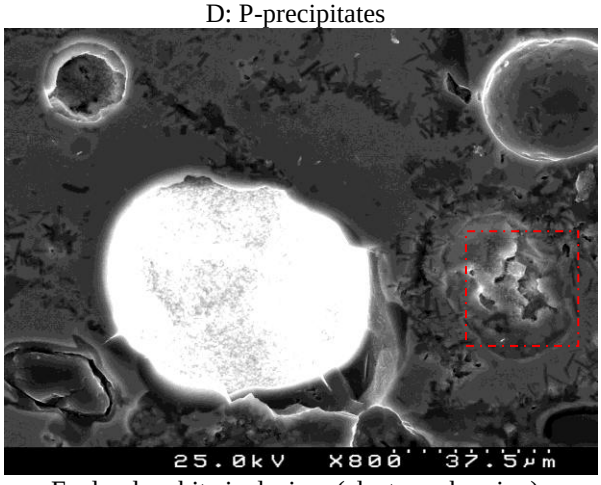

F: cloudy white inclusion, (electron charging)

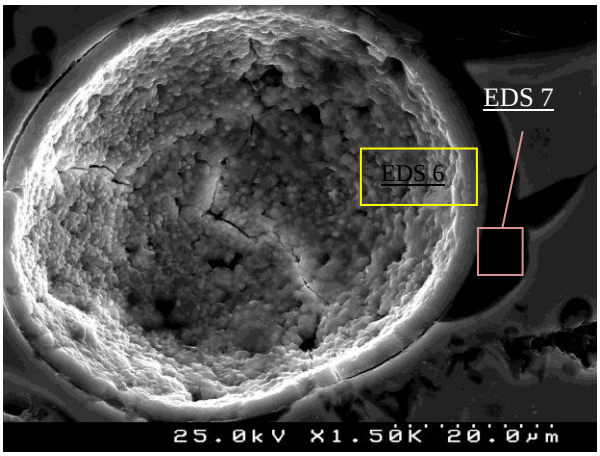

G: hole + crystallized particle like inner coating

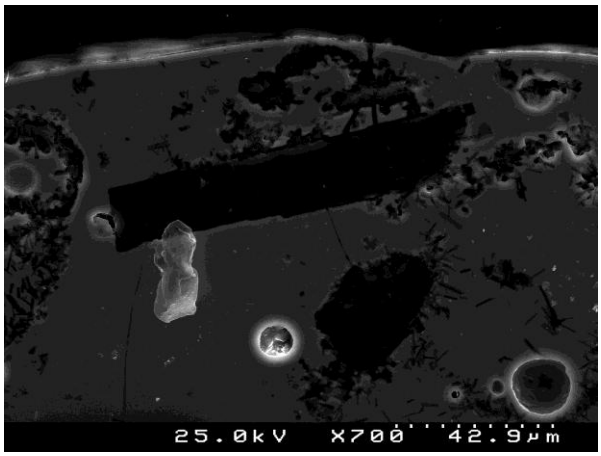

H: prismatic crystals with black contrast

Figure23. SEM images of sample HBR-0206

Table 12. EDS results of sample HBR-0206 (mol. %)

SEM Paste/ Glaze	Na_2O	MgO	Al_2O_3	SiO_2	K_2O	CaO	TiO_2	P_2O_5	MnO	Fe_2O_3	CuO	SnO_2	PbO	Si/Pb ratio
Paste (A)	3.1	5.0	9.7	55.0	2.8	15.5	1.2	--	--	3.4	--	--	4.4	-
“cuerda seca” (B)	--	--	8.3	52.8	2.0	18.1	--	--	12.5	5.0	--	--	1.3	40.95
General glaze (C)	--	--	6.0	55.3	3.9	11.7	--	--	--	2.7	--	--	20.5	2.70
Top top layer (C)	--	4.8	7.5	47.5	2.9	15.1	0.9	7.4	--	2.5	--	--	11.4	4.17
Interface (C)	2.1	--	19.5	67.2	7.6	--	--	--	--	--	--	--	3.7	17.99
P-precipitates (D) (*EDS 4)	--	--	--	--	--	50.3	--	16.4	--	--	--	--	33.3	-
P-precipitates-black prisms (D)	--	--	10.4	72.7	14.3	--	--	--	--	--	--	--	2.6	28.42
Around sphere (E) (*EDS 5)	--	--	5.9	48.2	1.9	12.7	--	--	--	2.4	--	--	29.0	1.66
Cloudy white grains (F)	--	--	--	8.7	--	46.0	--	16.5	--	--	--	--	28.7	0.30
White hole (G) (*EDS 6)	--	--	2.9	16.2	--	36.6	--	13.4	--	1.3	--	--	29.7	0.55
Black around white hole (G)	--	--	5.9	48.2	1.9	12.7	--	--	--	2.4	--	--	29.0	1.66

SEM Paste/ Glaze	Na_2O	MgO	Al_2O_3	SiO_2	K_2O	CaO	TiO_2	P_2O_5	MnO	Fe_2O_3	CuO	SnO_2	PbO	Si/Pb ratio
Black prisms (H) (*EDS 7)	--	--	10.4	72.7	14.3	--	--	--	--	--	--	--	2.6	28.43

Table 13. EDS results of sample HBR-0206

element / zones	Pb	P	Ca
Edge of top layer (C)	9.46	12.30	12.59
P-precipitates (D)	28.63	28.12	43.25
Cloudy white inclusion (F)	24.67	28.30	39.53
White hole (G)	25.24	22.79	31.10

a) X-ray diffraction

The pastes of these two samples were analyzed by X-ray diffraction, table 4.

The paste of sample CR/CSP/0022 is composed of quartz and silicates derivative of kaolin in presence of calcium that may indicate that the sample was fired at a temperature close to 900°C due to the simultaneous formation of anorthite and augite (Moropoulou 1995).

HBR-0206 is only composed of quartz and derivatives of kaolin crystalline phases. Indeed, the mullite appears around 1050°C the hypothetical firing temperature of this sample. Gehlenite and anorthite are formed at lower temperatures, table 3 (Cultrone, 2001)

3.4HBR-0072 and HBR-0207

3.4.1*Microscopy*

In these two samples, phosphor was found at the surface of the glaze and inside the ceramic body. The two samples show a similar type of morphology figures 24 and 25 that is visibly different from those of previous samples.

HBR-0072

The EDS analyses of sample HBR-0072 show [table 14/15] that phosphor is concentrate in the white areas at the top of the glaze (cross-section) in layers that seems to be sediments. The figure B of the

surface of the glaze (face) shows different kinds of black contrasted zones: elongated prismatic crystals and circular ones. All the black formations are composed of silicates.

As there is no trace of phosphor inside the volume of the glaze, its presence at the interface between glaze and ceramic body can be explained by migration trough the porosity of the ceramic body to the interface.

This sample is composed of regular elements that are usually used to make lead-silica glazes. One can found only traces of copper (table 14) that together with iron becomes the origin of the green colour of the glaze.

A: face, general view green glaze

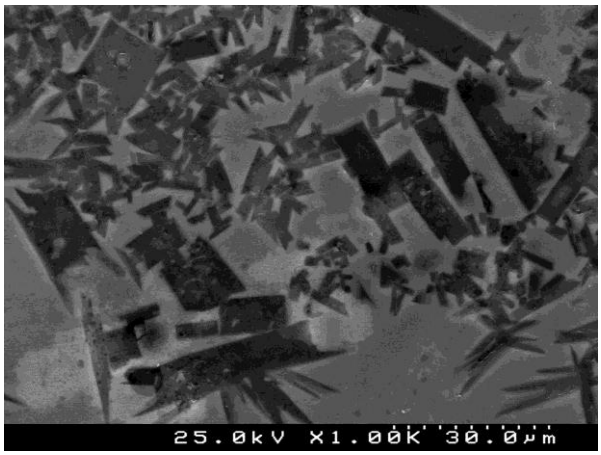

B: face, details black prismatic crystals in green glaze

C: face, general view brown glaze

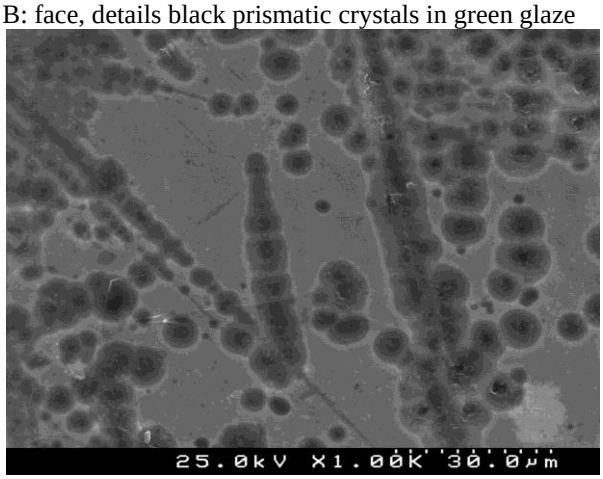

D: face, details black spots brown glaze

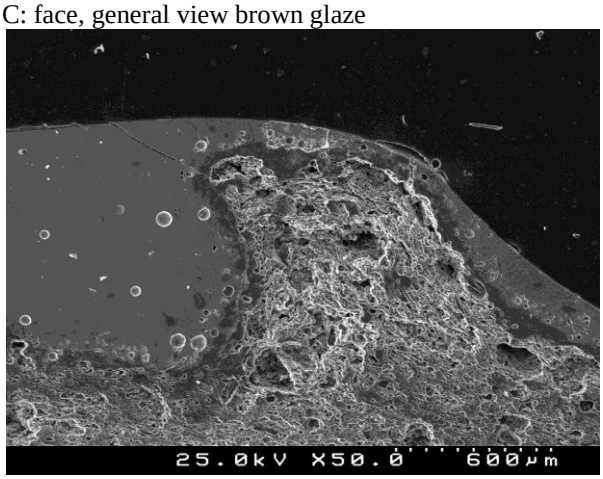

E: cross-section= general view paste & glaze

Figure24. SEM images of sample HBR-0072

Table 14. EDS results of sample HBR-0072 (mol. %)

SEM paste/ glaze	Na_2O	MgO	Al_2O_3	SiO_2	K_2O	CaO	TiO_2	P_2O_5	MnO	Fe_2O_3	CuO	SnO_2	PbO	Si/Pb ratio
paste	4.1	5.6	9.9	51.1	0.7	20.2	0.7	2.2	--	3.9	--	--	1.6	31.11
(A) general green glaze	7.1	3.5	4.1	56.0	3.0	8.9	--	3.6	--	1.3	--	--	12.6	4.46
(A) grey zone green glaze	8.4	5.2	5.2	51.7	3.3	6.6	--	--	--	1.3	1.2	--	17.3	2.99
(B) black sticks	3.5	--	4.4	71.1	4.0	4.1	--	--	--	1.1	--	--	11.9	5.96
(C) general view brown glaze	6.5	3.2	6.1	58.0	4.4	6.9	--	--	--	1.5	--	--	13.4	4.32
(D) black spots	5.6	3.0	6.5	58.2	5.6	7.4	--	--	--	1.4	--	--	12.2	4.76
(E) top mountain	9.5	5.0	5.6	52.8	3.6	5.7	--	--	--	2.2	--	--	15.7	3.36
(E) interface	5.9	5.9	8.9	50.7	1.9	15.0	--	3.1	--	3.8	--	--	4.8	10.65
(E) white crystals	8.4	5.5	4.3	25.9	2.8	23.6	--	9.2	--	1.8	--	--	18.6	1.39
(E) sedimentation	--	1.3	4.6	39.1	1.7	34.2	--	10.2	--	1.8	--	--	7.2	5.43

Table 15. EDS results of sample HBR-0072

element / zones	Pb	P	Ca
(A) general green glaze	10,54	6,03	7,50
(E) interface	3,85	5,09	12,11
(E) white crystals	14,67	14,59	18,65
(E) sedimentation	6,08	17,27	28,87

HBR-0207

In sample HBR-0207, phosphor, calcium and lead are concentrated in the white crystal-like precipitates (figures B and C) which also have specific relative ratio of these three elements [table 17] close to the proportions already observed in the previous samples.

The black area in (figure A) and the black crystallizations (figure D) correspond to a silicate-rich [table 16] zone which is taken as representative of the bulk of the glaze.

The SEM images of the cross-section show a layer at the top of glaze corresponding to a deposit of phosphate, Figure 25 E.

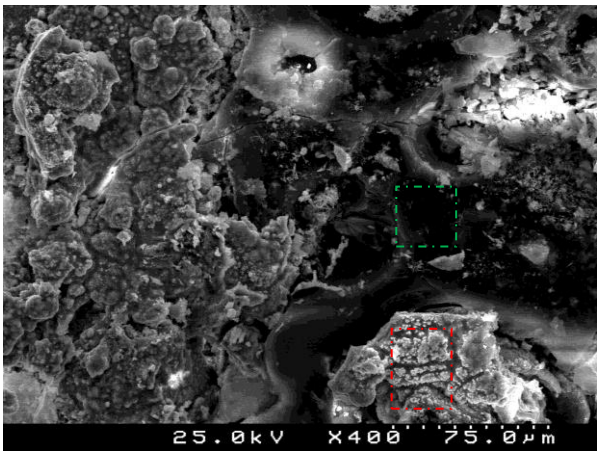

A: face, general view

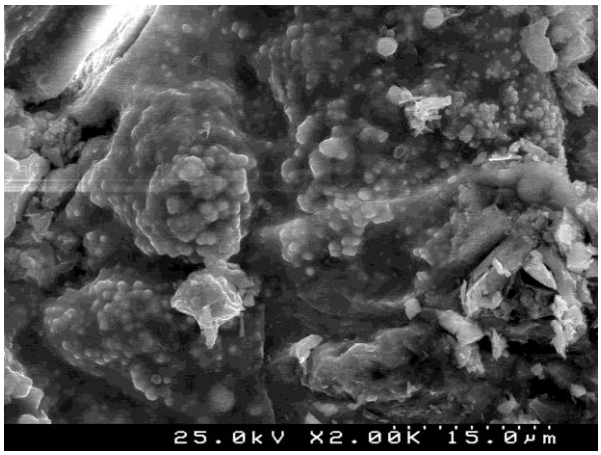

B: face, details of white crystals 1

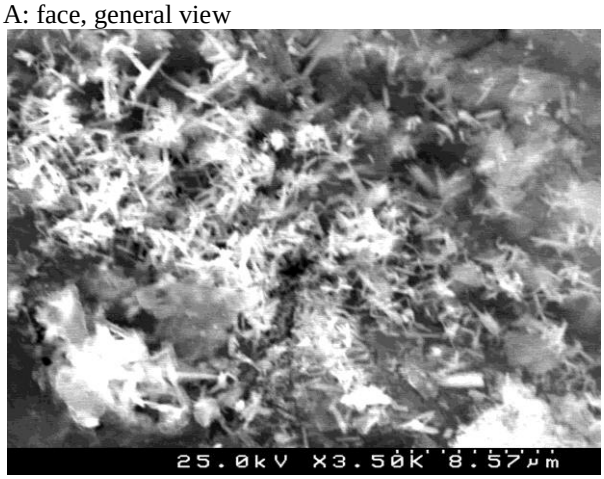

C: face, white crystals 2 in black part

D: cross-section, general view

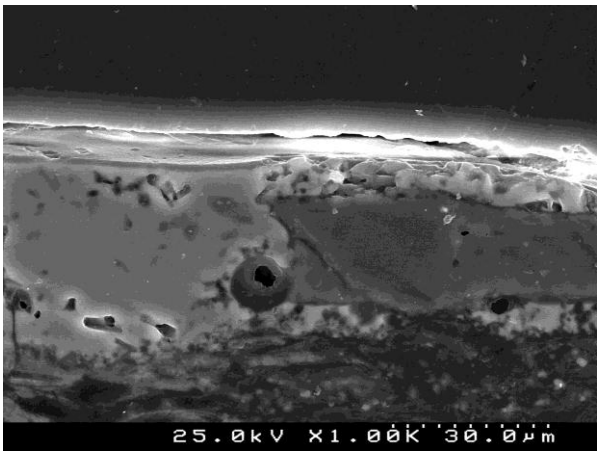

E: cross-section, details of glaze

Figure25. SEM images of sample HBR-0207

Table 16. EDS results of sample HBR-0207 (mol. %)

SEM paste/ glaze	Na_2O	MgO	Al_2O_3	SiO2	K_2O	CaO	TiO_2	P_2O_5	MnO	Fe_2O_3	CuO	SnO_2	PbO	Si/Pb ratio
paste	3.4	5.4	10.2	52.5	--	21.0	1.8	--	--	3.0	--	--	2.8	18.60
(A) general glaze	--	--	6.7	37.0	--	17.0	--	8.1	--	1.5	--	15.3	14.3	2.58
(A) black part	--	--	6.5	73.8	--	7.5	--	--	--	0.9	--	6.2	5.1	14.59
(B)white crystals 1	--	--	4.0	8.8	--	36.4	--	15.8	--	0.7	--	6.4	27.9	0.32
(C) white crystals 2 in black zone	11.4	7.5	6.1	42.0	--	6.0	--	1.5	--	0.6	--	21.5	3.3	12.55
(D) glaze	8.7	3.2	4.2	58.2	4.7	5.5	--	--	--	1.4	--	--	14.2	4.09
(D) top white crystals	--	--	4.9	30.6	--	--	--	--	--	0.7	--	55.7	8.1	3.79
(D) grey prisms	--	0.3	0.6	46.8	1.2	46.5	--	--	--	0.7	--	--	3.8	12.27
(D) black prisms	--	--	2.6	66.0	7.6	5.4	--	--	--	3.1	--	--	15.3	4.31

Table 17. Selected EDS results of sample HBR-0207

element / zones	Pb	P	Ca
(A) general glaze	12.31	13.98	14.59
(B) white crystals 1	23.11	26.26	30.16
(C) white crystals 2 in black zone	2.80	2.5	5.00

In these two samples in the zones where there is phosphor, calcium, lead these elements are present in the same relative ratio as already reported for the four previous samples. One can exclude the hypothesis that the presence of phosphor had the same origin in all samples. Nevertheless, one sees a completely different typology in these two samples that may be explained by a different use of the phosphorous.

Traces of titanium are detected by EDS in the pastes these two samples. Titanium can be characteristic of the region of extraction of the clay. It may mean that the clays from the same geological formation were used to make the two pottery pieces.

3.5 X-ray diffraction

X-ray analyses performed on the paste of samples HBR-0072 and HBR-0207 show silicates and derivates of kaolin.

In the sample HBR-0072, the presence of anorthite but not of mullite may indicate that the firing temperature was around 900°C. Anorthite is a derivative of kaolin obtained by addition of calcium that could come from the augite which is a silicate mineral with the elements (Ca, Mg, Fe...) or from the diopside ($CaMgSi_2O_6$). Diopside also forms by the reactions occurring during firing.

The sample HBR-0207 shows almost the same composition as sample HBR-0072 with the exception the mineral diopside. The composition show that the temperature used to fire the pottery was around 900°C, too, table 3.

4. Discussion

4.1 Phosphorous pollution from weathering

In the case of samples HBR-0207 and HBR-0072 one can think that the phosphorous matter observed by EDS comes from an external source. Indeed, for those samples, phosphor was only found at the surface of the glaze and can be seen as a sediment layer.

Since the samples were found under a Christian cemetery and bones are composed of calcite and calcium phosphates (Morgulis 1931); one can think that the phosphor found in the sample came from the dissolved bone material following the runoff water. Phosphate could also come from the products of agriculture.

This hypothesis is confirmed by the presence of phosphor also in the ceramic body which was never detected in the remaining samples whereas the ceramic body is the softer and more porous part of the pottery piece.

The two samples do not have the same glaze composition. The main difference concerns the elements tin and copper which are chromogenic elements. In sample HBR-0207 homogeneous distribution of tin was observed in the glaze, giving the whitish colour. Copper was not found in sample HBR-0207 but traces were observed in sample HBR-0072. This late sample is green, copper mixed with iron being usually used to make this colour.

These two samples present similarities than can be explained by a common origin. In addition to the special morphology of samples HBR-0206 and CR/CSP/0022, one observed the presence of a sediment layer at the top of the glaze that seems to come also from external pollution.

4.2 Technical phosphorous

4.2.1 *Precipitates*

This morphology was found in the samples HBR-0206 and CR/CSP/0022, as described above in section 3.3 Chap 4. Details of a spherical particle of phosphorous matter and results of EDS 7 show lead, calcium and phosphor only. The EDS 5 corresponds to the zone around the sphere. EDS 5 shows that this zone is composed of elements of the glaze (Al, Si, K, Fe, Ca and Pb); there being trace of phosphor here. Around the sphere, there is a boundary-like, thin layer that separates it from the glaze. It is important to notice that the amount of lead and calcium decreased outside the sphere; the lead decreases less (from 29% inside the sphere against 26% in the outside) whereas calcium decreases abruptly (from 40% inside against 11% outside), also section 3.3 Chap 4, tables 11, 13.

Figure 23-G represents a cavity describe in section 3.3 Chap 4. The EDS 1 of the wall material shows a composition corresponding to a mixture of glaze elements including Ca, and Pb and the phosphor. The content of lead, calcium and phosphor in the wall presents a similar ratio as in the other phosphorous spheres of this study in previous section, and but it also has elements (Al, Si, Fe) of the glaze (Viti 2003). EDS 5 was performed just next to the pore limits, but no trace of phosphor is

detected, as it was already observed above around the phosphorous spheres of previous sample, figure 23 section 3.3 Chap 4.

With these analyses and because similar behaviour was already observed in man-made glasses (bioglass) in literature (Radev and al. 2010), one cannot exclude the working hypothesis that the phosphor and the calcium are coming from a source of raw materials used in the making of these glazes that could be bone ashes. Indeed, hydroxyapatite (Ca_5 $(PO_4)_3(OH)$) is the main mineral compound of bones. One can suppose that under certain conditions, bones ashes/calcium phosphates present in the ceramic were either included by the potters or, otherwise, come from pollution where they react with the glaze and precipitate calcium-lead phosphates. The present study tends to lead to the assumption of a technical phosphor added by the potters because of the "boundaries" that are always present around the spheres. Indeed, the features of fractures around these inclusions can be explained because of high temperature shrinkage that could appear during cooling stage from firing.

In order to have a better understanding of the phosphorous phases, all the results obtained with EDS were plotted in ternary diagrams, the SiO_2-PbO-CaO diagrams giving evidence of reactions inside the glaze, and $PO_{5/2}$-PbO-CaO diagrams exposing potential relationships with the hydroxyapatite ($Ca_5(PO_4)_3(OH)$) coming from bone ashes that could have reacted with the lead contained in the glaze.

In the two projections of the quaternary phase diagram in figure 26, the pink squares correspond to the sample HBR-0206 and the blue ones to the sample CR/CSP/0022. In the phosphor/calcium/lead system the perimeter delimited by the red dashed line corresponds to the phosphate glass forming range (Sajai 2012), and the blue dashes to the glass miscibility gap (Tulyaganov 2000, Tulyaganov 2004). In the SiO_2/PbO/CaO system the pink dashes correspond to lead and calcium in equal weight amount.

One can firstly observe that the two samples display similar composition relationships for the phosphor repartition inside the glaze as well as a similar glaze composition. These plots in these diagrams confirm that there are free-phosphorous zones in the glaze compositions and that the high phosphor precipitates are always found with the same relative values of lead, calcium and phosphorous.

The diagram can represent a silica-lead glaze made of a silica raw material and a special mixture in fixed and almost equal weight proportions of a lead containing source (PbO) with calcium and phosphor coming from the bone ashes, the glaze becoming glass-phase-separated during firing or slow cooling inside the kilns. But, literature also gives some images of ancient glasses and glazes with the similar morphology of bands and zoning all coming from weathering (Casellato and al. 2007, Chiva and al. 2004, Croveri and al. 2010, Mahé-le Carlier and al. 2000).

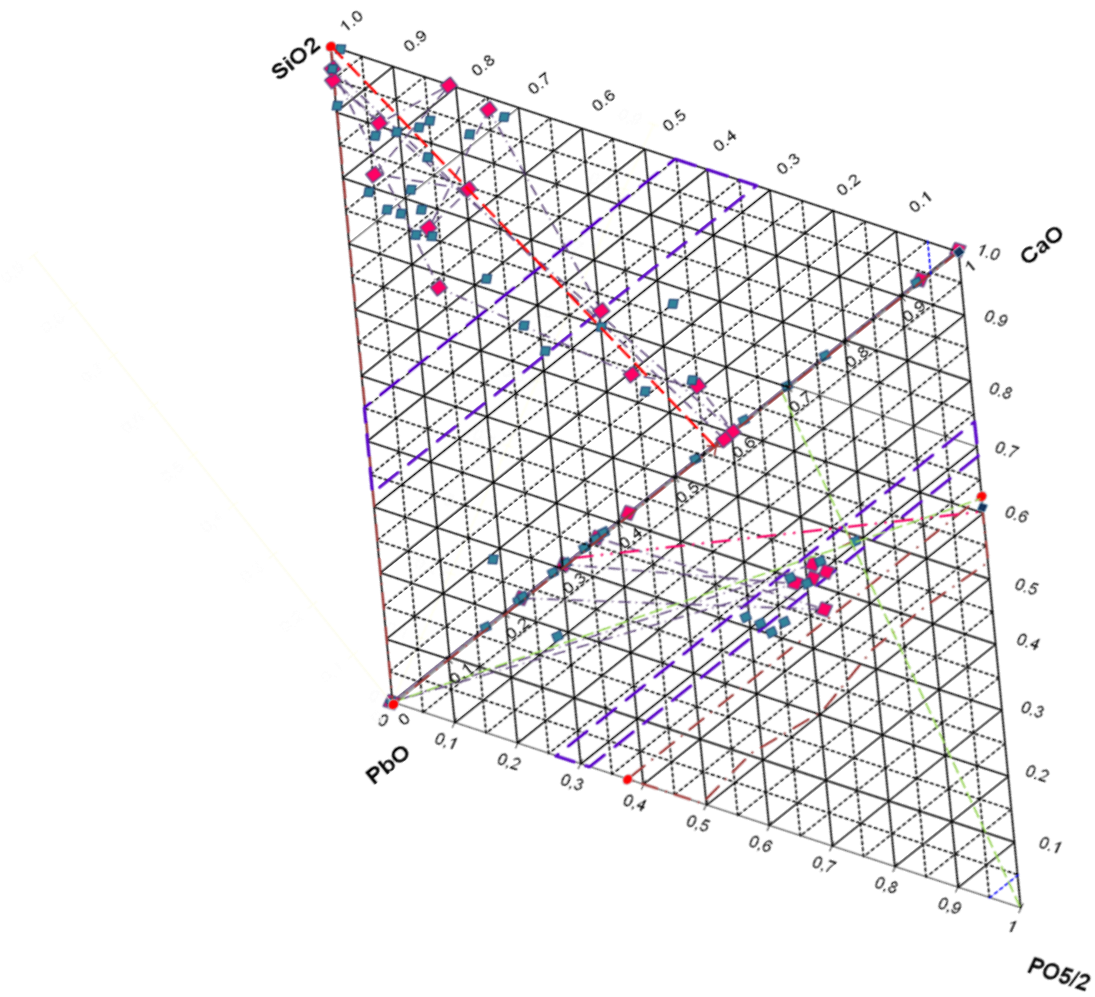

Figure 26: HBR-0206 and CR/CSP/0022 projections of the composition into the pertinent ternary phase diagrams

4.2.2 *Gradients of concentration*

Two samples, HBR-0001 and CR/CSP/0023, presented stratigraphy or zoning. This morphology is characterized by closely spaced layers seen as lines in cross-section, forming circles around large particles. Sample HBR-0001 was selected for further analysis of the element concentration at the transitions from the inclusions to the zoned areas. Preliminary study of the zoned area of sample CR/CSP/0023 (figure 18-E) corroborates the results obtained with sample HBR-0001.

EDS line scans were performed in order to establish the reaction paths that may have leaded to layered zone formation by detecting presence of gradients in element composition near the

glaze/inclusion internal interfaces. In sample HBR-001, the layers in the zoned matrix contour the relevant inclusions, or are parallel to outer boundaries of the zoned area. There are many different points inside the glaze that dictated layer zone orientations on local scale. This part of study aims to make a distinction of the origin of the layered zones in the glazes, the one that explains it as originating from weathering of the glaze in contact with burial fluids and contaminants from the alternative explanation of the formation of the layered zones in the SiO_2-P_2O_5 glazes under examination, as being due to effects of glass phase immiscibility during firing or at early stages of cooling of the glazed piece. Both processes of layer formation inside the glaze as seen, the spinodal reaction with glass phase separation at high temperature, or the weathering at soil temperature ranges, require diffusion of the chemical elements inside the glaze, or trough the glaze remnant of the Na, K ions leaching processes (Chiva 2004; Croveri 2010; Henshaw 2010; Mahé-Le Carlier 2000; Paynter 2011; Verita 2000).

Four different sites were characterized by EDS elemental line profiling. Thre are shown: (figures 27) the transition at the edges on both right and left sides of a quartz inclusion in the glaze, the right and left sides, (figures 28) the matrix contacting a Pb-P-Ca rich spherical particle and this particle itself and in (figures 29) a fractured Si rich glazed zone contacting Pb-P-Ca rich area and Pb-P-Ca rich inclusions of with angular shapes and small dimensions.

EDS was performed at the limit of the high silica inclusion (black grain). The EDS 1 (table 6) shows glaze elements (Fe, Cu, Si, Sn) and the three element lead/calcium/phosphor in high quantity with the same ratio that found in other samples. Lead, calcium and phosphor were not measured in the silica inclusion by EDS of inside area.

In order to understand how these zoning lines are formed and if there really is a gradient coming out of the large particles, line scans were performed from the silica particle away towards the matrix parallel to the lines (Figure 27). EDS counts of silicon, lead, phosphor and calcium were measured to confirm the correlation between silica and the other elements that has already observed in EDS of the given areas. Changes of carbon concentration were also evaluated to investigate the formation of carbonates (SEM samples are C coated, only net changes in C counting would be relevant). The C profile shows a quasi constant behaviour. Its concentration corresponds to the conductive carbon layer that was deposited during sample preparation. The jump of the intensity of C signal corresponds to the crack around the inclusion of silica. The carbon presence attributed to carbonates can be neglected.

Line scans show that coming out of high silica inclusion, Si concentration decrease rapidly and is compensated by the concentration of lead, calcium and phosphor that have to increase. The concentration of these three elements (Pb, P, and Ca) increases in moving away from the silica inclusion but always retain nearly constant values of their ratio (given as 30%, 35% and 35%, respectively, in EDS 1). Traces of calcium, lead and phosphor in similar relative proportion are found well inside the high silica inclusion at the starting of this line scan (23µm).

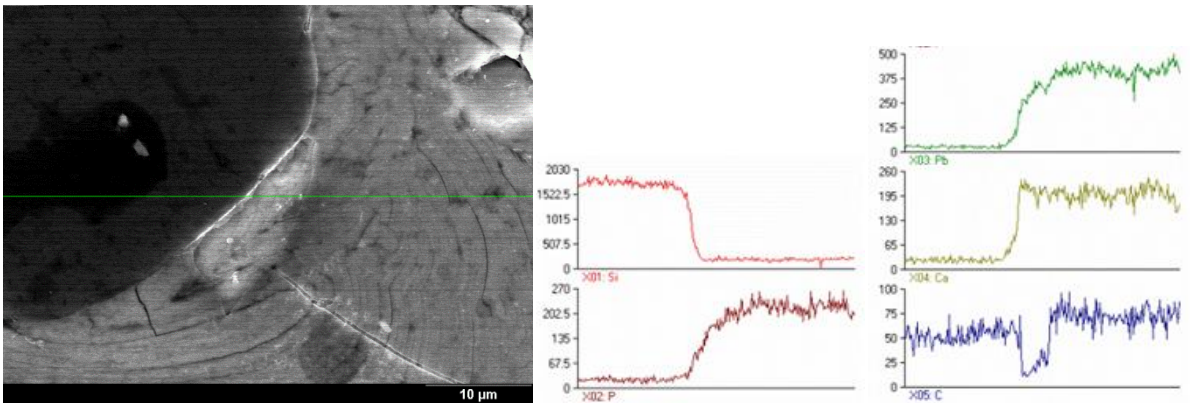

Figure 27. SEM (BSE) figure of the sample HBR-0001, details of a quartz inclusion and line scan; in pink Si, in red P, in green Pb, in brown Ca and in blue C

The figure 21-H shows a phosphor-rich inclusion that can be interpreted as a phosphorous source leading to the zoning by de-mixing inside with the glaze. The EDS of this area (EDS 2 table 9) would support such hypothesis. Indeed, in addition to glaze elements (silicon, aluminium and copper) one finds again high quantity of Pb, P, and Ca and in similar ratio of the three elements.

As above, the line scan (figure 28) performed in direction close to the normal of lines of the zoning shows a correlation between the quantity of Si and the other three elements Pb, P, and Ca. In those measurements, silicon decrease when the profile is getting closer to the inclusion with a quasi symmetrical evolution of phosphor and lead together, whereas Ca stays constant all along the path. It is interesting to notice that there is a strong link between the two inclusions (high silica and high phosphor) as the composition at the end of the line scan path coming from the silica inclusion to matrix correspond to the beginning of the path going to the phosphorous inclusion. These results suggest possible ionic diffusion processes between one sources of silicon and one source of Pb/P/Ca elements inside the glaze of this sample.

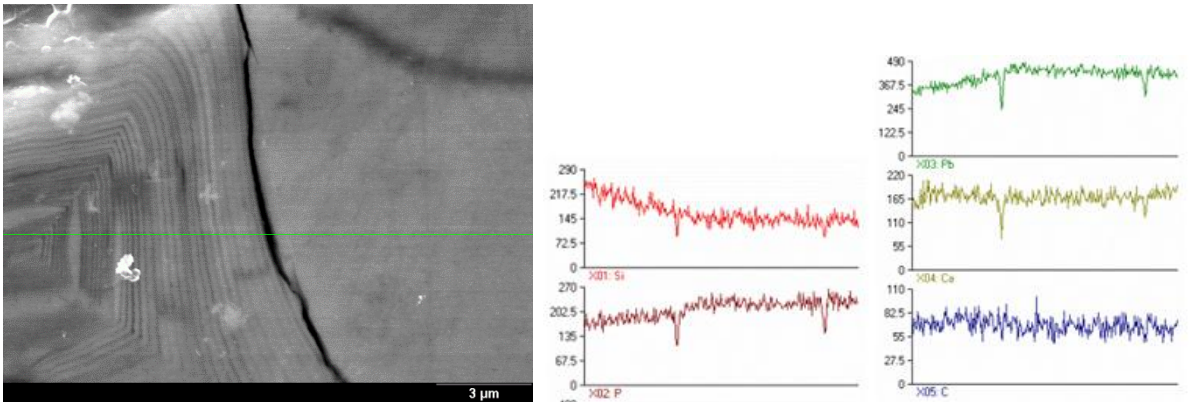

Figure 28. SEM (BSE) figure of the sample HBR-0001, details on a phosphorous grain and its line scan; in pink Si, in red P, in green Pb, in brown Ca and in blue C

The zone showed in figures 19-G is very different from the two zones in figures 27 and 28. In this area, glass like area rich in silica is surrounded by many particles of angular shapes which separate it from the glaze matrix with zoning. The area has composition similar to the others areas with the same proportion of Pb/P/Ca elements.

Line scans (green in figure 29) were performed in this area coming from the matrix at the left, crossing the glassy silica area and arriving to the clear inclusions on the glazed surface in the right (epoxy is see at the limit on the right). In this series of line scans three other elements (Fe), Cu and Sn) were included too. Those three elements are found in small amounts and their composition can be considered constant within the scatter of the line scan measurements,
Here again, a similar behavior of silicon, lead, calcium and phosphor as described above is observed. Coming from the matrix, silicon is low and lead, phosphor and calcium are high, approaching the silica phase; silicon increase and phosphorous, lead and calcium decrease together. The first jump of those three last elements corresponds to the clear grains and the last one to the glaze top layer. In those zones, silicon decreases again. With these results, one can say that the clear grains and the matrix have the same composition and that the matrix with the zoning has the same concentration in Pb, Ca and P as the overall glaze.

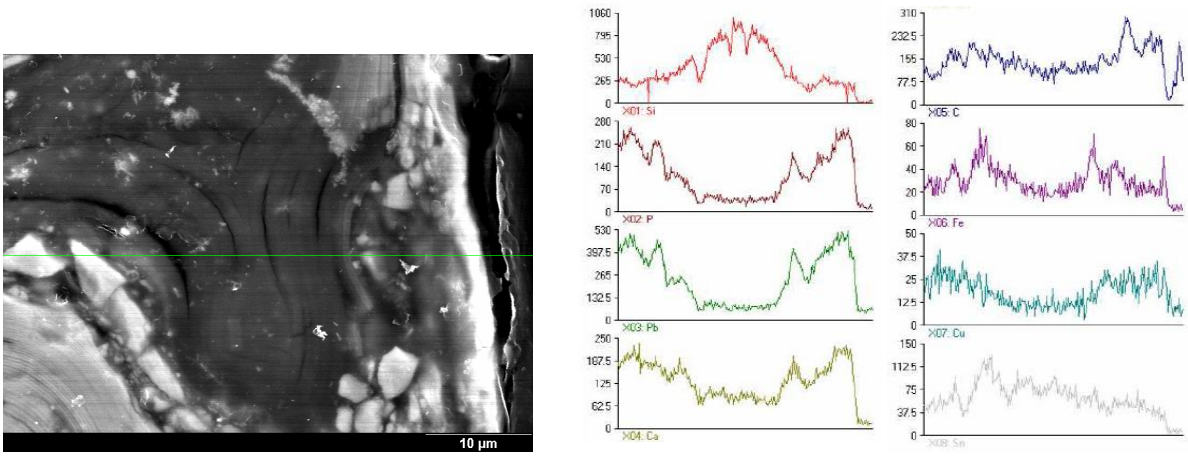

Figure 29. SEM (BSE) figure of the sample HBR-0001, details on a phosphorous grain and its line scan; in pink Si, in red P, in green Pb, in brown Ca, in blue C, in purple Fe, in turquoise Cu and in grey Sn

These results are interesting and as for the case of phosphorous-precipitates can be interpreted as a bone ashes reaction with the glaze. Indeed, when one plots all the EDS results of the two samples HBR-0001 and CR/CSP/0023, figure 30 one observe the trends analogous to those reported for samples CR/CSP/0022 and HBR-0206 (figure 26) characterized by a high concentration of points clustering in the bone ashes-PbO region in the CaO/PbO/PO5/2 ternary phase diagram and the same distribution of Si, Ca and Pb in the other diagram.

Until now, one could not find a consistent explanation of this morphology in the bibliography; the high content of Pb, P and Ca in almost fixed quantitative proportions, as determined in the glaze of sample

HBR-0001, could equally be the result of intentional man action of the potter, as well as it would be explicable on qualitative grounds by weathering.

The use of plant ashes specifically selected for the task, or furnace ashes just picked on place, in the formulation of glass, enamels and glaze frits was known early before the developments in glass and opaque glass tesserae (*opus sectile*) technologies of the Roman empire (Croveri 2010; Paynter 2011). Following Colomban 2004; 2005, the presence of calcium phosphate in the body and glaze of ancient ceramics was early explained in Kingery and Freestone works (Kingery 1984; Freestone 1998) as linked to the practice of adding bone ash in making white enamels, said to be an Islamic technique of opacification, the process being recognized in Islamic enameled glasses from 13-14th century and in the production of some Iznik ceramics (Anatolia, Turkey), (Henderson 1989, Schibile 2012). It is narrow the time span between the historical period of the shreds from Islamic period of Mértola and the tentative dating of the Islamic enameled glasses with calcined bone added in. The most widespread explanation for the detection of phosphor in ancient glazes of ceramics shreds still is contamination.

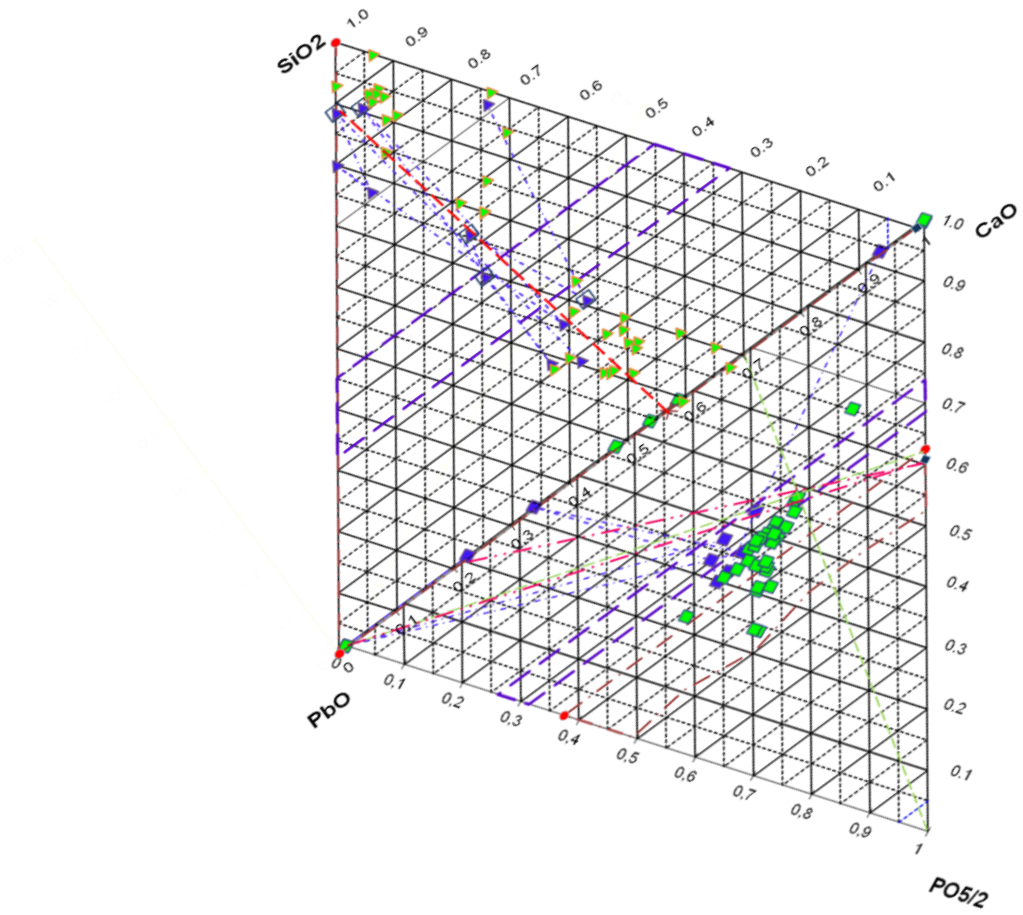

Figure 30. **HBR-0001 and CR/CSP/0023 projections of EDS results into pertinent ternary phase diagrams**

The study of this set of “cuerda seca” samples shows different faces of the behavior of phosphor. In two of out of the six historical samples of Mértola, the phosphor can be considered as due to weathering because it was only found at the surface of the glaze like a sediment layer. In the four others samples, phosphor was found in important quantity inside de the glaze with no trace in the ceramic body. These cases can hardly be considered as pollution because of the abscence of phosphor in the paste. In those samples, two categories of morphologies were observed: spheres of phosphor matter in a phosphorous free environment and gradients of phosphor and glaze base materials (Si, Ca...) coming from neighbor phosphor and silicate sources.

The samples presenting a sediment layer at their surface can be considered as altered by the phosphorous pollution coming from runoff water through the bone material of the cemeteries and septic pits.

In two others cases (samples HBR-0206 and CR/CSP/0022) and (samples HBR-0001 and CR/CSP/0023), one can formulate the hypothesis of the use of bone ashes include in the glaze mixture by the potters..

Phosphor in ancient ceramics was already observed. Indeed, phosphor and calcium reacting with lead-rich environment, by ionic diffusion may create either precipitates or zoning. This hypothesis has still to be confirmed by more experiments. Raman spectroscopy has been performed in order to identify nature of chemically bonding in phosphorous-rich regions. The first results did not show any carbonate in a different way as found, for instance, by Chiva (2004). That somehow strengthens the hypothesis about the use of a technological phosphor. In future work, Transmission Electron Microscopy will be necessary in order to clarify if one is dealing with precipitation form weathering or high-temperature glass phase separation. These results could be an interesting progress since until now the use of phosphor in glass and glaze technology was reported only from the 13-14th centuries onwards (Colomban 2004, 2005).

Chapter 5 - Conclusions and suggestions of further work

This study of one set of six ceramic shreds from the archeological site of Mértola and another small set of four other samples collected from Aveiro grounds represented a crossing between science and archeology for the author.

The study of the set of six archaeological samples of “cuerda seca” type has been useful at two levels: firstly, to understand how to analyze ancient samples in a non-destructive (as possible) way and second how to figure their history,

The archeological camp of Mértola provided the samples and the history. Since ancient times, localization of Mértola at the most northerly navigable point of Guadiana river, give to this town a strategically position for the economical and cultural trades in regional networks and through Mediterranean maritime routes. Mértola became one of the communication centers in Garb Al-Andalus. Pieces of “cuerda seca” Islamic ceramics were found in large amount in Mértola. The six pieces of this study came from two sites of this camp: form under the Christian cemetery and from a sceptic pit. The results of this study lead to the following conclusion on these samples

a) All six samples have lead-silica glazes that show different conditions of preservation.

b) The use of tin as opacifier is found in the glazes of four of these pieces but not in HBR-0072 and HBR-0206 samples

c) The green color of the glaze of sample HBR-0072 is due to Fe (1.1 – 3,8 mol. %) and this sample may not be of “cuerda seca” type. Cu was rarely found in points submitted to EDS analysis and the brown color in the thicker trace is correlated to staining of the surface. Diopside was only detected in the paste of this piece which has negative a* coordinates in the CIELab system of color.

d) The color of the pastes of samples HBR-0206 and CR/CSP/0023 have the largest red components which are correlated to low calcium contents and the presence of mullite from higher firing temperatures.

The SEM/EDS and XRD analyses show different composition and morphology of the four samples of other set. Because of complex composition, thickness and decoration style and the presence of elements such barium one can say that

- Sample (1) MSJ-TILE-3 25-REST is the most recent ceramic tile of this series.
- On the contrary, the not so precise composition the sample (4) MSJ-TILE-3 25-3C, its thickness and the blue-yellow colouring on white glaze opacified by tin indicates that it must be the older sample of the set.
- It was more difficult to differentiate the samples (2): ESG-POT-3 24 and (3): RMS-TILE-3 31-3C as they have similar compositions; these two samples are probably from the same age.

The analyzes of glazes of the six samples from Mértola show three different glazes morphologies in SEM that after EDS determination of the composition of main features in the glaze structure and EDS line profile analysis revealed the presence of two types of phosphor distribution: one originating from

weathering and other that could be hypothetically linked to the use of phosphor bearing materials added by the potters to compound the glazes.

Until now, the second hypothesis has still to be confirmed by new analyzes of others. Optical observation with reflected polarized light corroborated the effect of glaze composition in creating zoning. Raman spectroscopy performed on sample HBR-0001, also tends to corroborate the hypothesis of a high temperature process, eventually with the use of bone ashes as raw material, because peaks characteristic to O-H and PO_4 bonds of the (Pb) hydroxypromorphite.Ca hydroxyapatite solid solution were detected in Pb/P/Ca inclusions in a silicate glassy matrix.

Suggestions for further work:

The introductory study of the set of six samples received from Mértola in the short time available left many open questions, that are present as suggestions for future work in the following:

- Increase the statistical confidence of the measurements of the chemical composition of the pastes and areas of glaze which are clearly free of weathering by taking larger numbers of EDS spectra and by calculating the averages of the values of concentration of the chemical elements;

- Identification of links between composition of pastes and glazes of the samples of this set and other ceramic pieces of the large collection of “cuerda seca” Islamic ceramics of the Mértola archaeological site studied to the present time;

- The real structure of the glaze of sample HBR-0001 that is complex and lead to the present tentative of an alternative interpretation of the origin of phosphor in this glaze, needs to be further investigated with a new cross-section confirming, or not, the observed dispersion of phosphorous matter;

- Transmission electron microscopy with EDS will be needed for studying the hydroxtypyromorphite/ Calcium hydroxyapatite solid solution, refine chemical profile analysis of the phosphor ion combined with lead and Ca ions and investigate the extent of diffusion of these elements into silica/quartz inclusions.

- micro-Raman spectrometry of the inclusions and layers deposited inside large pores to separate carbonates form precipitation of phosphates.

References

Basso P, “Cerâmica Farmacêutica e a arte de curar”, CTT Correios de Portugal, (2009).

Casellato U, Fenzi F, Riccardi MP, Osmida GR, Vigato PA. Case study. Physico-chemical and mineralogical study of ceramic findings from Mary City - Turkmenistan. Journal of Cultural Heritage 8 (2007) 412-422

Chiva L, Gómez JJ, Estall V, Núñez I, JCarda JB, Study and Characterization of Islamic Ceramic Tiles from Onda-Castellon (Spain). 34th International Symposium on Archaeometry. Pub. Nº 2.621 Institución «Fernando El Católico» (Excma. Diputación de Zaragoza). ISBN: 84-7820-848-8. Zaragoza, Spain. (2004) 439-445

Ciobanuc. S, Andronescu E., Stoicu A., Florea O, Le Coustumer P, Galaup S, Djouadi A, Mevellec J.Y, Musa I, Massuyeau F, Prodan A. M., Lafdi Khalid. Trusca R., Pasuk I., Predoi D, Influence of annealing treatment of nano-hydroxyapatite bioceramics on the vibrational properties**,** Digest journal of nanomaterials and biostructures vol. 6, no 2, april - june (2011), p. 609 – 624

Colomban Ph, Milande V, Lucas H. On-site Raman analysis of Medici porcelain. Journal of RAMAN Spectroscopy. 35 (2004) 68–72

Colomban Ph. Recent Case Studies in the Raman Analysis of Ancient Ceramics: Glaze Opacification in Abbasid Pottery, Medici and 18th century French Porcelains, Iznik and Kûtayha Ottoman Fritwares and an Unexpected Lapis Lazuli Pigment in Lajvardina Wares. Mater. Res. Soc. Symp. Proc. Vol. 852 (2005) OO8.4.1-OO8.4.8

Croveri P, Frag Jane t D . Cotter - Howell Salà I, Ciliberto E. Analysis of glass tesserae from the mosaics of the ‘Villa del Casale’ near Piazza Armerina (Enna, Italy). Chemical composition, state of preservation and production technology. Applied Physics A 100 (2010) 927-935

Cultrone Giuseppe, Rodrigez-Navarro Carlos, Sebastian Eduardo, Cazalla Olga and Jose De La Torre Maria, Carbonate and silicate phase reactions during ceramic firing, Eur. J. Mineral. 13 (2001), 621-634

Déléry Claire, « Dynamiques économiques sociales et culturelles d’al-Andalus à partir d’une étude de la céramique de cuerda seca (seconde moitié du Xesiècle-première moitié du XIIIe siècle) », PhD Thesis, Université de Toulouse, Tome III (2006)

Déléry Claire, Dynamique économique, sociales et culturelle d’al-Andalus à partir d’une étude de la céramique de cuerda seca (seconde moitié du Xe siècle-première moitié du XIIIe siècle), Mélanges de la Casa de Velazquez, 38-1 (2008), 335-338.

Encyclopedia Universalis, http://www.universalis.fr/ (August 2012)

Ferraro J. R., Nakamoto K., Brown C. W., *Introductory Raman Spectroscopy*, Elsevier (2003).

Figueiredo, Gomes Celso de Sousa The prelude of Porcelain in Portugal: the first experiments”, June 2007

Figueiredo M.O., Pereira da Silva T. and Veiga J.P., Ancient glazed ceramic tiles: a long term study from the remediation of environmental impact to the non-destrcutive characterization of

materials, Proceeding of the International Seminar on conservation of Glazed Ceramic Tiles: research and practice, Lisbon, LNEC, april 15-16 (2009).

Freestone IC, Stapleton CP. In Gilded and *Enamelled Glass from the Middle East*, Ward R (ed). British Museum Press: London, 1998; chapt. 24. (*cited by Colomban Ph 2004, as ref. 31*)

Gardiner D. J, Graves P. R. *Practical Raman Spectroscopy*, Springer, (1989).

Gomes, C. S. Figueiredo. The prelude of Porcelain in Portugal: the first experiments",June 2007.

Gomez M. Susana, "New perspectives in the study of Al-Andalus Ceramics, Mértola (Portugal) and the Mediterranean Maritime Routes in the Islamic Period", Al-Masaq, Vol. 21 (april 2009), n1.

Hadrich A., Lautie A. and Mhiri T., Monoclinic to hexagonal phase transition and hydroxyl motion in calcium–lead hydroxyapatites studied by Raman spectroscopy, *J. Raman Spectrosc. (*2001); 32: 33–40

Hadrich A., Lautie A. and Mhiri T, Vibrational study and fluorescence bands in the FT–Raman spectra of Ca10−*x*Pb*x*(PO4)6(OH)2 compounds, Spectrochimica Acta Part A 57 (2001) 1673–1681

Henderson J. In *Iznik*, Raby J (ed). Alexandria Press: London, 1989; chapt. V (*cited by Colomban Ph 2004, as ref. 32*)

Henshaw CM. Early Islamic Ceramics and Glazes of Akhsiket, Uzbekistan. PhD Thesis, University College of London (2010)

Kingery DW, Smith D. In *Ancient Technology to Modern Science*, vol. I, Ceramics and Civilization, [24] Kingery DW (ed). American Ceramic Society: Columbus, OH, 1984; 273. (*cited by Colomban Ph 2004, as ref. 3*)

Mahé-Le Carlier C, Le Carlier de Veslud C, Ploquin A, Royer JJ. L'altération naturelle des scories de la métallurgie ancienne : un analogue de déchets vitrifiés. Earth and Planetary Sciences 330 (2000) 179–184

Marii F, Rehren T, Archeological coloured glass cakes and tesserae from Petra Church. AIHV Annales du 17e Congrés (2006) 295-300

Mihailova B., Kolev B., Balarew C., Dyulgerova E., L. Konstantinov, Vibration spectroscopy study of hydrolyzed precursors for sintering calcium phosphate bio-ceramics, JOURNAL OF MATERIALS SCIENCE 36 (2001) 4291 – 4297

Molera J, Vendrell-Saz M. Chemical and Textural Characterization of Tin Glazes in Islamic Ceramics from Eastern Spain. Journal of Archaeological Science 28 (2001) 331–340

Morgulis S, Studies on the chemical composition of bone ash, Journal of Biological Chemistry 93 (1931) 455-466

Paqueton, Henri and Ruste Jacky, Microscopie Electronique à Balayage, Principe et équipement, Technique de l'Ingénieur, (2004) 865-866

Paynter S, Dungworth D, Tyson R, Graham K, Taylor M, Hill D. *Archaeological Evidence for Glassworking. Guidelines for Best Practice*. Ed. David M. Jones, English Heritage Publishing. (2011)

Pereira M., De Lacerda -Aroso T., Gomes M.J.M., Mata A., Alves L.C. and Ph. Colomban, "Ancient Portuguese Ceramic Wall Tiles ("Azulejos"): Characterization of the Glaze and Ceramic Pigments", Journal of Nano Research, Vol 8 (2009) pp 79-88

Radev Lachezar, Hristov Vladimir, Michailova Irena, Fernandes Maria Helena V., Miranda Isabel Salvado M., “In vitro bioactivity of biphasic calcium phosphate silicate glass-ceramics in CaO-SiO2-P2O5 system”, *Processing and Application of Ceramics* **4** [1] (2010) 15-24]

Raskovska A., Minceva - Sukarova B., Grupce O. and Colomban Ph., Characterization of pottery from Republic of Macedonia II. Raman and infrared analyses of glazed pottery finds from Skopsko Kale, *J. Raman Spectrosc.* 2010, *41*, 431–439

Rousseau Jean-Jacques and Gibaud Alain, “Cristallographie géométrique et radiocrystallographie: cours et exercices corrigés”, DUNOD, 3e édition

Sajai N, Chahine A, Et-Tabirou M, Taibi M, Mazzah A. Structure and properties of (50-x)CaO-xPbO-50P2O5 metaphosphate glasses. Optoelectronics and Advanced Materials – Rapid Communications 6 (1-2), (2012) 99 – 103

Schanda, J (2007). Colorimetry. Wiley-Interscience. p. 61. ISBN 978-0-470-04904-4. http://books.google.com/?id=uZadszSGe9MC&pg=PA61&dq=lab+color+6-29+16-116 (August 2012).

Schibille N, Degryse P, Corremans M, Specht CG. Chemical characterisation of glass mosaic tesserae from sixth-century Sagalassos (south-west Turkey): chronology and production techniques. Journal of Archaeological Science 39 (2012) 1480-1492

Tanevska V, Philippe Colomban, BiljanaMinceva- Sukarova and Orhideja Grupce, Characterization of pottery from the Republic of Macedonia I: Raman analyses of Byzantine glazed pottery excavated from Prilep and Skopje (12th–14th century), *J. Raman Spectrosc.* 2009, *40*, 1240–1248

Tulyaganov DU. Phase equilibrium in the fluorapatite-anorthite-diopside system, Journal of the American Ceramic Society 83 (12) (2000) 3141-3146

Tulyaganov DU, Agathoupoulos S, Fernandes MH, Ventura JM, Ferreira JMF. Preparation and crystallization of glasses in the system tetrasilicic mica-fluorapatite-diopside, Journal of the European Ceramic Society 24 (2004) 3521-3528

Verita M. Technology and deterioration of vitreous mosaic tesserae. Reviews in Conservation (IIC) 1 (2000) 1-19. www.viks.sk/chk/revincon5.doc (August 2012)

Verità M, James L, Freestone I, Henderson J, Nenna M-D, Schibille N, *Glossary of Mosaic Glass Terms*, ed by B. Bjornholt (Centre for Byzantine Cultural History, University of Sussex, 2009). http://www.sussex.ac.uk/byzantine/research/mosaictesserae/publications (August 2012)

Verità M. 'Glass mosaic tesserae of the Neonian Baptistry in Ravenna: nature, origin, weathering causes and processes', Proceedings of the Conference: Ravenna Musiva, 22-24 October 2009

Viti C, Borgia I, Brunetti B, Sgamellotti A, Mellini M. Microtexture and microchemistry of glaze and pigments in Italian Renaissance pottery from Gubbio and Deruta. Journal of Cultural Heritage 4 (2003) 199–210

Weaver Robert, Rediscovering Polarized Light Microscopy, American Laboratory, October 2003, pp55-61

Annex

Annex 1: EDS results of face analyses of the more recent samples MSJ-TILE-3 25-REST and MSJ-TILE-3 25-3C corresponding respectively a, b), c) line design, deep blue and rough zone on the glaze MSJ-TILE-3 25-REST and d), e) whitish blue and dark blue on the glaze MSJ-TILE-3 25-3C, related to the Chapter 3 (preliminary study), section 3.2.1, figure 16.

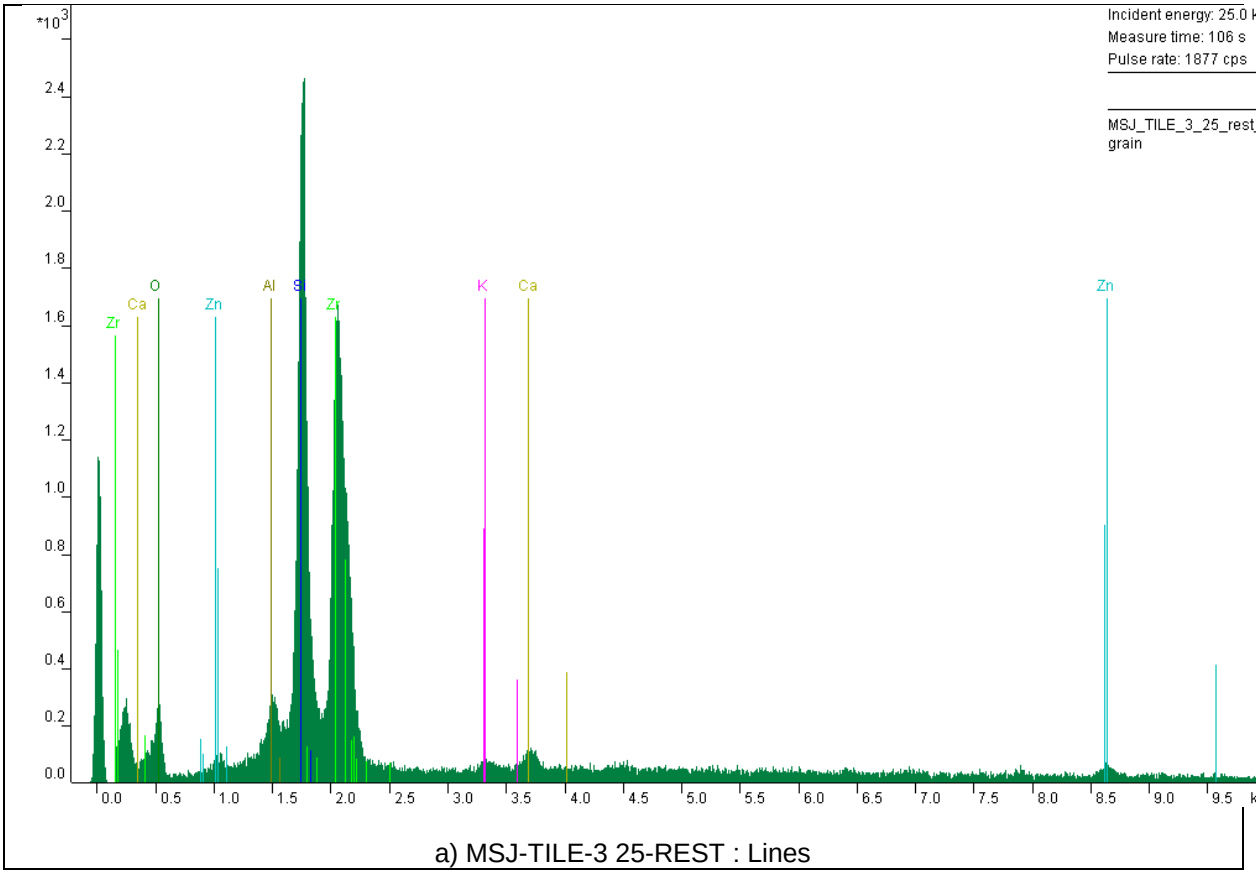

a) MSJ-TILE-3 25-REST : Lines

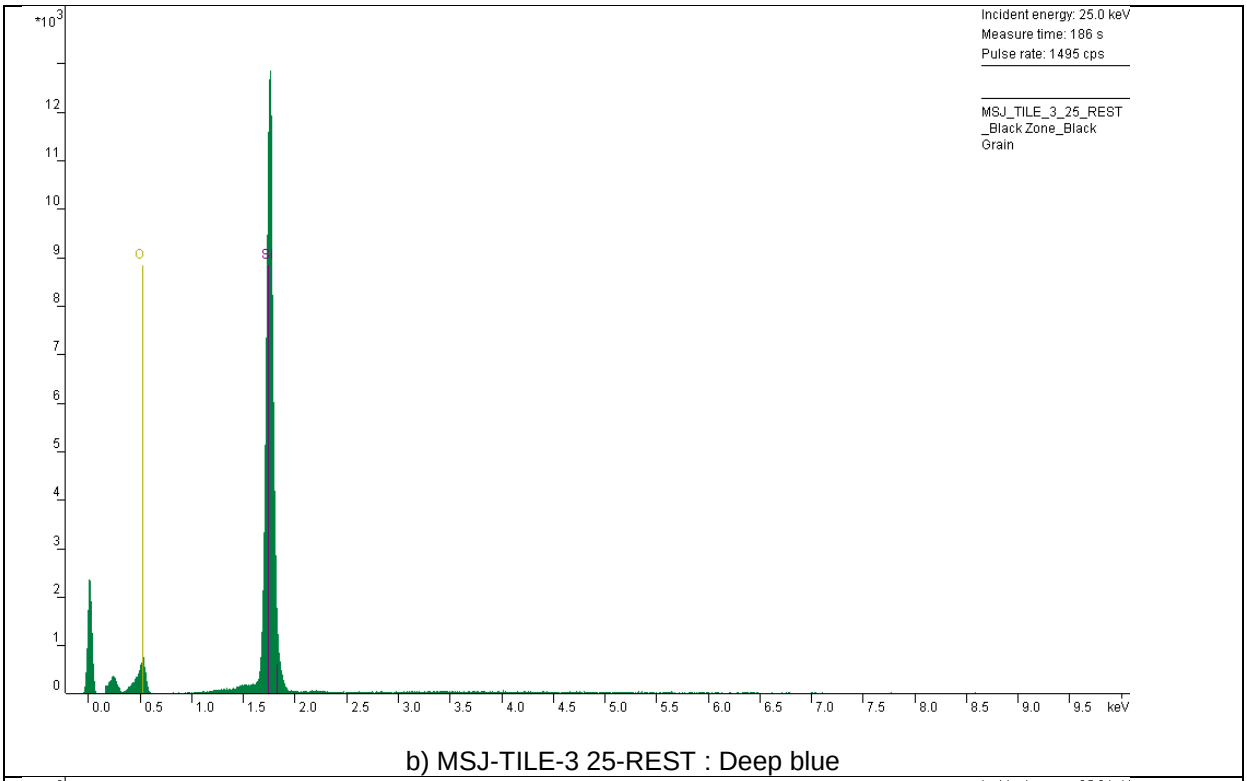

b) MSJ-TILE-3 25-REST : Deep blue

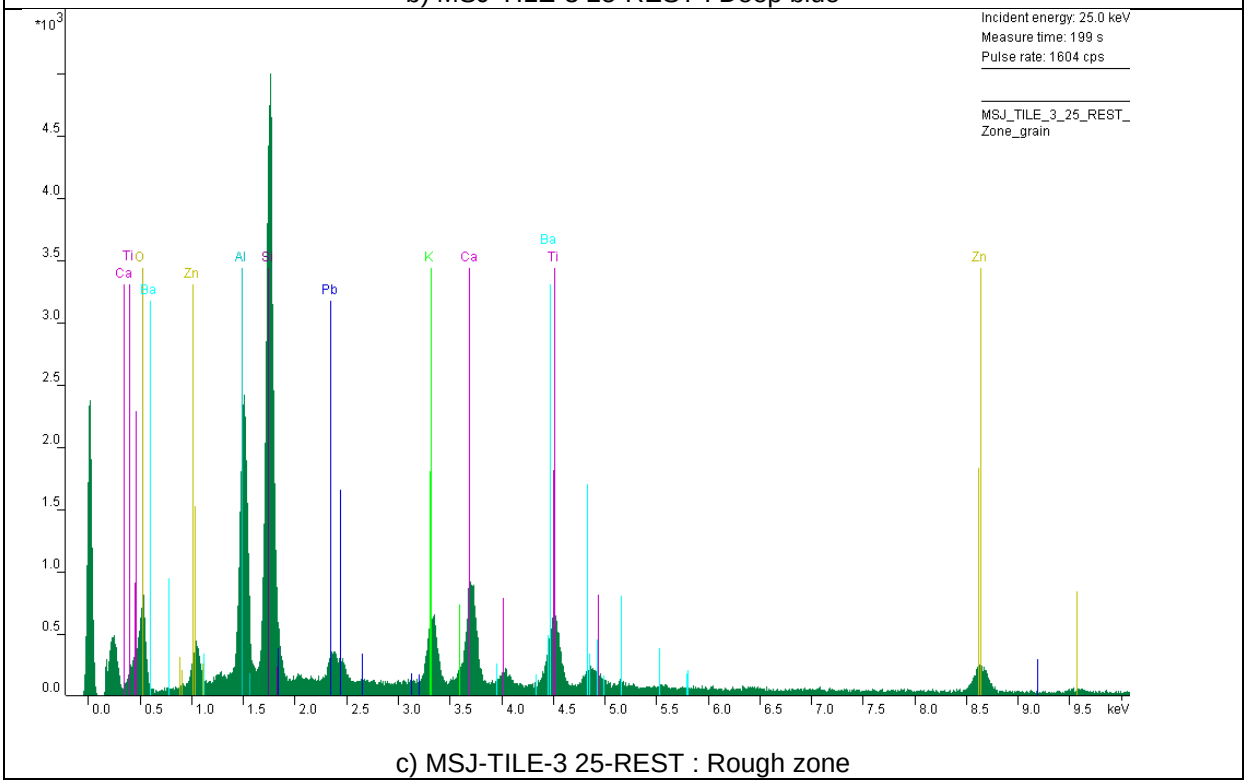

c) MSJ-TILE-3 25-REST : Rough zone

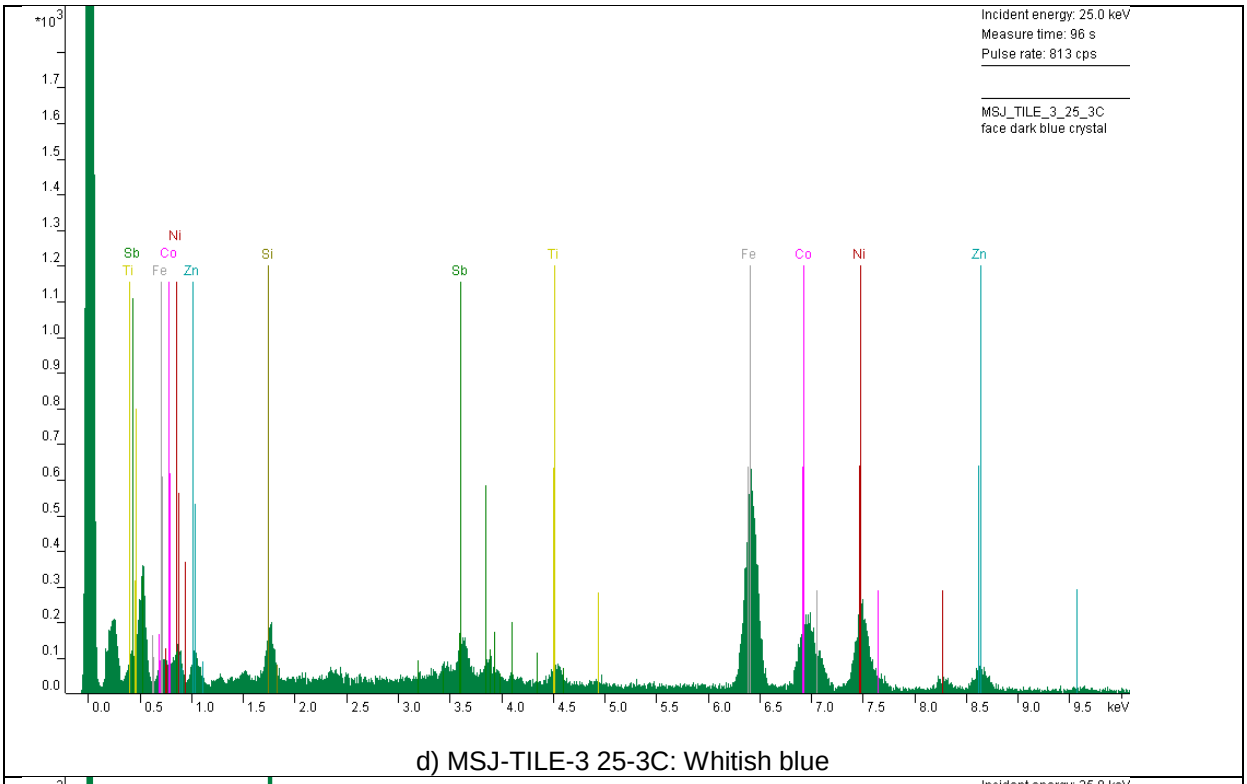

d) MSJ-TILE-3 25-3C: Whitish blue

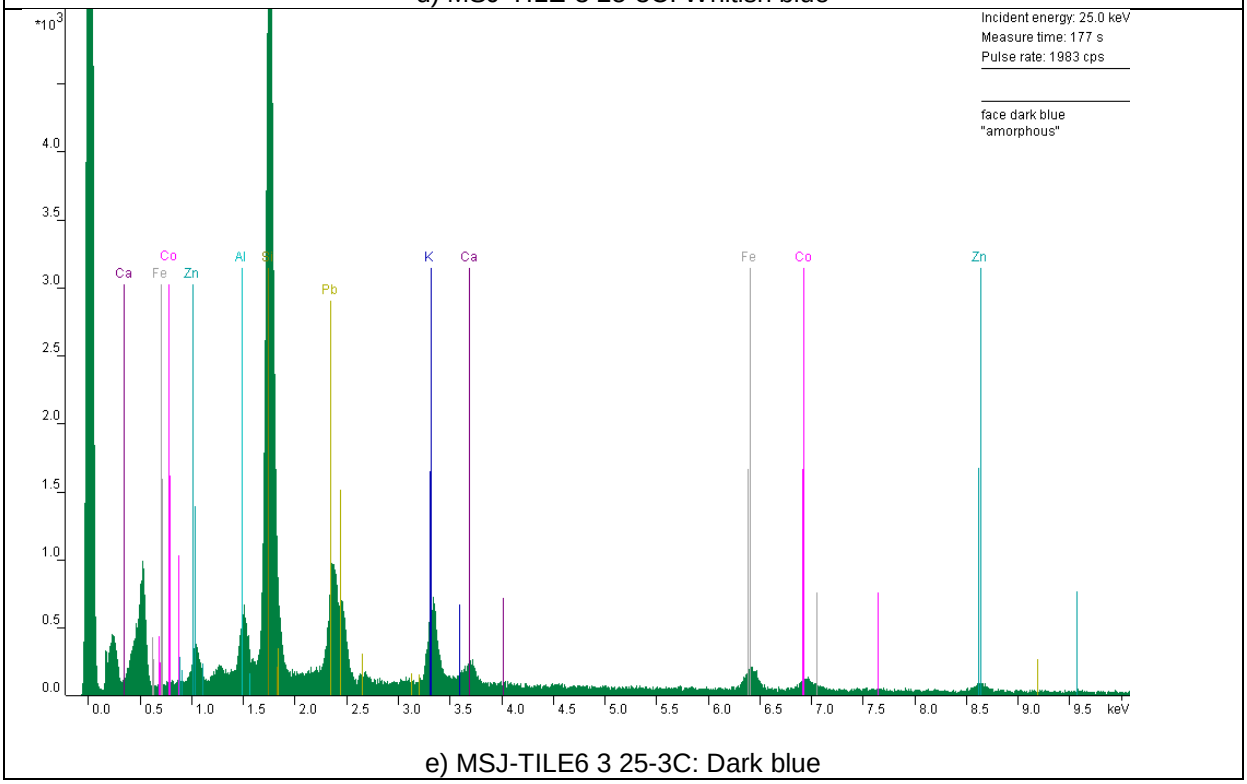

e) MSJ-TILE6 3 25-3C: Dark blue